



U.S. Department  
of Transportation  
**Federal Railroad  
Administration**

## **Tank Car Operating Environment Study–Phase I**

---

Office of Research and  
Development  
Washington, DC 20590

**Notice**

This document is disseminated under the sponsorship of the Department of Transportation in the interest of information exchange. The United States Government assumes no liability for its contents or use thereof.

**Notice**

The United States Government does not endorse products or manufacturers. Trade or manufacturers' names appear herein solely because they are considered essential to the objective of this report.

| <b>REPORT DOCUMENTATION PAGE</b>  |  |  | <i>Form approved</i><br>OMB No. 0704-0188 |
|---|--|--|---|
| Public reporting burden for this collection of information is estimated to average 1 hour per response, including the time for reviewing instructions, searching existing data sources, gathering and maintaining the data needed, and completing and reviewing the collection of information. Send comments regarding this burden estimate or any other aspect of this collection of information, including suggestions for reducing this burden to Washington Headquarters Services, Directorate for Information Operations and Reports, 1215 Jefferson Davis Highway, Suite 1204, Arlington, VA 22202-4302, and to the Office of Management and Budget, Paperwork Reduction Project (0702-0288), Washington, D.C. 20503  |  |  |   |
| <b>1. AGENCY USE ONLY (Leave blank)</b>   | <b>2. REPORT DATE</b><br>October 2007  | <b>3. REPORT TYPE AND DATES COVERED</b>                        |   |
| <b>4. TITLE AND SUBTITLE</b><br>Tank Car Operating Environment Study-Phase I  | <b>5. FUNDING NUMBERS</b><br>DTFR53-93-C-0001<br>Task Order No. 208            |  |   |
| <b>6. AUTHOR(S)</b><br>Kevin Koch   |  |  |   |
| <b>7. PERFORMING ORGANIZATION NAME(S) AND ADDRESS(ES)</b><br>Transportation Technology Center, Inc.<br>P.O. Box 11130, Pueblo, CO 81001   | <b>8. PERFORMING ORGANIZATION REPORT NUMBERS</b>                               |  |   |
| <b>9. SPONSORING/MONITORING AGENCY NAME(S) AND ADDRESS(ES)</b><br>U.S. Department of Transportation<br>Federal Railroad Administration<br>Office of Research and Development<br>1120 Vermont Avenue, NW<br>Washington, DC 20590   | <b>10. SPONSORING/MONITORING AGENCY REPORT NUMBER</b><br><br>DOT/FRA/ORD-07/22 |  |   |
| <b>11. SUPPLEMENTARY NOTES</b>  |  |  |   |
| <b>12a. DISTRIBUTION/AVAILABILITY STATEMENT</b><br>This document is available through National Technical Information Service, Springfield, VA 22161.  | <b>12b. DISTRIBUTION CODE</b>  |  |   |
| <b>13. ABSTRACT</b><br>This report documents the results of controlled testing conducted during the first phase of a tank car operating environment program involving the Association of American Railroads, the Railway Supply Institute (formerly the Railway Progress Institute), the Federal Railroad Administration, and Transport Canada. Strain gages, accelerometers, and an instrumented coupler were installed on a stub sill tank car during this phase of testing. This car was then subjected to a series of tests applying a range of forces to the coupler. These included the application of controlled vertical forces, car-to-car impact tests, and a short duration over-the-road test. Results showed that significant correlation could be established between strain gage output and output from the instrumented coupler. This indicates the strong possibility that longitudinal and vertical coupler forces can be inferred only from the output from four strain gages installed on the stub sill. Results also showed a correlation between accelerometer output (in the form of a shock response spectrum (SRS)) and peak longitudinal coupler forces, especially for impact forces above 400,000 pounds. This indicates a possibility that SRS values from only two accelerometers can be used to infer the magnitude of peak coupler forces that occur during yard impacts. During Phase II of this investigation, this transducer system will be tested under standard in-service conditions to further prove the concept and usefulness towards establishing tank car coupler force operating environment profiles. |  |  |   |
| <b>14. SUBJECT TERMS</b><br>Tank car coupler forces, railcar impact test, correlation of accelerometer data with coupler forces   |  |  | <b>15. NO. OF PAGES</b><br>77             |
|   |  |  | <b>16. PRICE CODE</b>                     |
| <b>17. SECURITY CLASSIFICATION</b><br>UNCLASSIFIED  | <b>18. SECURITY CLASSIFICATION OF THIS PAGE</b><br>UNCLASSIFIED                | <b>19. SECURITY CLASSIFICATION OF ABSTRACT</b><br>UNCLASSIFIED | <b>20. LIMITATION OF ABSTRACT</b>         |

### Approximate Conversions to Metric Measures

| Symbol        | When You Know | Multiply by | To Find     | Symbol |
|---------------|---------------|-------------|-------------|--------|
| <b>LENGTH</b> |               |             |             |        |
| in            | inches        | *2.50       | centimeters | cm     |
| ft            | feet          | 30.00       | centimeters | cm     |
| yd            | yards         | 0.90        | meters      | m      |
| mi            | miles         | 1.60        | kilometers  | km     |

| Symbol          | When You Know | Multiply by | To Find            | Symbol          |
|-----------------|---------------|-------------|--------------------|-----------------|
| <b>AREA</b>     |               |             |                    |                 |
| in <sup>2</sup> | square inches | 6.50        | square centimeters | cm <sup>2</sup> |
| ft <sup>2</sup> | square feet   | 0.09        | square meters      | m <sup>2</sup>  |
| yd <sup>2</sup> | square yards  | 0.80        | square meters      | m <sup>2</sup>  |
| mi <sup>2</sup> | square miles  | 2.60        | square kilometers  | km <sup>2</sup> |
|                 | acres         | 0.40        | hectares           | ha              |

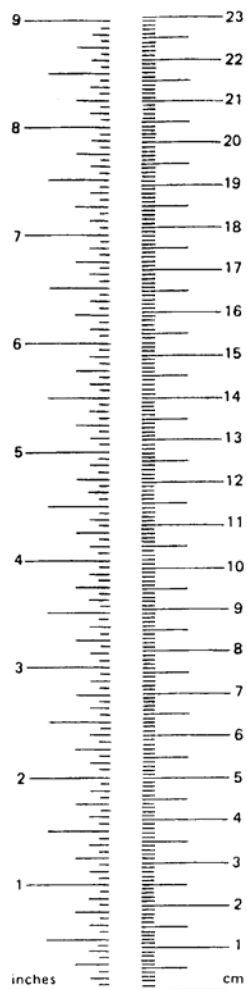
| Symbol               | When You Know        | Multiply by | To Find   | Symbol |
|----------------------|----------------------|-------------|-----------|--------|
| <b>MASS (weight)</b> |                      |             |           |        |
| oz                   | ounces               | 28.00       | grams     | g      |
| lb                   | pounds               | 0.45        | kilograms | kg     |
|                      | short tons (2000 lb) | 0.90        | tonnes    | t      |

| Symbol          | When You Know | Multiply by | To Find      | Symbol         |
|-----------------|---------------|-------------|--------------|----------------|
| <b>VOLUME</b>   |               |             |              |                |
| tsp             | teaspoons     | 5.00        | milliliters  | ml             |
| Tbsp            | tablespoons   | 15.00       | milliliters  | ml             |
| fl oz           | fluid ounces  | 30.00       | milliliters  | ml             |
| c               | cups          | 0.24        | liters       | l              |
| pt              | pints         | 0.47        | liters       | l              |
| qt              | quarts        | 0.95        | liters       | l              |
| gal             | gallons       | 3.80        | liters       | l              |
| ft <sup>3</sup> | cubic feet    | 0.03        | cubic meters | m <sup>3</sup> |
| yd <sup>3</sup> | cubic yards   | 0.76        | cubic meters | m <sup>3</sup> |

| Symbol                     | When You Know          | Multiply by                | To Find             | Symbol |
|----------------------------|------------------------|----------------------------|---------------------|--------|
| <b>TEMPERATURE (exact)</b> |                        |                            |                     |        |
| °F                         | Fahrenheit temperature | 5/9 (after subtracting 32) | Celsius temperature | °C     |

\* 1 in. = 2.54 cm (exactly)

### METRIC CONVERSION FACTORS



### Approximate Conversions from Metric Measures

| Symbol        | When You Know | Multiply by | To Find | Symbol |
|---------------|---------------|-------------|---------|--------|
| <b>LENGTH</b> |               |             |         |        |
| mm            | millimeters   | 0.04        | inches  | in     |
| cm            | centimeters   | 0.40        | inches  | in     |
| m             | meters        | 3.30        | feet    | ft     |
| m             | meters        | 1.10        | yards   | yd     |
| km            | kilometers    | 0.60        | miles   | mi     |

| Symbol          | When You Know                     | Multiply by | To Find       | Symbol          |
|-----------------|-----------------------------------|-------------|---------------|-----------------|
| <b>AREA</b>     |                                   |             |               |                 |
| cm <sup>2</sup> | square centim.                    | 0.16        | square inches | in <sup>2</sup> |
| m <sup>2</sup>  | square meters                     | 1.20        | square yards  | yd <sup>2</sup> |
| km <sup>2</sup> | square kilom.                     | 0.40        | square miles  | mi <sup>2</sup> |
| ha              | hectares (10,000 m <sup>2</sup> ) | 2.50        | acres         |                 |

| Symbol               | When You Know    | Multiply by | To Find    | Symbol |
|----------------------|------------------|-------------|------------|--------|
| <b>MASS (weight)</b> |                  |             |            |        |
| g                    | grams            | 0.035       | ounces     | oz     |
| kg                   | kilograms        | 2.2         | pounds     | lb     |
| t                    | tonnes (1000 kg) | 1.1         | short tons |        |

| Symbol         | When You Know | Multiply by | To Find      | Symbol          |
|----------------|---------------|-------------|--------------|-----------------|
| <b>VOLUME</b>  |               |             |              |                 |
| ml             | milliliters   | 0.03        | fluid ounces | fl oz           |
| l              | liters        | 2.10        | pints        | pt              |
| l              | liters        | 1.06        | quarts       | qt              |
| l              | liters        | 0.26        | gallons      | gal             |
| m <sup>3</sup> | cubic meters  | 36.00       | cubic feet   | ft <sup>3</sup> |
| m <sup>3</sup> | cubic meters  | 1.30        | cubic yards  | yd <sup>3</sup> |

| Symbol                     | When You Know       | Multiply by       | To Find                | Symbol |
|----------------------------|---------------------|-------------------|------------------------|--------|
| <b>TEMPERATURE (exact)</b> |                     |                   |                        |        |
| °C                         | Celsius temperature | 9/5 (then add 32) | Fahrenheit temperature | °F     |

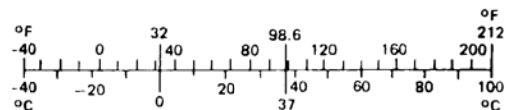


## Table of Contents

|                                    |    |
|------------------------------------|----|
| List of Figures.....               | v  |
| List of Tables .....               | vi |
| Executive Summary .....            | 1  |
| 1.0 Introduction.....              | 3  |
| 1.1 Background.....                | 3  |
| 1.2 Objectives .....               | 3  |
| 1.3 Approach.....                  | 4  |
| 1.4 Scope.....                     | 4  |
| 2.0 Test Description.....          | 7  |
| 2.1 Test Car.....                  | 7  |
| 2.2 Test Method .....              | 7  |
| 2.3 Instrumentation .....          | 11 |
| 2.4 Data Analysis.....             | 14 |
| 2.5 Summary of Results.....        | 17 |
| 2.6 Conclusions.....               | 35 |
| 3.0 Recommendations.....           | 37 |
| References.....                    | 39 |
| Appendix. Plots 1 through 22 ..... | 41 |
| Acronyms.....                      | 77 |



## List of Figures

|            |  |    |
|------------|--|----|
| Figure 1.  | VICX 1725 Tank Car Setup for Impact Test.....  | 7  |
| Figure 2.  | Force versus Time Trace.....   | 8  |
| Figure 3.  | FAST-High Tonnage Loop.....  | 10 |
| Figure 4.  | VICX Tank Car in FAST Train .....  | 7  |
| Figure 5.  | Accelerometer Locations–Overall Layout.....  | 11 |
| Figure 6.  | Accelerometer Locations–Details.....   | 12 |
| Figure 7.  | Strain Gage Locations.....   | 12 |
| Figure 8.  | Strain Gage Rosette 11, 12, and 13 and Strain Gage 19.....   | 13 |
| Figure 9.  | Data Acquisition Bricks Used During Impact Test .....  | 13 |
| Figure 10. | Examples of SRS Plot for Accelerometer 6.....  | 15 |
| Figure 11. | Measured (top) and Calculated LCF versus Time, April 15-16, 2003,<br>Test Car Near Front of Train .....                                  | 27 |
| Figure 12. | Measured LCF (top) and Calculated VCF versus Time, April 15-16, 2003,<br>Test Car Near Front of Train .....                              | 28 |
| Figure 13. | Measured (top) and Calculated LCF versus Time, April 14-15, 2003,<br>Test Car Near Rear of Train.....                                    | 29 |
| Figure 14. | Measured (top) and Calculated LCF versus Time During a 41-Second Time<br>Period, April 14-15, 2003, Test Car Near Rear of Train .....    | 29 |
| Figure 15. | Measured LCF (top) and Calculated VCF versus Time During a<br>41-Second Time Period, April 14-15, 2003, Test Car Near Rear of Train..... | 30 |
| Figure 16. | Measured LCF and Associated Longitudinal Acceleration at Location 6,<br>April 14-15, 2003.....   | 30 |
| Figure 17. | Measured LCF and Associated Longitudinal Acceleration at Location 18,<br>April 14-15, 2003.....  | 31 |
| Figure 18. | Typical Accelerometer Data Recorded April 20-22, 2003 .....  | 31 |
| Figure 19. | Cross Plot of Calculated LCF (y-axis) versus Measured LCF,<br>April 14-15, 2003.....   | 33 |
| Figure 20. | Cross Plot of Calculated LCF (y-axis) versus Measured LCF,<br>April 16-17, 2003.....   | 33 |
| Figure 21. | Cross Plot of Calculated LCF (y-axis) versus Measured LCF,<br>April 20-21, 2003.....   | 34 |
| Figure 22. | Cross Plot of Calculated LCF (y-axis) versus Measured LCF,<br>April 21-22, 2003.....   | 34 |

## List of Tables

|           |   |    |
|-----------|---|----|
| Table 1.  | Amplitude and Duration of Applied Vertical Force, Car Empty .....                             | 8  |
| Table 2.  | Amplitude and Duration of Applied Vertical Force, Car Loaded .....                            | 8  |
| Table 3.  | Summary of FAST Test .....  | 11 |
| Table 4.  | Peak LCF and VCF for Impact Sequence 1 .....  | 19 |
| Table 5.  | Peak LCF and VCF for Impact Sequence 2 .....  | 20 |
| Table 6.  | Peak LCF and VCF for Impact Sequence 3 .....  | 20 |
| Table 7.  | Peak LCF and VCF for Impact Sequence 4 .....  | 21 |
| Table 8.  | Estimated Linear Relationships, SRS Response versus Peak LCF–<br>Accelerometer Number 6 ..... | 24 |
| Table 9.  | Sample of Predicted Peak LCF Values Using SRS Data–<br>Accelerometer Number 6 .....           | 25 |
| Table 10. | Estimated Linear Relationships, SRS Response versus Peak VCF–<br>Accelerometer Number 6 ..... | 26 |



## EXECUTIVE SUMMARY

The Association of American Railroads (AAR), the Railway Supply Institute (formerly the Railway Progress Institute), the Federal Railroad Administration (FRA), and Transport Canada (TC) participated in a cooperative investigation of the operating environment of tank cars. Two technical groups cooperated on this project.

One of the groups, known as the Tank Car Operating Environment Task Force (TCOE-TF), evaluated a possible inverse relationship between the costs associated with the design/construction of tank cars and handling/operation of those cars. TCOE-TF would like to establish the credibility of a reasonably priced device that would collect reliable data for use in investigating the magnitude and direction of the largest forces encountered by tank cars during over-the-road service. The second group, the Stub Sill Working Group (SSWG), investigated the use of failure analysis to predict the proper inspection interval for stub sill tank cars. SSWG has a need to verify the full range of forces that tank cars experience in the railroad operating environment.

This investigation is part of an ongoing assessment of necessary components for a complete system optimization (i.e., to assure safety while minimizing total cost). Since the research needs are so closely related, the two groups agreed to work together to achieve both objectives.

The test program, designed with the requirements of these two groups in mind, was initially divided into three phases. Phase I, completed in April 2003, addressed the development and proof of a methodology to infer peak longitudinal coupler forces (LCF) and vertical coupler forces (VCF) from data collected using a relatively inexpensive set of transducers. Phase I also included the development of the inexpensive transducer and data collection package. Phase II is designed to follow Phase I and provide further data collection system development and further validation of a correlation process by eventually subjecting as many as five cars with the minimal transducer package to an uncontrolled over-the-road service environment. If Phases I and II are successful, Phase III will implement the installation of the inexpensive transducer packages on a larger number of tank cars to collect a more comprehensive set of environment data. This report addresses the results of the following testing that was completed under Phase I:

1. A series of controlled, car-to-car impact tests while recording acceleration versus time and strain versus time data from transducers mounted at numerous locations on the tank car. LCF was also recorded during each impact. The data from these tests was processed in an effort to determine if, under controlled impact conditions, a sufficient degree of correlation could be established between measured acceleration response and peak coupler forces (both longitudinal and vertical) or between strain output and peak coupler forces. The acceleration response versus coupler force correlation was analyzed using two methods:
  - Coupler force (longitudinal and vertical) versus peak acceleration values.
  - LCF and VCF versus shock response spectrum (SRS) curves generated from the peak acceleration values.

2. A series of tests applying upward vertical forces to the end of the tank car while recording the acceleration and strain output from the set of transducers. The vertical forces were designed to simulate the VCFs produced during over-the-road operations. Again, the data from these tests was processed in an effort to determine if, under controlled conditions, a degree of correlation could be established between measured vertical acceleration response and peak coupler forces (both longitudinal and vertical) or between strain output and peak coupler forces.
3. The final task of Phase I was to operate the test car in a train to record similar accelerometer and strain gage responses while the instrumented tank car was used in conditions more closely approximating over-the-road service. It was intended that completion of this task would meet the following objectives:
  - Confirm that relationships between strain gage or accelerometer output and peak coupler force can also be established for the lower magnitude coupler forces produced by normal train action. The results of the impact tests had allowed the study of these relationships for peak compressive forces greater than 250,000-300,000 pounds. It had also established the validity of such relationships for both tensile and compressive forces with magnitudes from near zero to 250,000-300,000 pounds.
  - Develop and prove the reliability of a power generation system (in a relatively controlled environment) that can provide consistent, long-term power for the onboard data acquisition hardware while being hidden from casual observation.

The results of Phase I testing have shown that strain values from gages strategically mounted to the stub sill can be used to calculate the magnitude of VCFs and LCFs during standard over-the-road operations, as well as during yard impact events. The results also indicate this as the preferred method for calculating coupler forces to be used in fatigue life predictions or damage tolerance analysis. The results also show that it is definitely possible to use SRS data to calculate or predict peak LCFs and VCFs occurring as a result of car-to-car impacts. This method, however, is most effectively used for impact events resulting in LCFs above 400,000-500,000 pounds. The preferred location for accelerometers to be used in this prediction process is near the longitudinal center of the car attached to the top of the tank structure. Accelerometers alone, however, are not suitable for the prediction of LCFs and VCFs that result from normal over-the-road operations.

## **1.0 Introduction**

### **1.1 Background**

AAR, the Railway Supply Institute (formerly the Railway Progress Institute), FRA, and TC funded a cooperative investigation of the operating environment of tank cars. AAR subsidiary Transportation Technology Center, Inc. (TTCI) conducted this evaluation at FRA's Transportation Technology Center (TTC), Pueblo, CO.

Two technical groups cooperated on this project. One of the groups, known as TCOE-TF, evaluated a possible inverse relationship between the costs associated with the design/construction of tank cars and handling/operation of those cars. The TCOE-TF would like to establish the credibility of a reasonably priced device that would collect reliable data that could be used to investigate the frequency and magnitude of the largest forces encountered by tank cars during over-the-road service. The second group, SSWG, investigated the use of failure or durability analysis to predict the proper inspection interval for stub sill tank cars. SSWG has a need to verify the full range of forces that tank cars experience in the railroad operating environment.

This investigation is part of an ongoing assessment of what is necessary for a complete system optimization (i.e., to assure safety while minimizing total cost). Since the research needs are so closely related, the two groups have agreed to work together to achieve both objectives.

### **1.2 Objectives**

This report addresses the results of Phase I of a possible three-phase program. The testing in Phase I had the following objectives:

1. Study, through controlled, on-track testing, the feasibility of estimating or calculating coupler force using only car-mounted accelerometer or strain readings. The body of data must show that such a correlation is possible with an acceptable degree of accuracy. The acceleration versus coupler force correlation will be tested using a minimum of two methods:
  - Coupler force (longitudinal and vertical) versus peak acceleration values.
  - LCF and VCF versus SRS curves generated from the peak acceleration values.
2. If the initial testing conducted in Phase I indicated a good possibility that reliable relationships can be defined, effort would then be directed toward the assembly and demonstration of an acquisition system that could be used to efficiently and reliably record and broadcast, or download, such data from one or more cars placed in extended over-the-road service.

### 1.3 Approach

The test program, designed with the requirements of these two groups in mind, was initially divided into three phases. Phase I, completed in April 2003, addressed the development and proof of a methodology to infer peak LCFs and VCFs from data collected using a relatively inexpensive set of transducers. Phase I also included the development of the inexpensive transducer and data collection package. This report discusses the results of Phase I. Phase II is designed to provide further data collection system development and further validation of a correlation process by eventually subjecting as many as five cars with the minimal transducer package to an uncontrolled over-the-road service environment. If Phases I and II are successful, Phase III will implement the installation of the inexpensive transducer packages on a possibly much larger number of tank cars to collect a more comprehensive set of environment data. The objectives of Phase I to successfully relate accelerometer or strain gage output to coupler force were attempted using the following methods:

- Peak coupler force (longitudinal and vertical) versus peak output from accelerometers.
- Peak LCF and VCF versus SRS curves generated from the peak acceleration values.
- LCF and VCF versus output from a small number of strategically placed strain gages.

Before a large-scale test program was undertaken, an initial or exploratory test was conducted in an effort to better establish some of the important parameters to be used in the subsequent Phase I testing, as well as gain more confidence in the validity of the correlation between acceleration data and coupler force or strain data and coupler force. During the initial testing, a large number of accelerometers and strain gages were placed at widespread locations on the tank car. This was done because of the uncertainty of which locations would provide the best correlation with coupler force. The primary focus, therefore, was to eventually eliminate most of the transducers and establish only a small number of accelerometer or strain measurement locations that could provide the best correlation. This step was vital if system complexity and expense were to be minimized.

### 1.4 Scope

Phase I testing included the controlled application of vertical force pulses to the end of the stub sill with the tank car empty and fully loaded, as well as the following impact sequences:

- *Sequence 1:* Empty, instrumented tank car rolling into loaded stationary 3-car anvil string at velocities of 2, 4, 6, and 8 mph. The hand and air brakes were set on the two stationary cars farthest from the impact.
- *Sequence 2:* Loaded, instrumented tank car rolling into loaded stationary 3-car anvil string at velocities of 2, 4, 6, and 8 mph. The hand and air brakes were set on the two stationary cars farthest from the impact.
- *Sequence 3:* Loaded, hopper car rolling into instrumented, loaded stationary tank car at velocities of 2, 4, 6, and 7 mph. The tank car was not coupled to any other cars. The hand and air brakes were set on the stationary tank car.
- *Sequence 4:* Loaded, hopper car rolling into instrumented, loaded stationary tank car at velocities of 2, 4, 6, and 6.5 mph. The tank car was the lead car in a loaded five-car anvil string. The hand and air brakes were set on all of the stationary cars.

The final task of Phase I was to record similar accelerometer and strain gage responses while the instrumented tank car was used in over-the-road conditions. The completion of this would meet the following objectives:

- Confirm that relationships between strain gage or accelerometer output and peak coupler force can also be established for the lower magnitude coupler forces produced by normal train action. The results of the impact tests have allowed the study of these relationships for peak compressive forces greater than about 250,000-300,000 pounds. It is important to establish the validity of such relationships for both tensile and compressive forces with magnitudes from near zero to 250,000-300,000 pounds.
- Develop and prove the reliability of a power generation system (again in a controlled environment) that can provide consistent, long-term power for the onboard data acquisition hardware while being hidden from casual observation.



## 2.0 Test Description

### 2.1 Test Car

The tank car used in this study had the following characteristics:

- Manufacturer: American Car and Foundry (pictured in Figure 1)
- Car number: VICX 1725 (Certificate of Construction No. 21826)
- Empty weight: 75,400 pounds
- Maximum weight with payload of water: 262,272 pounds
- Tank design: ACF 4-B-7188, 22,500-gallon capacity
- Underframe design: ACF 4-B-7190 stub sill
- Coupler design: 6 1/4x8 Type E, Top and Bottom Shelf
- Draft gear design: Cardwell Westinghouse Mark 50 all-steel design (friction wedges plus springs)



Figure 1. VICX 1725 Tank Car Setup for Impact Test

### 2.2 Test Method

#### 2.2.1 *Low Frequency Vertical Forces Applied to Sill, Simulating In-Train Forces*

A vertical force pulse was applied to the end of the sill in the upward direction. This test was conducted with the car both empty and loaded with water. A hydraulic cylinder created the force pulse, and the shape of this pulse was essentially one-half of a sine wave. Tables 1 and 2 provide the duration of the half-sine wave shapes, as well as the peak amplitude of the vertical force applied. Figure 2 shows an illustration of a typical force versus time trace and the term “ $t/2$ .” Each test condition was repeated at least three times.

**Table 1. Amplitude and Duration of Applied Vertical Force, Car Empty**

| Peak Force (pounds) | t/2 (seconds) |
|---------------------|---------------|
| 10,000              | .25           |
| 10,000              | .50           |
| 10,000              | 1.0           |
| 15,000              | .25           |
| 15,000              | .50           |
| 15,000              | 1.0           |
| 20,000              | .25           |
| 20,000              | .50           |
| 20,000              | 1.0           |

**Table 2. Amplitude and Duration of Applied Vertical Force, Car Loaded**

| Peak Force (pounds) | t/2 (seconds) |
|---------------------|---------------|
| 21,800              | .25           |
| 30,900              | .50           |
| 35,800              | .25           |
| 51,600              | .50           |

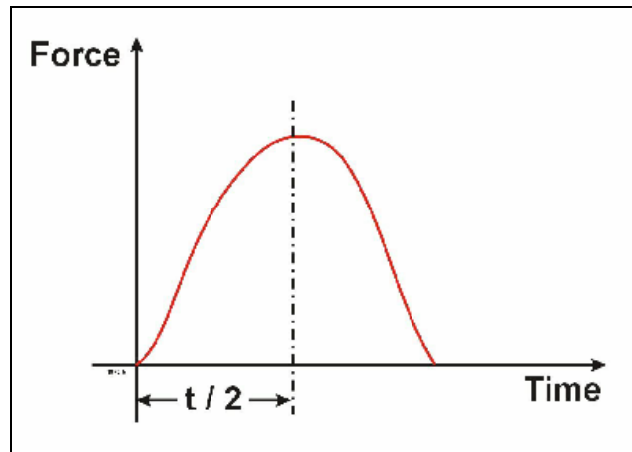


**Figure 2. Force versus Time Trace**

### **2.2.2 Controlled Impact Testing**

The following summarizes the conditions for impact sequences 1 through 4. For all sequences, the impacts occurred at the A-end of the instrumented tank car.

- *Impact Sequence 1:* Empty, instrumented tank car rolling into stationary, loaded 3-car anvil string at velocities of 2, 4, 6, and 8 mph. The air and hand brakes were set on the two anvil string cars farthest from impact. The anvil group of cars remained essentially stationary for all but the 8-mph impacts. During the 8-mph tests, 3 to 5 inches of



movement upon impact occurred. The height of the tank car coupler was approximately 1.5 inches higher than that of the mating stationary cars.

- *Impact Sequence 2:* Loaded, instrumented tank car rolling into loaded stationary 3-car anvil string at velocities of 2, 4, 6, and 8 mph. The air and hand brakes were set on the two anvil string cars farthest from impact. Movement of the anvil string after impact ranged from about 12 inches at 2 mph to over 40 inches at 8 mph. The heights of the couplers on the tank car and the mating anvil car were within .25 inch of each other.
- *Impact Sequence 3:* Loaded, hopper car rolling into instrumented, loaded stationary tank car at velocities of 2, 4, 6, and 7 mph. The tank car was not coupled with any other cars. The gross weight of the hammer car was 261,764 pounds. The air and hand brakes were set on the tank car. Tank car movement after impact ranged from about 2 feet at 2 mph to about 20 feet at 7 mph. A maximum impact velocity of 7 mph was used in order to limit the maximum LCF to around 1.25 million pounds. Coupler height again matched to within 0.25 inch.
- *Impact Sequence 4:* Loaded, hopper car rolling into instrumented, loaded stationary tank car at velocities of 2, 4, 6, and 6.5 mph. This was the same hopper car used in sequence 3. The tank car was the lead car in a loaded five-car anvil string. The air and hand brakes were set on all cars in the anvil string. Tank car movement after impact ranged from about 2 inches at 2 mph to about 17 inches at 6.5 mph. A maximum impact velocity of 6.5 mph was used to limit the maximum LCF to around 1.25 million pounds. Coupler height again matched to within .25 inch.

### ***2.2.3 Testing at TTC's Facility for Accelerated Service Testing (FAST)***

The High Tonnage Loop (HTL) at FAST is a 2.7-mile closed track consisting of a main loop and a bypass loop (see Figure 3). This track is used primarily for heavy axle load and bridge testing and research. The loaded instrumented tank car was included in the FAST train as it proceeded with its normal operating schedule. Some of the basic parameters of this loop include the following:

- Each lap includes up to four 5-degree curved sections (Sections 3, 7, 31, or 38) and one 6-degree curve (Section 25).
- During each main loop lap, the train travels over three turnouts (Sections 25, 27, and 35). During each bypass loop lap, the train travels through two turnouts (Sections 27 and 35), over one turnout (Section 23), and over three more turnout frogs in Section 36.
- Normal operating speed is approximately 40 mph.
- A number of minor grades are included in the HTL, ranging from 0.4 to 0.9 percent.
- During the test period, the train included 75-78 cars with the travel direction of both clockwise and counterclockwise (see Table A-1 in the appendix).

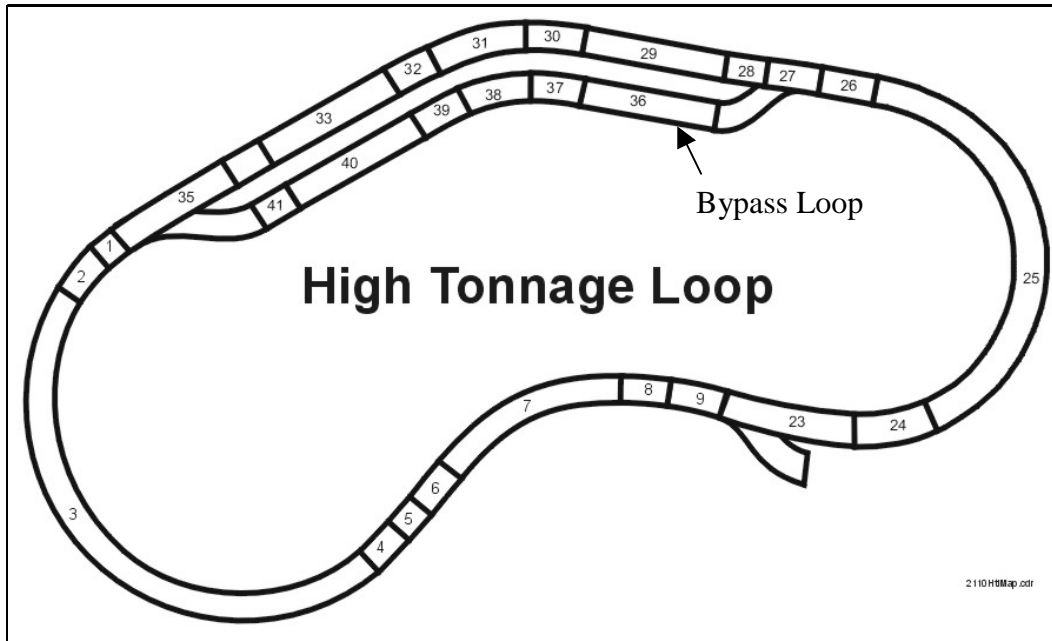


**Figure 3. HTL at FAST**

The loaded instrumented tank car was allowed to run in the FAST train for 13 nights from March 23, 2003, to April 22, 2003. The tank car was near the front of the train for part of the test period and near the rear of the train for the remainder (Figure 4). Table 3 briefly summarizes the completed testing. Table A-1 in the appendix provides additional details.



**Figure 4. VICX Tank Car in Test Train at FAST**

**Table 3. Summary of Test Results at FAST**

| Dates           | Laps Completed | Hours of Running | Approximate Miles Traveled |
|-----------------|----------------|------------------|----------------------------|
| 3/23/03–3/24/03 | 129            | 8.7              | 398                        |
| 3/24/03–3/25/03 | 86             | 6.0              | 232                        |
| 3/25/03–3/26/03 | 124            | 8.6              | 335                        |
| 3/26/03–3/27/03 | 134            | 8.9              | 362                        |
| 3/30/03–3/31/03 | 127            | 8.9              | 343                        |
| 3/31/03–4/1/03  | 130            | 8.8              | 351                        |
| 4/7/03–4/8/03   | 135            | 9.3              | 365                        |
| 4/13/03–4/14/03 | 122            | 8.7              | 329                        |
| 4/14/03–4/15/03 | 135            | 8.8              | 365                        |
| 4/15/03–4/16/03 | 129            | 8.9              | 348                        |
| 4/16/03–4/17/03 | 90             | 6.3              | 243                        |
| 4/20/03–4/21/03 | 71             | 5.0              | 192                        |
| 4/21/03–4/22/03 | 130            | 8.9              | 351                        |
| Totals          | 1,542          | 159.8            | 4,169                      |

### 2.3 Instrumentation

Originally, 38 single accelerometers and 22 strain gages were installed on the car. Figures 5, 6, and 7 show the locations of these transducers. Figure 8 shows strain gage locations 11, 12, and 13. Figure 9 shows the installation of the data acquisition hardware on the tank car. For each accelerometer location shown, except for numbers 11 and 12, one vertical axis and one longitudinal axis accelerometer are installed. At locations 11 and 12, only longitudinal accelerometers were installed. The accelerometers used at the center and impact end (A-end) of the car had a capacity of  $\pm 100$  g, while those used on the end of the car opposite the impact had a capacity  $\pm 50$  g. An instrumented coupler was also installed at the car's impact end to record the LCF.

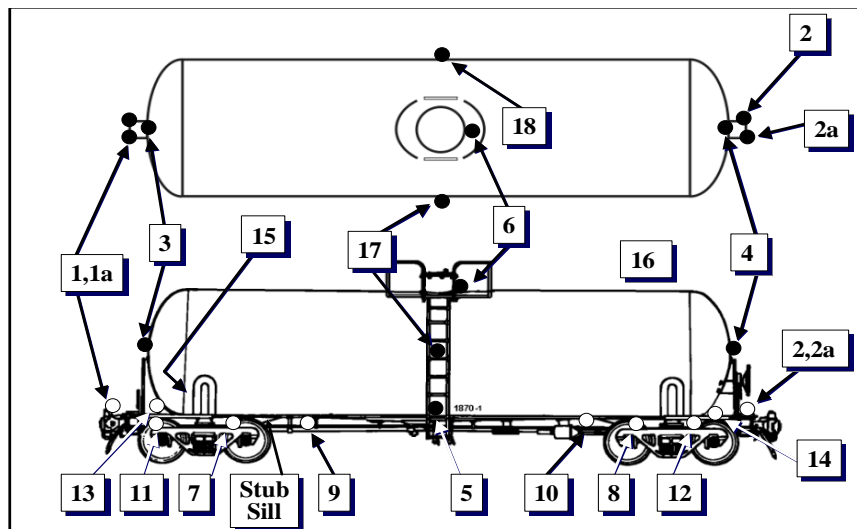


**Figure 5. Accelerometer Locations—Overall Layout**

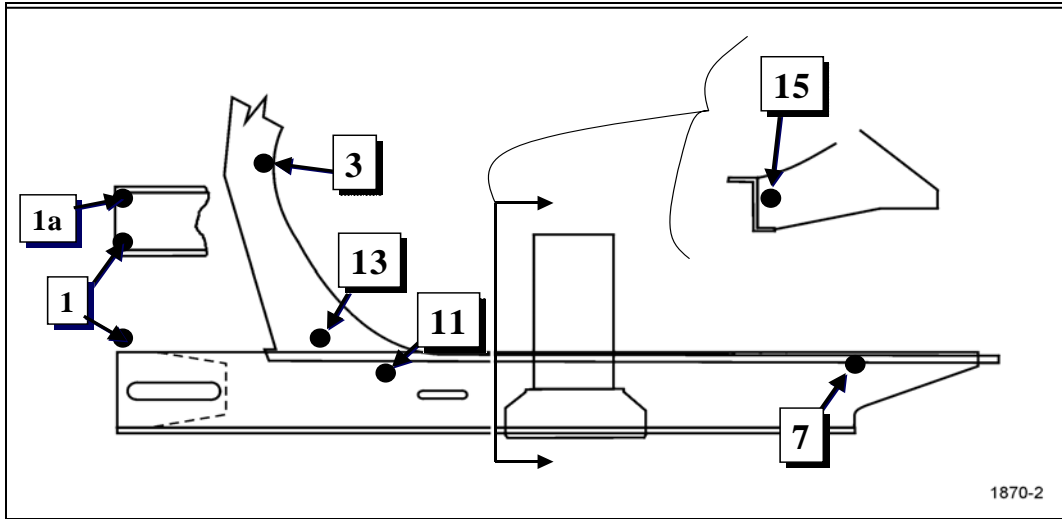


Figure 6. Accelerometer Locations—Details

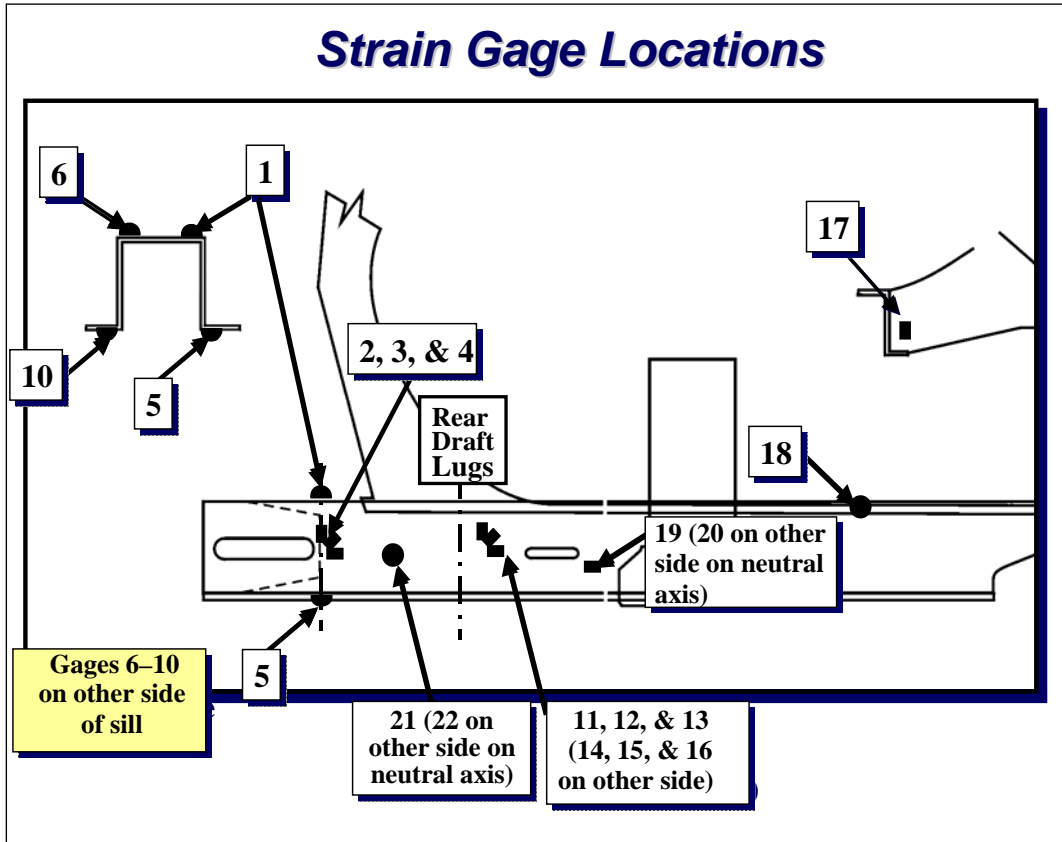
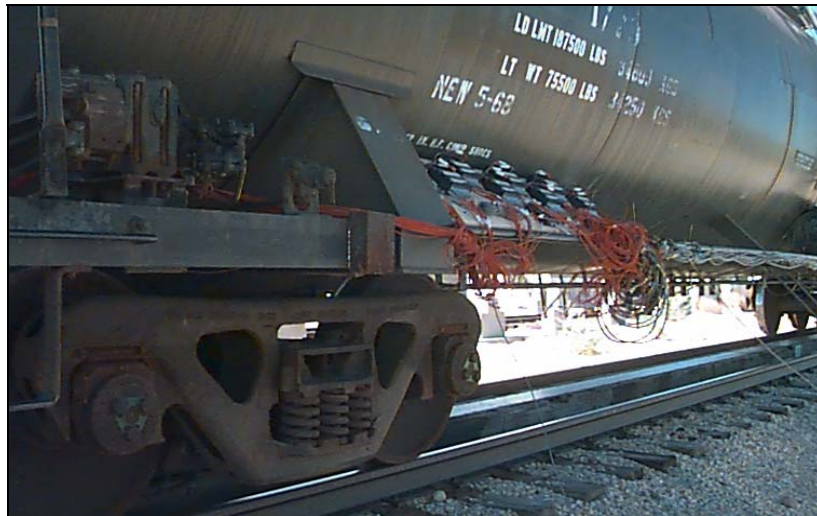


Figure 7. Strain Gage Locations



**Figure 8. Strain Gage Rosette 11, 12, and 13 and Strain Gage 19**



**Figure 9. Data Acquisition Bricks Used During Impact Test**

Before any testing began, a quasi-static calibration procedure was performed to relate strain gage response to LCF and VCF. This calibration procedure involved two tasks. During the first, compressive and tensile loads of up to 300,000 pounds were applied to the instrumented coupler. Response from all of the strain gages was recorded, and relationships of coupler force versus strain were established for each gage. For the second task, vertical forces of up to 20,000 pounds upward (positive) to 20,000 pounds downward (negative) were applied to the end of the stub sill on the A-end of the car. A calibrated load cell, installed between a hydraulic cylinder and the sill, measured these forces. Again, the response from each strain gage was recorded as the forces were applied, and relationships of coupler forces versus strain were established for each gage.

During the controlled, dynamic vertical force test, data was recorded for all strain gages but only for the following accelerometers: 1 vertical and longitudinal, 1A vertical and longitudinal, 11 longitudinal, 13 longitudinal, 3 vertical and longitudinal, 15 vertical and longitudinal, 5 vertical and longitudinal, and 6 vertical and longitudinal.

During the first impact test (Sequence 1), the output from all transducers was recorded, and the data was processed. Decisions about which longitudinal and vertical accelerometer locations to study in detail were based on the shape of the acceleration versus time curve and the characteristics of the associated Fast Fourier Transfer (FFT) plots. If an acceleration versus time plot showed a distinct low frequency displacement, the associated FFT plot also indicated very little high frequency response. Longitudinal accelerometer locations 2, 2A, 5, 6, 8, 9, 12, 11, 13, 14, 16, 17, and 18 and vertical accelerometer locations 1, 1A, 2, 2A, 5, 6, 14, and 18 generally exhibited this type of response. Of the transducers listed above, the output of locations 18, 9, 6, and 5 demonstrated the best correlation between peak longitudinal acceleration and peak LCF. As a result, for all subsequent impact tests, data was recorded for all transducers, but that data was processed only for this most significant subset. The following lists those transducers:

- Strain Gages: Numbers 21-22, 8, 19, and 20
- Vertical Accelerometers: Numbers 1, 1A, 2, 2A, 5, 6, 9, 10, and 18
- Longitudinal Accelerometers: Numbers 1, 1A, 2, 2A, 5, 6, 9, 10, and 18

During testing at FAST, data was recorded and stored for 10 accelerometers, 4 strain gages, and 1 instrumented coupler. Examination of the data from all of the previous impact sequences revealed which transducers provided responses that could best be correlated to LCF and VCF. This analysis helped determine which of the transducers would be used for the FAST test. These transducers are listed below:

- Strain Gages: Numbers 21-22, 19, and 20
- Vertical Accelerometers: Numbers 5, 6, 9, 10, and 18
- Longitudinal Accelerometers: Numbers 5, 6, 9, 10, and 18

Data was reduced and examined only for the accelerometer locations of primary interest. Those locations were Number 6 vertical and longitudinal and Number 18 vertical and longitudinal, as well as the strain gages and instrumented coupler. These four accelerometers are near the center of the car and were proven by impact test data to be the most useful for the estimation of peak VCFs and LCFs. The strain gages used (8, 19, 20, and 21-22) are all located on the A-end stub sill (Figure 7).

## **2.4 Data Analysis**

### **2.4.1 *Impact and Controlled Vertical Force Test***

- Data for all tests was collected at a rate of 5,000 samples per second. The data collection system was activated approximately 0.5 seconds before impact and collected data for a duration of 3 seconds.
- The data collected from the transducers listed above was in the form of acceleration versus time and strain versus time.
- VCF was calculated using the strain output from strain gages 21 and 22 that were mounted on the neutral axis of the stub sill. These two shear gages were connected in a half-bridge circuit so that they were sensitive primarily to vertical force applied to the stub sill. The relationship between the output from strain gages 21 and 22 and vertical force had been established during static and dynamic calibration tests performed before any impact tests and is shown in the following equation:

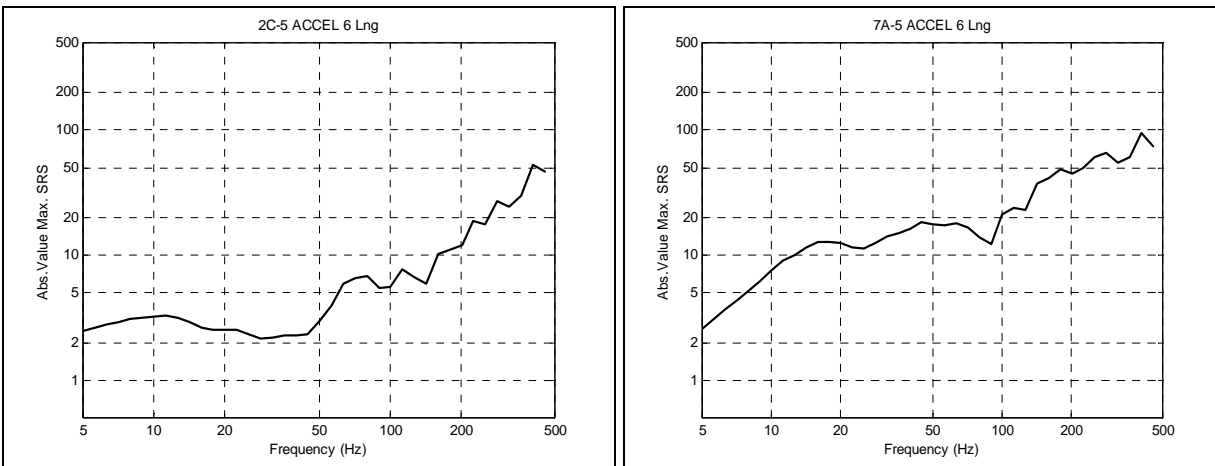
$$\text{Calculated VCF (kip)} = -0.16 \times (\text{Gage 21/22 microstrain} + 0.5 \times \text{Coupler Force})$$

Where gage 21/22 microstrain is the output from strain gages 21/22 and coupler force is the longitudinal force output from the instrumented coupler.

Since the available instrumented couplers only measure longitudinal force, vertical force must be derived in this manner.

- The data from the transducers listed above was used to evaluate correlations between the following measurements:
  - Peak strain from strain gages 19 and 20 versus peak LCF
  - Peak longitudinal acceleration versus peak LCF
  - Peak vertical acceleration versus peak VCF
  - Maximum longitudinal SRS versus peak LCF
  - Maximum vertical SRS versus peak VCF
  - Average longitudinal SRS values over 5-50 Hz versus peak LCF
  - Average vertical SRS values over 5-50 Hz versus peak VCF
  - Average longitudinal SRS values over 10-100 Hz versus peak LCF
  - Average vertical SRS values over 10-100 Hz versus peak VCF

The correlation of average SRS values and peak LCF and VCF values has proven to be the best one for the estimation of coupler forces using accelerometer output. This is in large part due to the considerable amount of high frequency content in the acceleration versus time traces produced by the impact forces. SRS analysis does not describe the shock itself but its influence on a set of idealized, single-degree of freedom (SDOF) mechanical systems. To convert acceleration versus time data to SRS, the actual acceleration response (acceleration at each time step T) is applied to a number of SDOF systems. Each SDOF system has a unique natural frequency. A maximum response value is obtained for each of these SDOF systems. A SRS plot is then created when these maximum response values are plotted against frequency. An average SRS value over the frequency range 5 to 50 Hz would just be the average of all of the individual response values between 5 and 50 Hz. Figures 10(a) and 10(b) are examples of SRS plots for accelerometer 6 at impact velocities of 2 and 7 mph, respectively.



10(a)

10(b)

Figure 10. Examples of SRS Plot for Accelerometer 6

### 2.4.2 Testing at FAST

Data was recorded from transducers and one instrumented coupler on the VICX 1725 tank car during 13 nights of operation on the track at FAST between March 23, 2003, and April 22, 2003. The FAST train operated 4 nights a week during this time period, but problems with the data acquisition system limited the nights during which data could be recorded. The problems encountered during the first 8 nights of testing were as follows:

- Frequent computer shutdown and reboot due to vibration and data throughput limitations. The device that allows the computer to automatically reboot did not provide enough time for a scan disk operation.
- Excessive signal noise and spikes due primarily to poor analogue-to-digital card connection.
- Large zero load and electronic offsets in the signal due to a software problem.

Of the 13 nights in which attempts were made to record data, useful information was obtained from 9 nights. For 5 of these nights, the test car was located 6 cars from the end of the train. For the remainder of the nights, the test car was located four to eight cars from the last locomotive. Three to eight hours of data were recorded each night.

All data channels were sampled at either 4,096 samples per second (for 9 nights) or 2,048 samples per second. The sample rate was reduced by half for 4 of the nights in an effort to determine if that rate was the cause of problems with the data acquisition computer.

The data was processed using the following steps:

- The full night of data for each channel was inspected to determine if any of the specified thresholds had been exceeded. The Matlab™ signal processing toolbox was used to perform this task. The thresholds were set as follows:
  - Accelerometer 5 longitudinal, accelerometer 6 longitudinal, or accelerometer 18 longitudinal:  $> 5 \text{ g}$  or  $< -5 \text{ g}$ .
  - Strain gages 21/22:  $> 100 \text{ microstrain}$  or  $< -100 \text{ microstrain}$ .
  - Instrumented coupler:  $> 80,000 \text{ pounds positive (buff)}$  or  $< 140,000 \text{ pounds negative (draft)}$ .

These values were chosen as a first cut to allow the isolation of the most meaningful data and to somewhat reduce the size of the data analysis task for this short test.

- Data files were created and stored in 45-second increments. Using a Matlab macro, all of the 45-second files that demonstrated values exceeding any of the thresholds were tagged for subsequent inspection. Again using a Matlab macro, these files were then concatenated in a way that allowed the data to be combined into one large file. This allowed inspection of all data at one time.
- Based primarily on the longitudinal coupler values observed in this set of data, a subset of files was then selected for further, closer examination. The result was that data recorded over the entire night had been reduced to the 1 to 2 hours of data that was of the most interest.
- Initially, the data receiving this closer examination was from the following channels: instrumented coupler, strain gage 21/22, strain gage 19, and strain gage 20. This reduced set



of data was converted to a format that could be used with computer software developed by nCode International called Fatimas™. During the conversion process, the coupler force and strain gage data was decimated from the original sample rate (either 4,096 or 2,048 samples/second) to 256 samples per second. nCode Fatimas is a fatigue analysis software but also has significant capabilities to process, condition, and evaluate large amounts of data. This software can be used to digitally filter data, remove obvious spikes, concatenate short files into longer files, and perform mathematical operations using the data from separate files.

- Within Fatimas, the selected strain gage and coupler force files were subjected to spike removal if required and filtered with a 30 Hz low pass filter. The strain gage and coupler force data was then used in the following sequence to compute LCF and VCF:

$$\text{Calculated VCF (kip)} = -0.16 \times (\text{Gage 21/22 Microstrain} + 0.5 \times \text{Coupler Force})$$

$$\text{Calculated LCF (kip)} = -1.24 \times (\text{Gages 19 and 20 Microstrain} - 1.36 \times \text{Calculated VCF})$$

Where gage 21/22 microstrain is the output from strain gages 21/22, coupler force is the output from the instrumented coupler (in thousands of pounds or kips), and gages 19 and 20 microstrain is the average of the output from gages 19 and 20.

Positive LCF values are compressive, and positive VCF values are upward. These relationships were established using the data collected during the static load calibration tests conducted in September 2000 (before the initial impact testing).

- Finally, acceleration versus time data collected during the nights of April 14-15, April 15-16, and April 20-21 was inspected. This set of data was chosen based on the magnitude of the coupler forces recorded during these time periods. Only the data from accelerometers 18 longitudinal, 18 vertical, 6 longitudinal, and 6 vertical were inspected. SRS analysis was performed for a total of 9 events where either compressive or tensile coupler forces of over 150,000 pounds were measured. The average SRS response over frequencies of 5-50 Hz and 10-100 Hz were then compared to peak LCF values recorded during the same event.

## **2.5 Summary of Results**

### **2.5.1 Controlled Vertical Force Test**

#### **2.5.1.1 Strain Gage Response**

- Strain gages 8 and 21-22 were not the most responsive to vertical force input, but they were the most responsive gages that were least affected by longitudinal force input. The sensitivity of gage 8 was approximately 0.00431 microstrain per pound of vertical force. The sensitivity of gages 21-22 was approximately 0.00633 microstrain per pound of vertical force (see Plot A-1 in the appendix).
- Strain response for all gages was essentially linear with increasing vertical force.
- The rate at which load was applied made little significant difference in the relationship between strain and applied peak load for a particular gage.
- Standard deviation values were calculated based on the three repetitions at each test condition. These values indicated that the repeatability of the response of all strain gages was essentially equivalent.

### 2.5.1.2 Accelerometer Response

- No detectable output existed from any of the accelerometers until a peak load of at least 13,000-15,000 pounds was applied.
- At a pulse duration of 2 seconds, a peak force amplitude of at least 20,000 pounds was required to generate any detectible acceleration response. Plots A-2 and A-3 in the appendix show estimated linear relationships between peak acceleration and vertical force amplitude for vertical accelerometers 1 and 1A. Using these plots, the peak vertical force can be roughly estimated:
  - From accelerometer 1:
    - 8,354.3 × (peak accel.) + 11,977 for a 0.5-second pulse duration
    - 11,162 × (peak accel.) + 11,940 for a 1.0-second pulse duration
  - From accelerometer 1A:
    - 12,984 × (peak accel.) + 10,894 for a 0.5-second pulse duration
    - 29,583 × (peak accel.) + 7,433.8 for a 1.0-second pulse duration

As an example, at a force pulse duration of 0.5 second, a peak 0.5 g output from Accelerometer 1 would predict a peak vertical force of about 16,200 pounds while a similar output value from accelerometer 1A would yield a peak vertical force of 17,400 pounds. If the same 0.5 g output came during an event of about 1.0 second in duration, the accelerometer 1 relationship would yield a peak vertical force of about 17,500 pounds while the accelerometer 1A relationship would result in an estimate of about 22,200 pounds.

- Due to the scatter of this data, these are only rough estimations. At a pulse duration of 2 seconds, a peak force amplitude of at least 20,000 pounds was required to generate any detectible acceleration response.
- Responses were recorded for both longitudinal and vertical accelerometers. The most responsive vertical accelerometers were at the 1 and 1A positions while the most responsive longitudinal accelerometer was at the 3 position.

## 2.5.2 Controlled Impact Tests

### 2.5.2.1 Peak Coupler Forces versus Impact Velocity

Plot A-6 in the appendix shows two very significant relationships between impact velocity and peak LCF. For all loaded car impacts (Sequences 2 through 4), the peak LCF versus impact velocity relationship is essentially horizontal for impact velocities between 2 and 4 mph. Peak LCF only varies between about 350,000 and 500,000 pounds for impact events in this velocity range. As impact velocities increase to 6 and 8 mph, however, suddenly a very steep slope with peak LCF values increasing significantly exists. This is likely an indication that the draft gear is performing as designed. At velocities up to about 5 mph, movement occurs within the draft gear, and the friction wedges and internal springs produce the required reaction forces. At velocities above 5 mph, however, the draft gear has likely reached its deflection capacity, resulting in a sudden rise in the force transmitted from the gear to the car structure. The data indicates that for this loaded car, impact velocity could be used to estimate peak LCF in the following manner:

- For velocities from 2-5 mph, peak LCF = 350,000 to 500,000 pounds
- For velocities above 5 mph, peak LCF = 440,000 × (velocity - 5) + 440,000

The last 440,000 value in this equation is the point on the y-(force) axis at which the function intersects the 5-mph x value.

Plot A-6 also shows that the peak LCF versus impact velocity relationship for Sequence 1 (empty car) again is significantly different from the loaded car relationships. The Sequence 1 data indicates a more constant relationship between velocity and peak LCF with no significant change in slope between 5 and 6 mph. This could indicate that the characteristics of the draft gear changed between the Sequence 1 and Sequence 2 impacts or that due to the lower kinetic energy levels during Sequence 1, the draft gear never reached its deflection limits.

Plots A-7 through A-10 in the appendix show that throughout all of the impact sequences, a relatively good relationship exists between measured peak LCF and calculated peak VCF. The weakest correlation was observed from the data recorded during Impact Sequence 3 (single car-to-single car). Generally, the peak VCF can be estimated by using the following function:

$$\text{Peak VCF} = (0.11 \text{ to } 0.12) \times (\text{Peak LCF})$$

In all impact cases, the peak VCF was in the upward (away from track) direction.

Tables 4-7 give a summary of the recorded peak LCF and calculated peak VCF values for all four impact sequences. These tables illustrate that the coupler forces at a given impact velocity were about 30 to 40 percent greater during the loaded car impacts (Sequences 2-4) than during the empty car tests. They also reveal that Sequence 4 generally produced the highest coupler forces per mph of impact velocity.

**Table 4. Peak LCF and VCF for Impact Sequence 1**

| <b>Velocity at Impact<br/>(mph)</b> | <b>Measured Peak LCF<br/>(lbs)</b> | <b>Calculated Peak VCF<br/>(lbs)</b> |
|-------------------------------------|------------------------------------|--------------------------------------|
| 2.5                                 | 374,743                            | 51,320                               |
| 2.0                                 | 254,972                            | 38,060                               |
| 3.0                                 | 242,145                            | 34,790                               |
| 4.5                                 | 444,059                            | 52,900                               |
| 5.0                                 | 541,853                            | 70,230                               |
| 3.8                                 | 593,849                            | 63,700                               |
| 5.9                                 | 618,556                            | 55,920                               |
| 6.1                                 | 582,814                            | 59,960                               |
| 6.2                                 | 808,052                            | 98,490                               |
| 8.0                                 | 1,051,530                          | 116,680                              |
| 7.8                                 | 970,455                            | 105,310                              |
| 7.9                                 | 1,003,544                          | 126,950                              |

**Table 5. Peak LCF and VCF for Impact Sequence 2**

| <b>Velocity at Impact<br/>(mph)</b> | <b>Measured Peak LCF<br/>(lbs)</b> | <b>Calculated Peak VCF<br/>(lbs)</b> |
|-------------------------------------|------------------------------------|--------------------------------------|
| 3.0                                 | 469,000                            | 44,600                               |
| 2.9                                 | 495,000                            | 53,500                               |
| 2.6                                 | 500,000                            | 50,600                               |
| 2.4                                 | 445,500                            | 39,600                               |
| 2.4                                 | 408,000                            | 52,500                               |
| 3.3                                 | 479,600                            | 36,800                               |
| 4.2                                 | 495,000                            | 58,200                               |
| 4.1                                 | 442,000                            | 55,340                               |
| 4.1                                 | 485,700                            | 44,810                               |
| 4.2                                 | 404,400                            | 44,700                               |
| 6.1                                 | 1,108,000                          | 118,080                              |
| 6.1                                 | 1,057,000                          | 115,040                              |
| 6.1                                 | 1,050,000                          | 113,790                              |
| 7.4                                 | 1,346,600                          | 149,400                              |
| 7.2                                 | 1,275,900                          | 142,600                              |
| 7.5                                 | 1,374,600                          | 149,400                              |

**Table 6. Peak LCF and VCF for Impact Sequence 3**

| <b>Velocity at Impact<br/>(mph)</b> | <b>Measured Peak LCF<br/>(lbs)</b> | <b>Calculated Peak VCF<br/>(lbs)</b> |
|-------------------------------------|------------------------------------|--------------------------------------|
| 3.0                                 | 338,880                            | 46,300                               |
| 2.8                                 | 408,110                            | 52,000                               |
| 2.7                                 | 419,870                            | 53,900                               |
| 2.4                                 | 420,070                            | 71,000                               |
| 2.2                                 | 377,970                            | 32,200                               |
| 2.3                                 | 373,140                            | 64,600                               |
| 4.2                                 | 380,720                            | 59,000                               |
| 4.1                                 | 396,580                            | 57,000                               |
| 4.2                                 | 350,260                            | 71,700                               |
| 4.2                                 | 344,510                            | 54,700                               |
| 5.1                                 | 405,620                            | 44,400                               |
| 6.0                                 | 836,660                            | 133,000                              |
| 6.0                                 | 843,660                            | 85,000                               |
| 6.1                                 | 793,490                            | 72,000                               |
| 7.1                                 | 1,242,740                          | 137,800                              |
| 7.1                                 | 1,175,090                          | 141,700                              |
| 7.1                                 | 1,168,440                          | 127,100                              |

**Table 7. Peak LCF and VCF for Impact Sequence 4**

| <b>Velocity at Impact<br/>(mph)</b> | <b>Measured Peak LCF<br/>(lbs)</b> | <b>Calculated Peak VCF<br/>(lbs)</b> |
|-------------------------------------|------------------------------------|--------------------------------------|
| 2.4                                 | 399,520                            | 399,000                              |
| 2.2                                 | 369,360                            | 379,000                              |
| 2.2                                 | 418,040                            | 451,000                              |
| 2.2                                 | 392,030                            | 485,000                              |
| 4.1                                 | 529,760                            | 699,000                              |
| 4.0                                 | 396,480                            | 521,000                              |
| 4.1                                 | 415,790                            | 527,000                              |
| 5.0                                 | 443,980                            | 619,000                              |
| 6.0                                 | 1,134,080                          | 132,400                              |
| 6.1                                 | 1,111,210                          | 128,400                              |
| 6.0                                 | 1,091,080                          | 128,600                              |
| 6.4                                 | 1,235,730                          | 155,400                              |
| 6.9                                 | 1,333,100                          | 159,900                              |
| 5.8                                 | 1,023,790                          | 122,300                              |
| 6.3                                 | 1,185,110                          | 144,600                              |

#### *2.5.2.2 Strain Gage Response*

Strain gages at locations 15, 16, 19, and 20 proved to be the most consistent and most sensitive indicators of peak LCF. Of these four gages, the output of gage 20 proved to be the most consistent and sensitive.

The relationship between peak LCF and maximum strain from gage 20 was not a continuous linear relationship during Impact Sequence 1. Plot A-11 in the appendix shows that whether the strain versus peak LCF relationship is treated as a continuous or discontinuous function, an obvious change occurs in that relationship at coupler forces above about 600,000 pounds. Still, the relationship between peak strain and peak LCF at strain gage location 19 remains relatively consistent as peak LCF reaches maximum levels.

The fact that a significant difference existed between the strain response of gages at similar locations on either side of the sill (gage 19 versus gage 20) may indicate that, as the peak coupler forces reached levels above 600,000 pounds, the longitudinal forces into the rear draft lugs were not the same on one side of the sill as the other. This could result from slight misalignment of the coupler and draft gear or manufacturing tolerances locating the rear draft lugs. A contributing factor could also be that the point of application of the force is offset from the center of the sill's side plate. This could introduce out-of-plane, localized stresses on the plate surface that are difficult to predict. Plot A-11 shows that the strain versus peak LCF relationships for gages 20 and 19 actually diverge significantly at peak forces above about 600,000 pounds. One way to combat these effects could be to use an average of the outputs from gages 19 and 20 to predict or calculate LCF. Plot A-11 also shows a set of points created by averaging the output from gages 19 and 20.

Even though the data from gages 19 and 20 recorded during the loaded car impacts (Sequences 2 through 4) did not show the tendency to diverge at larger LCF values, averaging the output from these two gages still provided the best correlation between strain and peak LCF.

### 2.5.2.3 Accelerometer Response

Accelerometers 18, 9, 6, and 5 provided the best correlation between peak longitudinal acceleration and peak LCF. Plots A-12 and A-13 in the appendix show examples of these relationships. This trend was discovered as a result of the analysis of the Sequence 1 impact data. In all cases for Impact Sequence 1, discontinuous linear relationships appeared to provide the best fit for the data. As an example, for accelerometer 18, when output values were between 0 and about -2.5 g, the peak LCF could be estimated as:

$$-183,590 \times \text{peak acceleration}$$

However, for accelerations greater than -2.5 g, the peak LCF could be estimated as:

$$-20,561 \times (\text{peak acceleration}) + 430,000$$

Even though the relationships above could be estimated using peak acceleration versus coupler force data from Impact Sequence 1, further analysis demonstrated that a significantly better correlation between acceleration response and peak coupler force values could be obtained if calculated SRS values rather than peak acceleration values were used. As a result, for the remaining impact tests, emphasis was placed on the SRS versus coupler force relationships.

SRS calculations were performed on the Impact Sequence 1 output from the following longitudinal accelerometers: 1, 1A, 2, 2A, 5, 6, 8, 9, 11, 12, 13, 14, and 18. Shock response values were calculated for natural frequencies ranging from 5 to 500 Hz. The result was an SRS plot of response versus frequency for each accelerometer and each impact (see Figure 10 for examples).

Relationships were studied relating peak LCF with the following values from the Impact Sequence 1 SRS data:

- Peak SRS value over the 5-500 Hz range versus peak LCF.
- The average SRS value over the 5-500 Hz range versus peak LCF.
- The average SRS value over a restricted frequency range of 5-50.4 Hz versus peak LCF.
- The average SRS value over a restricted frequency range of 10-100.8 Hz versus peak LCF.

The last two relationships were studied because the response versus frequency plots were generally more linear within these frequency ranges. Attempts were made to apply continuous, as well as discontinuous, function relationships, but, again, it appeared that the discontinuous linear functions provide the best correlation of SRS response to peak LCF.

The output from accelerometer locations 1A, 2A, 5, 6, 18, 9, and 12 recorded during Impact Sequence 1 provide credible correlation between SRS response and peak LCF. The best correlation is generally provided by locations 12, 6, and 18. Plots A-14 and A-15 in the appendix show examples. As an example, using the average SRS response from accelerometer 6 over the 10-100.8 Hz range peak LCF could be estimated as follows:

$$\begin{aligned} \text{LCF} &= 231,620 \times (\text{average SRS response}) \text{ for average response values from 0 to 2.4, or} \\ \text{LCF} &= 30,097 \times (\text{average response}) + 460,000 \text{ for response values greater than 2.4} \end{aligned}$$

Plot A-17 in the appendix shows that a very distinct difference exists in the SRS versus LCF relationships between Sequence 1 (empty car) and Sequences 2 through 4 (loaded case). This difference could be due to the condition of the draft gear or to the significant change in the car's mass. The factors contributing to this difference are not fully understood at this point. It is therefore important to know the state of as many of the contributing factors as possible. Since car mass could be one of these important contributing factors, it remains important to be able to determine the car's mass during an impact. It is also important to recognize that a discontinuous or dual function appears to be the best approximation for the SRS versus peak LCF data from Sequence 1. One linear function fits the data fairly well at coupler forces below about 550,000 pounds. It is at these impacts that the draft gear is still effective and has not bottomed. However, a different linear function exists at coupler forces greater than 550,000 pounds. At coupler forces higher than 550,000 pounds, the draft gear does apparently go through its full range of travel, resulting in a distinctly different transfer function.

The data shows that for these impact conditions, the SRS versus peak LCF relationship may be represented reasonably well by a simple linear function of the form:

$$\text{Peak LCF} = m \times (\text{Average SRS Response}) + b$$

Where A is the slope, and B is the intercept constant.

Plots A-18 through A-21 in the appendix and Table 8 summarize some proposed linear SRS versus peak LCF relationships for a loaded, instrumented tank car during three different impact conditions (Impact Sequences 2 through 4). Plot A-21 also illustrates, however, that when all of the loaded tank car impact data is considered, the SRS versus peak LCF relationship might be best approximated by more than one function. For this car/draft gear combination, the change in relationship or function generally occurred at peak LCF values of about 400,000 to 500,000 pounds and again at about 1.0- to 1.1-million pounds, indicating the possibility of three functions to completely define the SRS versus peak LCF relationship.

**Table 8. Estimated Linear Relationships, SRS Response versus Peak LCF—  
Accelerometer Number 6**

| <b>Impact Sequence</b> | <b>Frequency Over Which SRS Values Averaged</b> | <b>Function Slope (m)</b> | <b>Function Intercept (b)</b> | <b>Coefficient of Determination (R<sup>2</sup>)</b> |
|------------------------|---|---------------------------|-------------------------------|---|
| 2                      | 5-50 Hz   | 97,046                    | 125,834                       | .925  |
| 3                      | 5-50 Hz   | 136,612                   | 13,476                        | .894  |
| 4                      | 5-50 Hz   | 128,634                   | 40,716                        | .926  |
| 2, 3, and 4            | 5-50 Hz   | 110,904                   | 101,369                       | .882  |
|                        |   |                           |                               |   |
| 2                      | 10-100 Hz                                       | 74,905                    | 109,071                       | .904  |
| 3                      | 10-100 Hz                                       | 96,763                    | -3,486                        | .840  |
| 4                      | 10-100 Hz                                       | 91,009                    | 40,896                        | .880  |
| 2, 3, and 4            | 10-100 Hz                                       | 83,731                    | 70,821                        | .865  |

Plots A-18 through A-21 of the appendix show the results of linear regression analysis of the SRS data produced from the output of accelerometer 6 during Impact Sequences 2, 3, and 4. Plots A-18 through A-20 show the results if the data from each impact sequence is considered separately, and Plot A-21 shows the results if the data from all three sequences is considered together. Each plot contains a scatter band (bounded by the dashed lines), illustrating the range of peak LCF values that could be expected to be calculated from a given SRS value with a 95 percent confidence level. Table 9 lists a sample of calculated peak LCF values using given SRS values of 4 g and 10 g for the 5-50 Hz data, and 6 g and 14 g for the 10-100 Hz data.

The information contained in Tables 8 and 9 show the following significant results:

- The Coefficient of Determination data in Table 8 indicates that a linear approximation is a better fit for the SRS data averaged over 5 to 50 Hz than that averaged over 10 to 100 Hz. This would also imply that the bands of scatter on each side of the best-fit, mean line are somewhat smaller for the 5 to 50 Hz data than for the 10 to 100 Hz data.
- For any measured SRS value, the estimated or calculated peak LCF value should fall within the ranges shown in the last column of Table 9 with a 95 percent confidence level. These ranges of peak LCF values could be significant, ranging from about  $\pm 45$  to 50 percent at the lower LCF values to  $\pm 20$  to 25 percent at the higher LCF values.
- Considering the range of estimated LCF values that are calculated for a given SRS value, the data from all impact sequences yield similar results. The implication is that, other than payload condition, knowledge of the details of an impact situation may not be required for this method of estimating peak LCF.



**Table 9. Sample of Predicted Peak LCF Values Using SRS Data—  
Accelerometer Number 6**

| <b>Impact Sequence</b> | <b>Frequency Over Which SRS Values Averaged</b> | <b>SRS Value Used to Calculate Peak LCF</b> | <b>Range of Calculated LCF Values (lb)</b> |
|------------------------|---|---|--|
| 2                      | 5-50 Hz   | 4   | 272,260 to 755,684                         |
| 3                      | 5-50 Hz   | 4   | 306,747 to 813,098                         |
| 4                      | 5-50 Hz   | 4   | 304,787 to 805,718                         |
| 2, 3, and 4            | 5-50 Hz   | 4   | 285,276 to 804,719                         |
|                        |   |   |  |
| 2                      | 5-50 Hz   | 10  | 843,304 to 1,349,246                       |
| 3                      | 5-50 Hz   | 10  | 1,102,023 to 1,657,160                     |
| 4                      | 5-50 Hz   | 10  | 1,070,675 to 1,583,438                     |
| 2, 3, and 4            | 5-50 Hz   | 10  | 1,164,740 to 1,699,919                     |
|                        |   |   |  |
| 2                      | 10-100 Hz                                       | 6   | 283,604 to 833,938                         |
| 3                      | 10-100 Hz                                       | 6   | 264,251 to 889,944                         |
| 4                      | 10-100 Hz                                       | 6   | 266,713 to 907,193                         |
| 2, 3, and 4            | 10-100 Hz                                       | 6   | 295,743 to 851,355                         |
|                        |   |   |  |
| 2                      | 10-100 Hz                                       | 14  | 872,452 to 1,443,030                       |
| 3                      | 10-100 Hz                                       | 14  | 1,016,915 to 1,685,504                     |
| 4                      | 10-100 Hz                                       | 14  | 991,449 to 1,638,609                       |
| 2, 3, and 4            | 10-100 Hz                                       | 14  | 960,783 to 1,525,771                       |

As shown in Plot A-22 in the appendix, considerable scatter exists in the peak vertical acceleration versus peak VCF data. As a result, even though a general trend of increasing peak vertical acceleration with increasing peak VCF exists, it is difficult to identify a function that satisfactorily defines a relationship between the two parameters from the data currently available.

Shock response calculations were performed on the output from the following vertical accelerometers: 1, 1A, 2, 2A, 5, 6, 14, and 18. Shock response values were calculated for natural frequencies ranging from 5 to 500 Hz. The result was an SRS plot of response versus frequency for each accelerometer and each impact. Relationships were studied relating peak VCF with the following values from the SRS data:

- Peak SRS value over the 5-500 Hz range versus peak VCF.
- The average SRS value over the 5-500 Hz range versus peak VCF.
- The average SRS value over a restricted frequency range of 5-50.4 Hz versus peak VCF.
- The average SRS value over a restricted frequency range of 10-100.8 Hz versus peak VCF.

The last two relationships were studied because the response versus frequency plots were generally more linear within these frequency ranges.

The last two types of relationships studied provided the best correlation between SRS response and peak VCF. Plots A-23 through A-26 in the appendix indicate that some fairly well-defined trends relating SRS data from vertical accelerometer 6 to peak VCF also exist. The SRS versus peak VCF relationships for accelerometer 5 are similar. As shown in Table 10, however, these relationships tend to be somewhat less defined than those established for the LCF response. As a result, for a given SRS value generated using data from either accelerometer 5 or 6, the predicted peak VCF would have a range of possible values larger than for the similar peak LCF predictions.

**Table 10. Estimated Linear Relationships, SRS Response versus Peak VCF—  
Accelerometer 6**

| Impact Sequence | Frequency Over Which SRS Values Averaged | Function Slope (m) | Function Intercept (b) | Coefficient of Determination (R <sup>2</sup> ) |
|-----------------|--|--------------------|------------------------|--|
| 2               | 5-50 Hz                                  | 5,542              | 20,235                 | .930   |
| 3               | 5-50 Hz                                  | 5,782              | 36,821                 | .753   |
| 4               | 5-50 Hz                                  | 9,997              | 15,087                 | .918   |
| 2, 3, and 4     | 5-50 Hz                                  | 5,905              | 32,661                 | .732   |
|                 |  |                    |                        |  |
| 2               | 10-100 Hz                                | 4,282              | 12,651                 | .901   |
| 3               | 10-100 Hz                                | 4,420              | 31,070                 | .761   |
| 4               | 10-100 Hz                                | 7,152              | 5,761                  | .919   |
| 2, 3, and 4     | 10-100 Hz                                | 4,535              | 25,031                 | .741   |

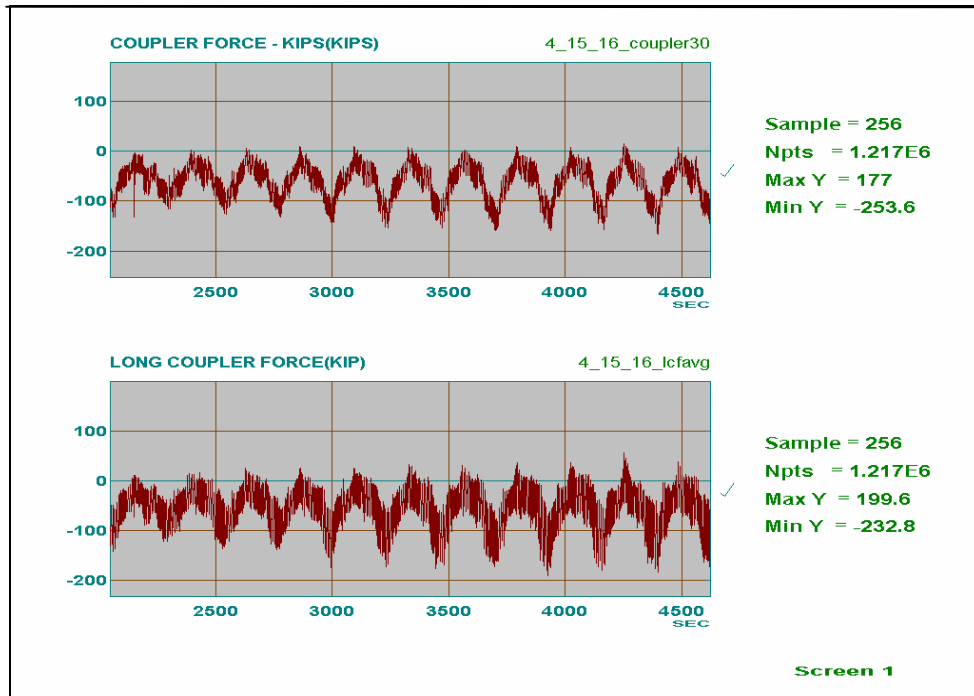
Engineers at the Volpe National Transportation Center performed additional analysis of the acceleration versus time data. A power spectral density (PSD) analysis was performed on each tank car acceleration history to determine the dominant frequencies in the response of the tank car structure. Accelerations in the vertical and longitudinal directions, with the tank empty as well as filled, were examined. The results of this analysis indicated that for an empty tank, the dominant excited frequencies for the tank structure were 0 Hz (rigid body motion) in the longitudinal axis and 13 Hz in the vertical direction. A vertical axis frequency of 100 Hz, likely excited by the stick-slip action of the draft gear, was also prominent in the empty car data collected during events when the stick-slip coupler forces were observed. PSD results from the full tank tests exhibit dominant peaks at 0 Hz in the longitudinal direction and at both 5 Hz and 23 Hz in the vertical direction [1][2].

### 2.5.3 Testing at FAST

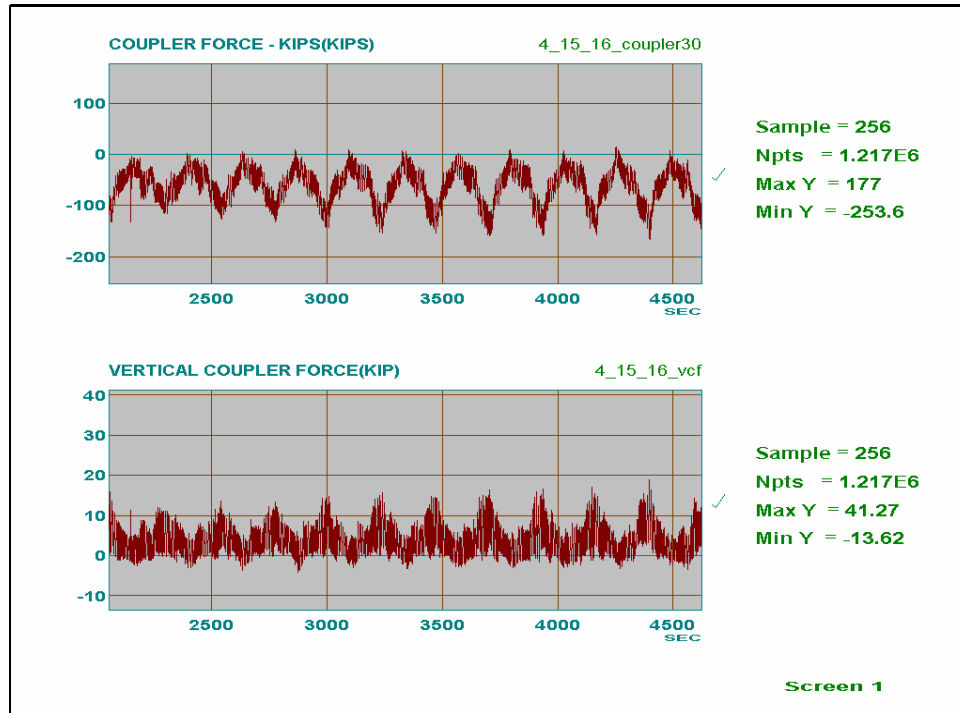
#### 2.5.3.1 Coupler Forces

Table A-1 in the appendix summarizes the test conditions and resulting coupler force measurements (LCF from coupler and VCF calculated) during the FAST test. In general terms, when the car was near the locomotives (near the front of the train), the LCF values were primarily tensile and varied from near 0 to 170,000-250,000 pounds. The mean value was about 60,000-70,000 pounds. The calculated VCF values were similar in character and varied from about 20,000-40,000 pounds upward to 6,000-13,000 pounds downward (negative values). Figure 11 shows typical measured LCF (top plot) and calculated LCF (lower plot) versus time

data for this car location. This data was recorded on the night of April 15-16, 2003, over a time period of approximately 45 minutes. Figure 12 shows the measured LCF and calculated VCF values for the same time period as the data in Figure 11. This plot demonstrates the relationship between LCF and calculated VCF for this operating environment. Output from accelerometers 6L, 6V, 18L, and 18V was insignificant during this time period. This 45-minute segment is indicative of the data recorded for the entire night with the car near the front of the train.



**Figure 11. Measured (top) and Calculated LCF versus Time, April 15-16, 2003, Test Car Near Front of Train**



**Figure 12. Measured LCF (top) and Calculated VCF versus Time, April 15-16, 2003, Test Car Near Front of Train**

By contrast, when the test car was near the end of the train, enough slack action existed to produce numerous events characterized by short duration buff and draft LCF. As shown in Table A-1 in the appendix, the values of the measured LCF were in order of magnitude from 160,000- to 263,000-pound compression to 150,000- to 270,000-pound tension. Figures 13 through 15 illustrate this. Figure 13 shows about 45 minutes of measured and calculated LCF data from the night of April 14-15, 2003. Figures 14 and 15 show a 41-second segment from the same time period.

### 2.5.3.2 Accelerometer Response

Tables A-2 and A-3 in the appendix and Figures 16 and 17 show some of the data from accelerometers 6L and 18L recorded during the night of April 14-15, 2003. This acceleration data was processed for the nine most significant LCF events recorded during the night. The peak acceleration values were less than 7 g, and SRS values were generally in the 2-3 g range.

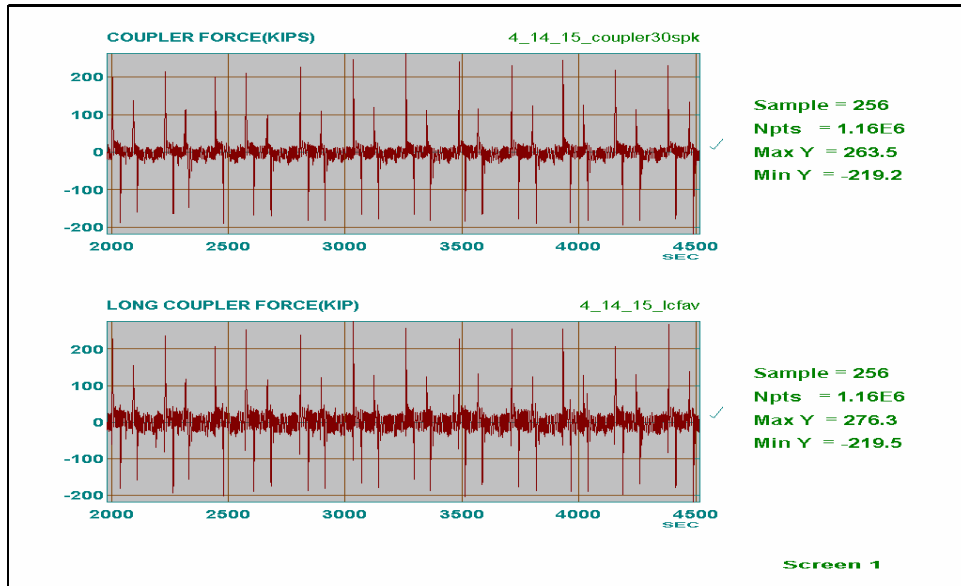


Figure 13. Measured (top) and Calculated LCF versus Time, April 14-15, 2003, Test Car Near Rear of Train

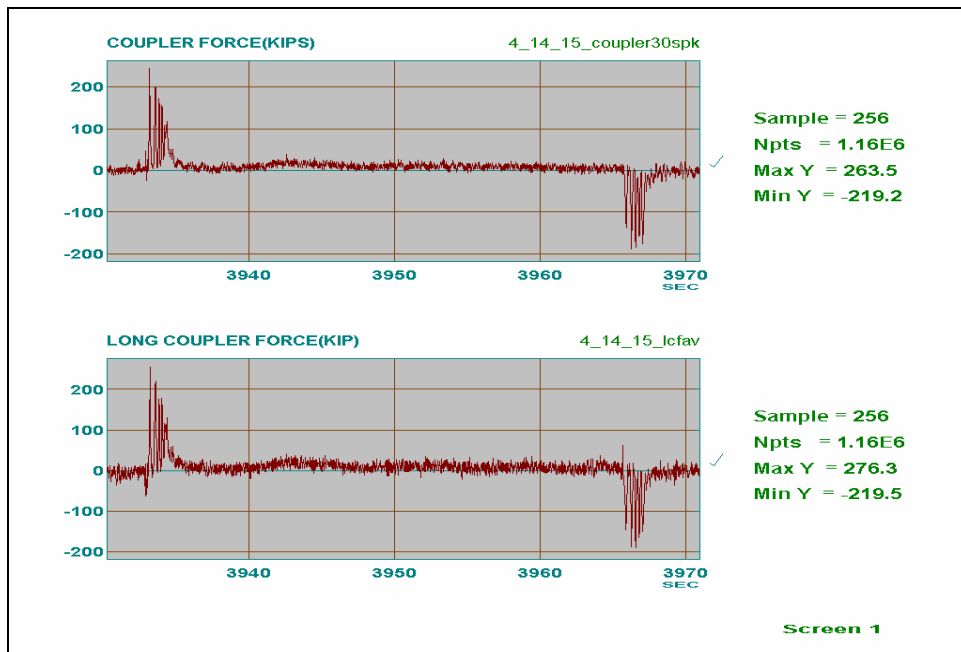
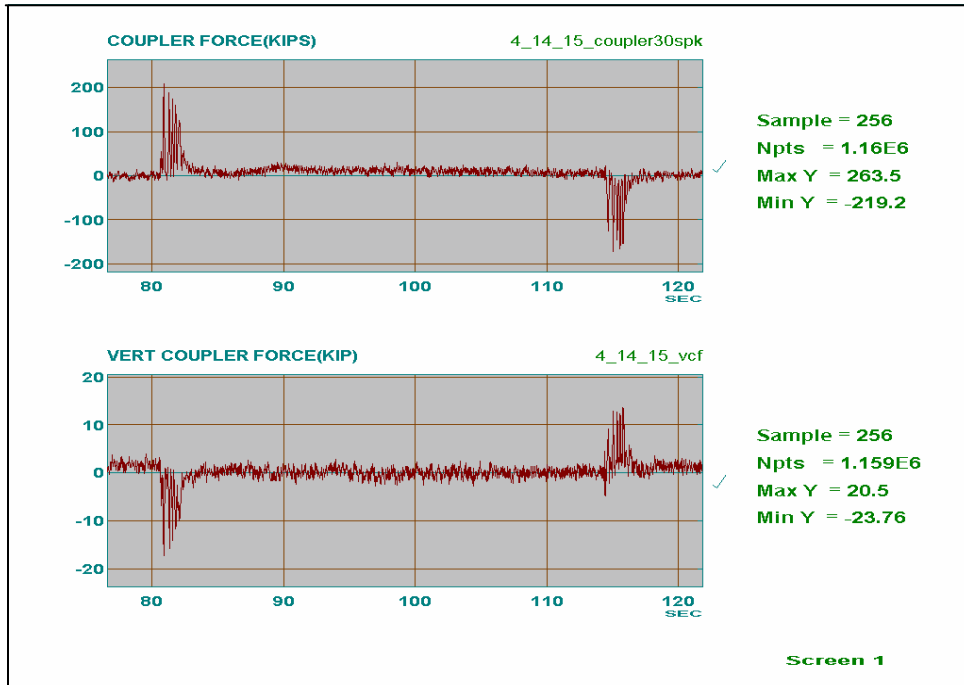
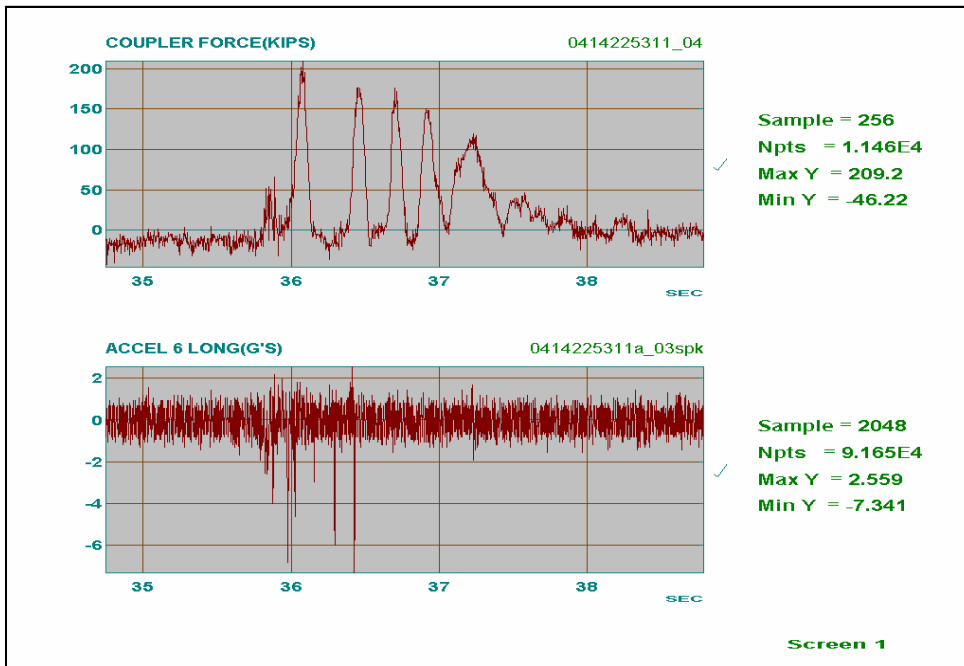


Figure 14. Measured (top) and Calculated LCF versus Time During a 41-Second Time Period, April 14-15, 2003, Test Car Near Rear of Train



**Figure 15. Measured LCF (top) and Calculated VCF versus Time During a 41-Second Time Period, April 14-15, 2003, Test Car Near Rear of Train**



**Figure 16. Measured LCF and Associated Longitudinal Acceleration at Location 6, April 14-15, 2003**

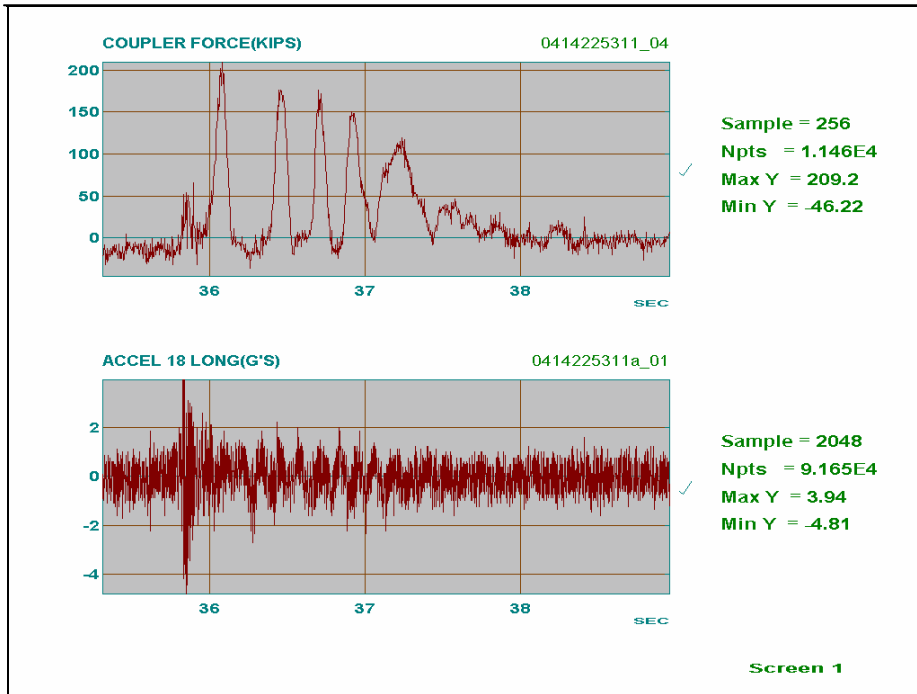


**Figure 17. Measured LCF and Associated Longitudinal Acceleration at Location 6, April 14-15, 2003**

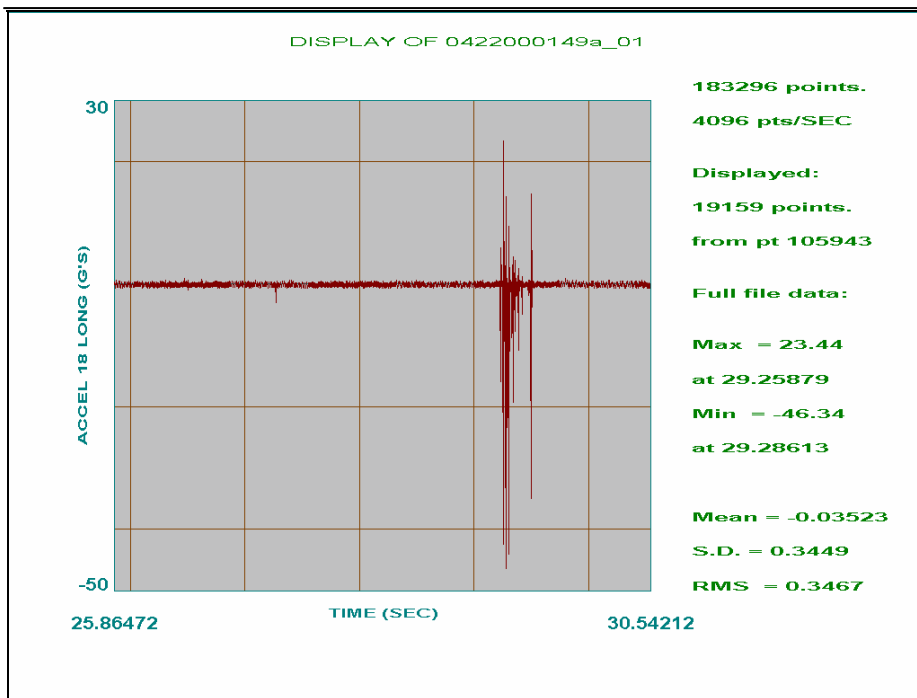


**Figure 18. Typical Accelerometer Data Recorded April 20-22, 2003**

Plots A-28 and A-29 in the appendix are plots of average SRS value versus measured peak LCF for the same events mentioned previously. Little correlation seemed to exist between peak LCF and average SRS values at this coupler relatively low (less than 300,000 pounds) force level. It must be recognized, however, that all of the LCF values in this small comparison were of the same general order of magnitude.

During the first 4 to 5 nights of testing, several problems occurred with the data acquisition system, including premature computer shutdown and data with considerable noise, spikes, and zero offsets. Much of this poor quality data was not processed. Most of the problems were eventually solved, and the result was significantly better data quality during the last 5 nights of testing. The problem of spikes in the acceleration data, however, was never totally solved. This problem may have resulted from amplifier connections that became intermittent during train action impacts. The peak acceleration values indicated by these spikes are not realistic or consistent with data recorded and illustrated in Figure 18 during previous nights when lower coupler force events occurred.

#### *2.5.3.3 Strain Gage Response*

Figures 19 through 22 are cross plots of recorded LCF values versus those calculated using the data from strain gages 19 and 20. These plots cover time spans of 1.25 to 2.34 hours (representing over 1 million data points) and demonstrate that the correlation is close to 1-to-1 with a relatively narrow band of scatter. This is especially true of the data recorded during the last 3 to 4 nights of testing. It was during this time period that the data quality was at its best. It is possible that the band of scatter could be reduced in width at higher LCF values (above 300,000 pounds) or if additional filtering was used.



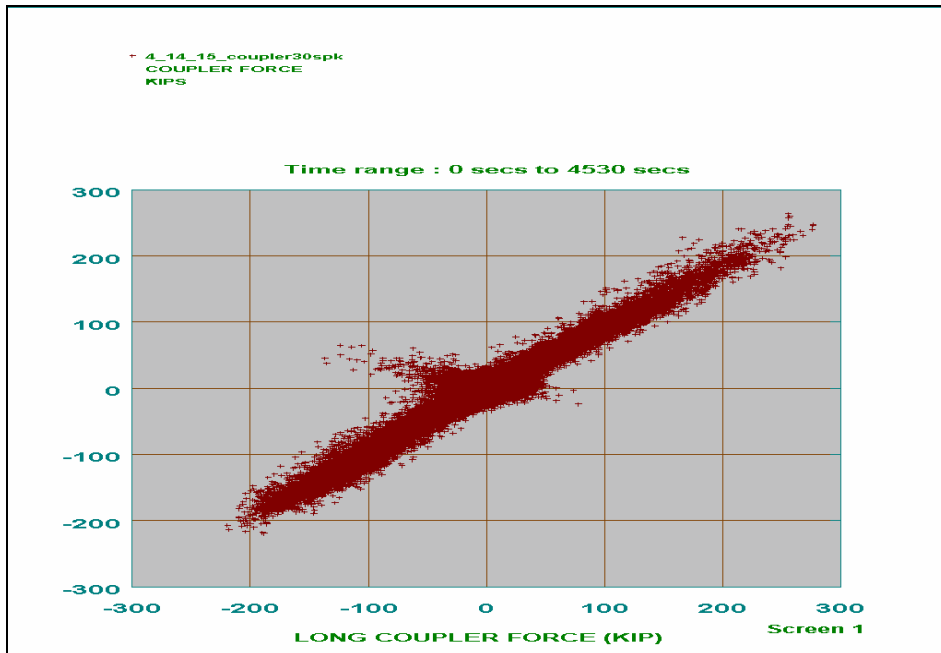


Figure 19. Cross Plot of Calculated LCF (y-axis) versus Measured LCF, April 14-15, 2003

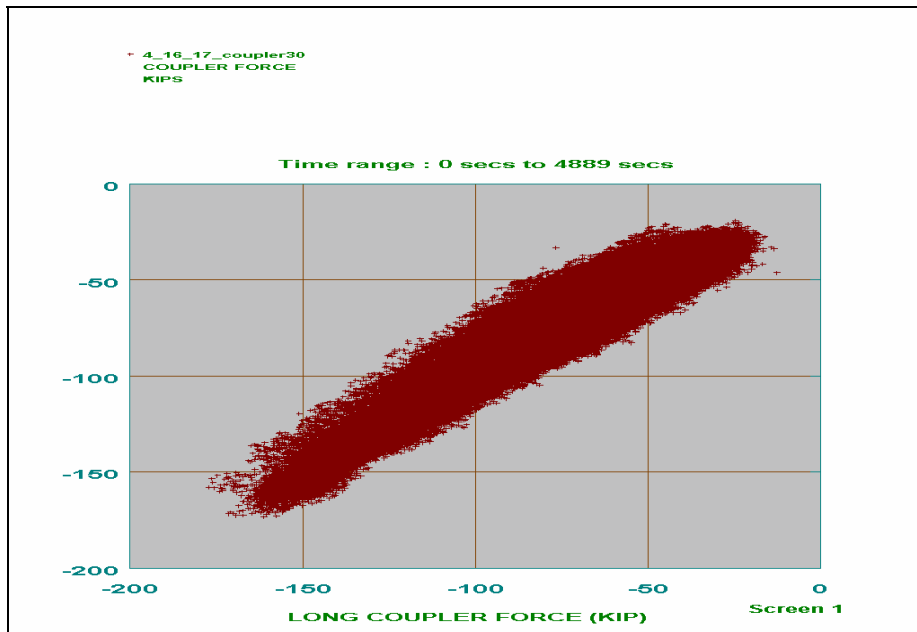


Figure 20. Cross Plot of Calculated LCF (y-axis) versus Measured LCF, April 16-17, 2003

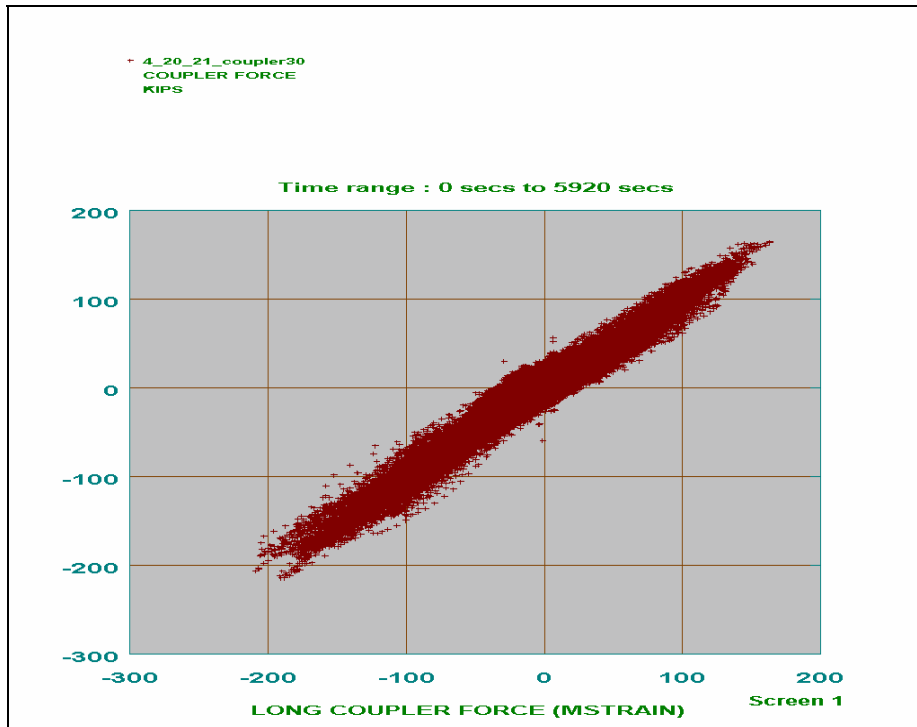


Figure 21. Cross Plot of Calculated LCF (y-axis) versus Measured LCF, April 20-21, 2003

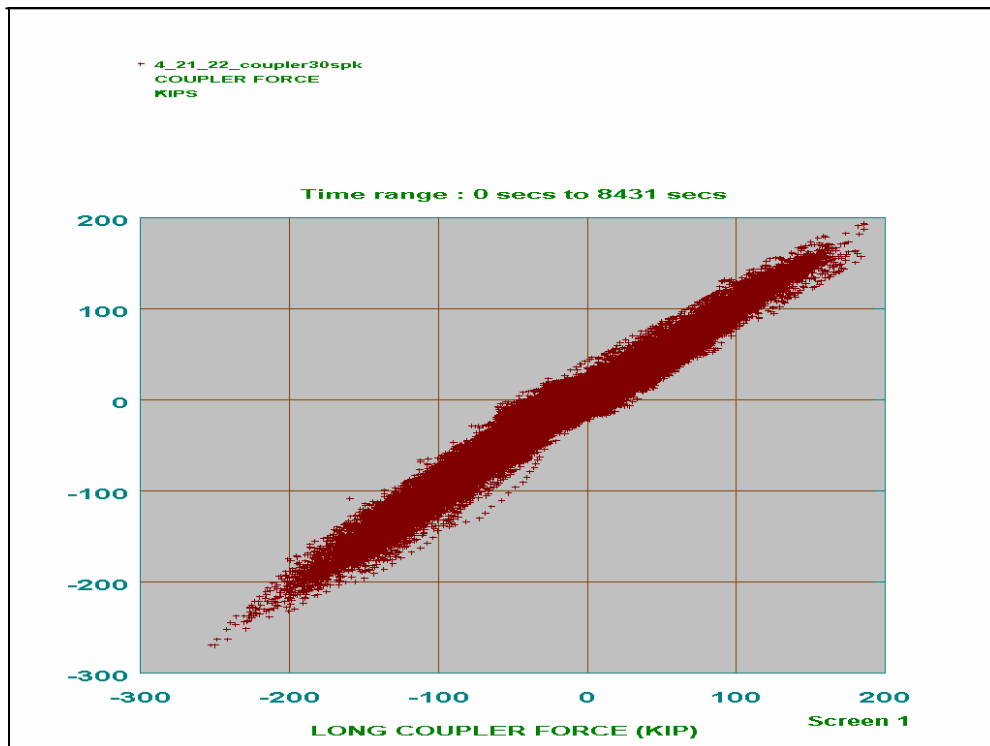


Figure 22. Cross Plot of Calculated LCF (y-axis) versus Measured LCF, April 21-22, 2003

## **2.6 Conclusions**

### **2.6.1 Controlled Vertical Force Test**

Phase I testing measuring accelerometer response resulting from controlled, low-magnitude, vertical force pulses applied to the end of the stub sill revealed that such acceleration responses (in the form of peak acceleration values) could not effectively be used in an estimation of peak VCF resulting from such low magnitude inputs. Plots A-4 and A-5 in the appendix illustrate two problems with this method. In both plots,  $T/2$  represents one-half of the time period of the vertical force pulse. The first area of concern is that as the rate of force input decreased ( $T/2$  increased), accelerometer response (in terms of the resulting peak vertical acceleration) became less sensitive to changes in magnitude of the maximum amplitude of the vertical force pulse. This is illustrated by observing the difference in the slopes of the curves estimated for the  $T/2 = 0.25$  and  $T/2 = 0.5$  tests in Plot A-5. The second and more serious problem with this method is that different peak force versus peak acceleration curves could develop depending on the duration of the vertical force pulse. As a result, if all that is known is the amplitude of the acceleration, two or more peak force values could be surmised. As an example using the data in Plot A-4, if a peak acceleration value of 0.38 g had been recorded, the calculated peak VCF could be estimated from 14,000 to 20,000 pounds depending on the rate at which the load was applied. These problems should effectively eliminate this method as a way to calculate in-train VCF at this time.

### **2.6.2 Impact Test**

The data from these tests provides the most accurate alternative to instrumented couplers for predicting peak LCF and the best option for predicting VCF. The strain versus peak LCF and VCF relationships do not appear to be significantly affected by impact severity or draft gear action. The variation of strain response for a given measured peak LCF appears to be significantly smaller than the variation of SRS response. If strain gages are used to indicate VCFs, it is recommended that they be placed in locations where they will be sensitive to those vertical forces but essentially unaffected by LCFs.

As Plots A-14 through A-21 in the appendix show, it is possible to use SRS data to estimate peak LCF that occur as a result of car-to-car impacts. This method shows the most promise for the purposes of indicating the severity of moderate to severe impacts (impact environment characterization) using accelerometer response. For the purposes of such impact environment characterization, the range or scatter of SRS response for a given peak LCF and some changes in SRS versus coupler force relationships as impact severity increases may not be unacceptable limitations. The longitudinal accelerometer at location No. 6 in Figure 5 (top surface of the tank shell near the longitudinal center line) has thus far proven to provide the best data for such predictions. Conversely test data has shown that the use of unfiltered (as recorded) peak accelerometer output (either positive or negative) cannot be used to reliably predict peak LCF during an impact event. Peak acceleration values that result from acceleration versus time data filtered at either 50 or 100 HZ have also proven to be a relatively poor predictor of peak coupler force resulting from impacts.

The data collected from Impact Sequences 1 through 4 indicates that SRS response cannot, at this time, be used very effectively to estimate peak VCF or LCF values for the purposes of performing crack growth, fatigue, or damage tolerance analysis. The reasons for this are as follows:

- Even for the best SRS versus peak LCF relationships, enough scatter exists in the data (regardless of the regression function used) that the resulting range of peak LCF values that might be predicted with a given SRS value is too broad to be effectively used in an accurate crack growth or damage tolerance analysis.
- The change of the SRS versus peak LCF relationship as impact forces increase (for a particular type of impact) most likely results from draft gear design or condition. It must be recognized that among different draft gear designs or even among draft gear of the same design but different ages, a wide variation can exist in force versus deflection performance. If this is the case, the effects on the SRS versus peak LCF relationship cannot be generalized in a way that can be applied to all possible draft gear/car combinations.

Since testing thus far has only involved one car/draft gear combination, the overall form of the peak LCF versus SRS relationship is only known for that one combination. At this time it must be assumed that the form of the LCF versus SRS relationship will be significantly different for any other car/draft gear combination. These factors again prevent any type of practical generalization or expansion of the relationships established thus far to cover all significant car/draft gear designs.

### ***2.6.3 Testing at FAST***

Analysis of the data revealed that at peak LCF values less than 300,000 pounds, the output from strain gages 20 and 19 could be used to make estimates of LCF as measured by the instrumented coupler. Figures 11, 13, 14, and 19 through 22 illustrate this. The response versus time traces in Figures 11, 13, and 14 illustrate the similar nature of the data from the instrumented coupler to that calculated using strain values from gages 19 and 20. Figures 19 through 22 show the similar data in a cross plot format and illustrate the accuracy and scatter of the LCF values calculated using strain gage output versus those measured by the instrumented coupler.

The data collected during this test confirmed that accelerometer response in the form of SRS values does not correlate well with either vertical or longitudinal peak coupler force at peak LCF values below 200,000 pounds.

Plots A-30 and A-32 in the appendix illustrate that at this coupler force level, correlation seemed to exist between peak LCF and SRS values averaged over frequency ranges of either 5 to 50 Hz or 10 to 100 Hz.

### 3.0 Recommendations

Conduct extended over-the-road trials to prove that: (1) strain gage response can be used to accurately predict LCFs and VCFs during uncontrolled, long-term service and (2) accelerometer response in the form of SRS values can be used to effectively monitor the level of LCFs and VCFs resulting from severe yard impacts. This could be accomplished within Phase IIA by installing a reduced set of transducers on a single stub sill tank car that would then be subjected to standard over-the-road conditions for 10,000 to 13,000 miles. Mileage could be accumulated in 6 to 8 weeks of testing. If the data collected during this trial test continue to suggest that these two methods of predicting coupler forces are valid and useful, three more cars—each of a different design—should be similarly instrumented and placed in similar extended service. This last step would be required to prove that the concept has true universal application.

The following transducers should be installed on the stub sill/tank structure:

- Instrumented coupler at each end of car.
- Strain gages at locations 19 and 20 on A-end of car.
- Strain gages at locations 19 and 20 on B-end of car.
- Strain gages at location 21/22 on A-end of car.
- Strain gages at location 21/22 on B-end of car.
- 100 g vertical and longitudinal accelerometers at location 6.
- 100 g vertical and longitudinal accelerometers at location 5.
- 100 g vertical and longitudinal accelerometers at location 18 (used as backup).

In addition, a set of strain gages should be applied to one of the bolsters to record data on bolster loads that can be compared with similar data collected in the stub sill tank car research project DOT/FRA/ORD/95-11, often referred to as FEEST II,<sup>3</sup> conducted in 1995. As the coupler force data from the proposed Phase IIA test is evaluated and compared with that recorded during the FEEST II test, it will be useful to also compare bolster load history as an indication of relative route severity.

Before on-track testing begins, the output of all strain gages should be re-calibrated against known loads, repeating the quasi-static process used before Phase I testing began.

The recorded data during over-the-road testing should be processed in a manner similar to that used for the FAST test of Phase I. Thresholds should be set to control the recording of acceleration data, and that data should only be recorded for the time that the values exceed the limits. The acceleration versus time data for each event should be converted to SRS values averaged over 5-50 Hz by software within the data acquisition system. As a result, the data downloaded for each significant acceleration event would be an SRS value averaged over a range of 5-50 Hz and a peak coupler force value. Based on the Volpe analysis, accelerometer data should be recorded at about 2,000 samples per second.<sup>1,2</sup>

Strain gage and coupler force data should be recorded continuously while car velocity is over 1.0 mph. This data can also be recorded at 2,000 samples per second but then decimated to 256 Hz to save onboard file space. This data should then pass through a 30-Hz digital filter before being processed. The filtered strain gage data should be processed using software on the data

acquisition computer so that the information available for download is in the form of calculated VCFs and LCFs versus time.

If the data recorded during this trial test continues to confirm an acceptable level of accuracy for the correlation of SRS response versus measured peak coupler force and coupler force calculated from strain data versus measured peak coupler force, a Phase IIB should be planned. In this phase, similar transducer/data acquisition systems would be installed on three more stub sill tank cars of three different contemporary designs. These 3 cars would also be subjected to 10,000 to 13,000 miles of over-the-road testing as a final confirmation of the system effectiveness and the usefulness of using cars designed differently from that of the Phase IIA car.

## References

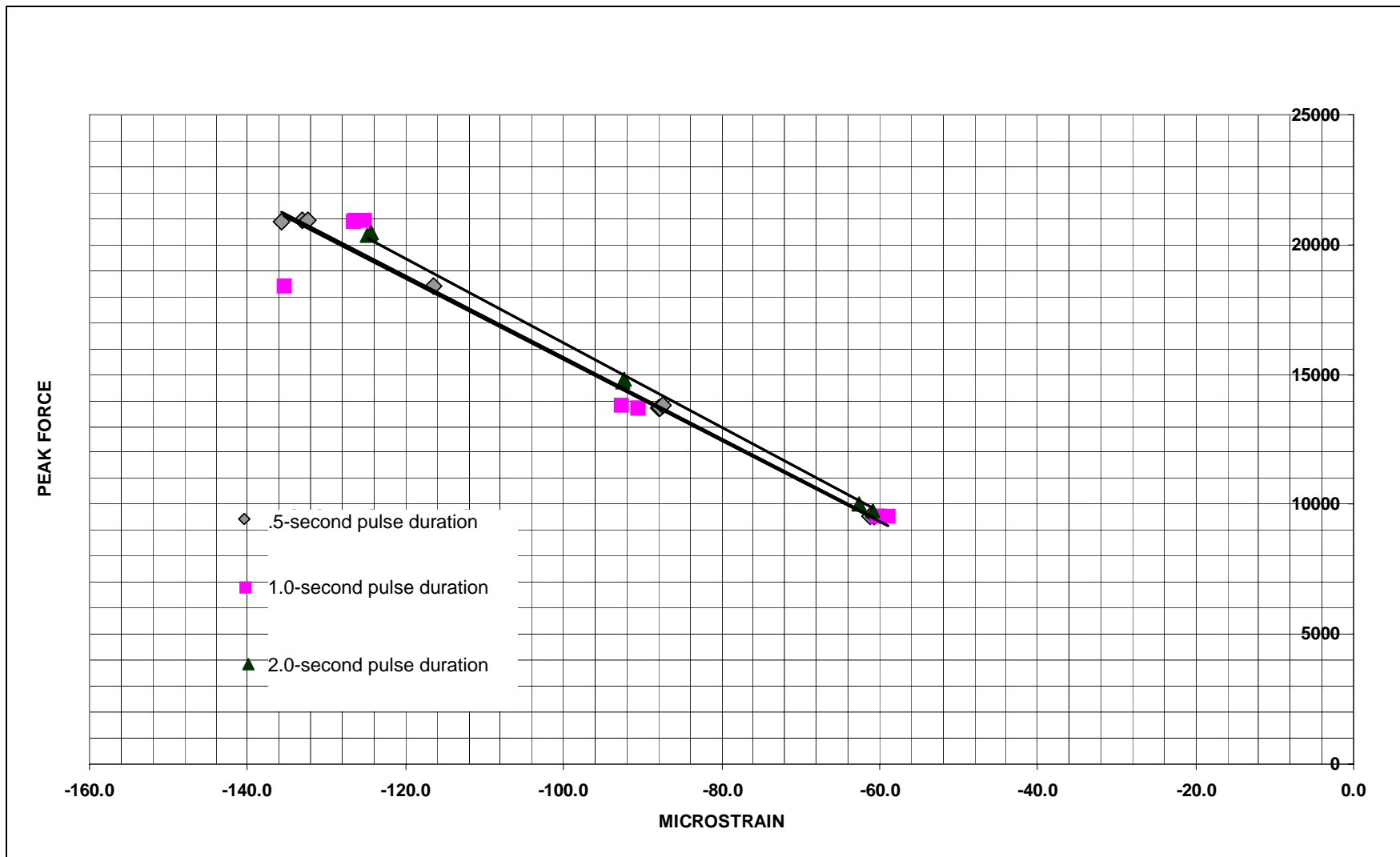
1. Lyons, M., Riddell, W., and Koch, K. "Analysis of Accelerations Measured During Full-Scale Tank Car Impact Tests," Report No. DOT/FRA/ORD-07/08, U.S. Department of Transportation, Federal Railroad Administration, April 2007.
2. Lyons, M., Riddell, W., and Koch, K. "Full-Scale Tank Car Impact Tests," American Society of Mechanical Engineers Report IMECE2003-44062, November 2003.
3. Cogburn, L. "Stub Sill Tank Car Research Project Results of a 15,000-Mile Over-the-Road Test," Report No. DOT/FRA/ORD-95/11, U.S. Department of Transportation, Federal Railroad Administration, September 1995.



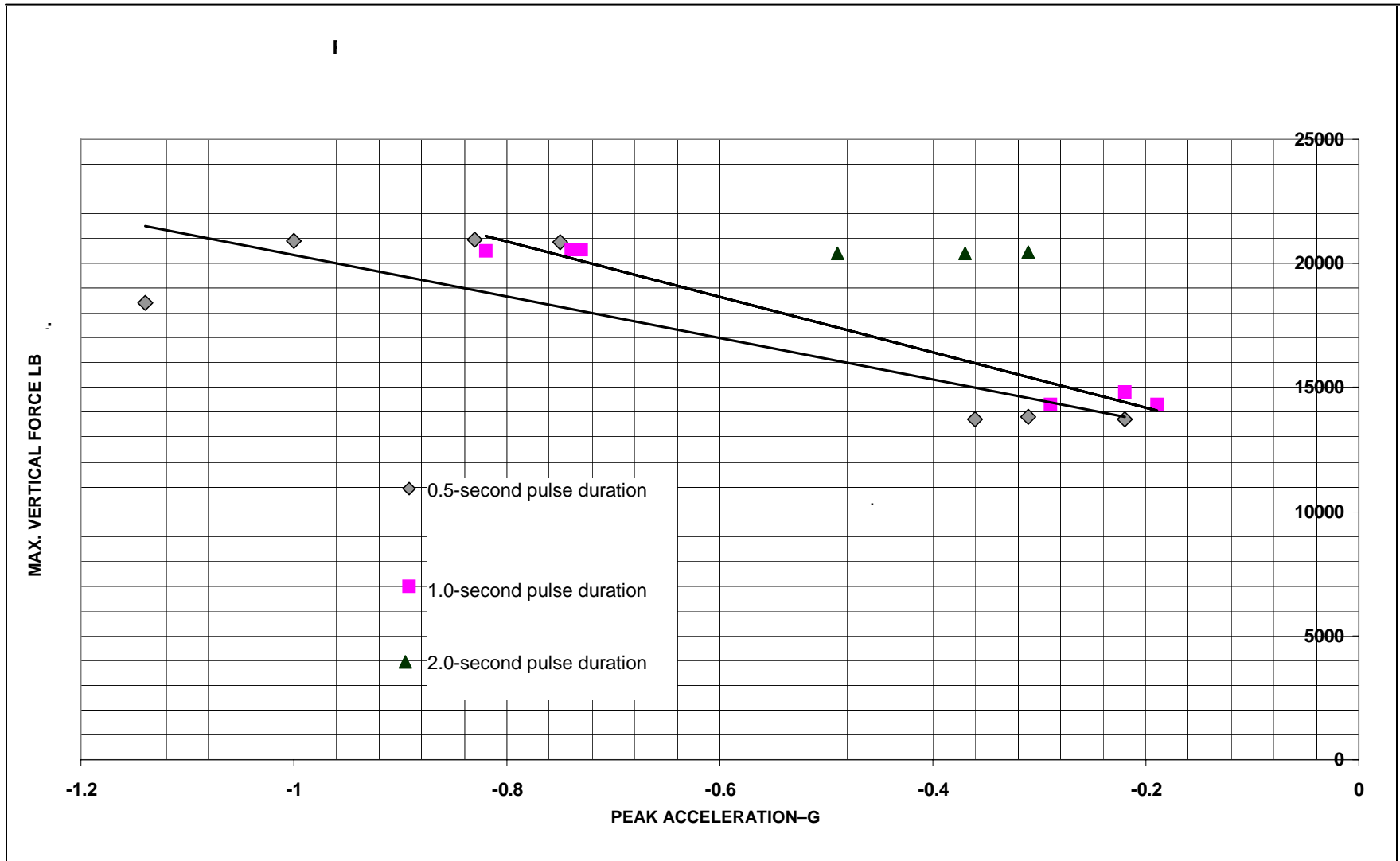


**Appendix.**

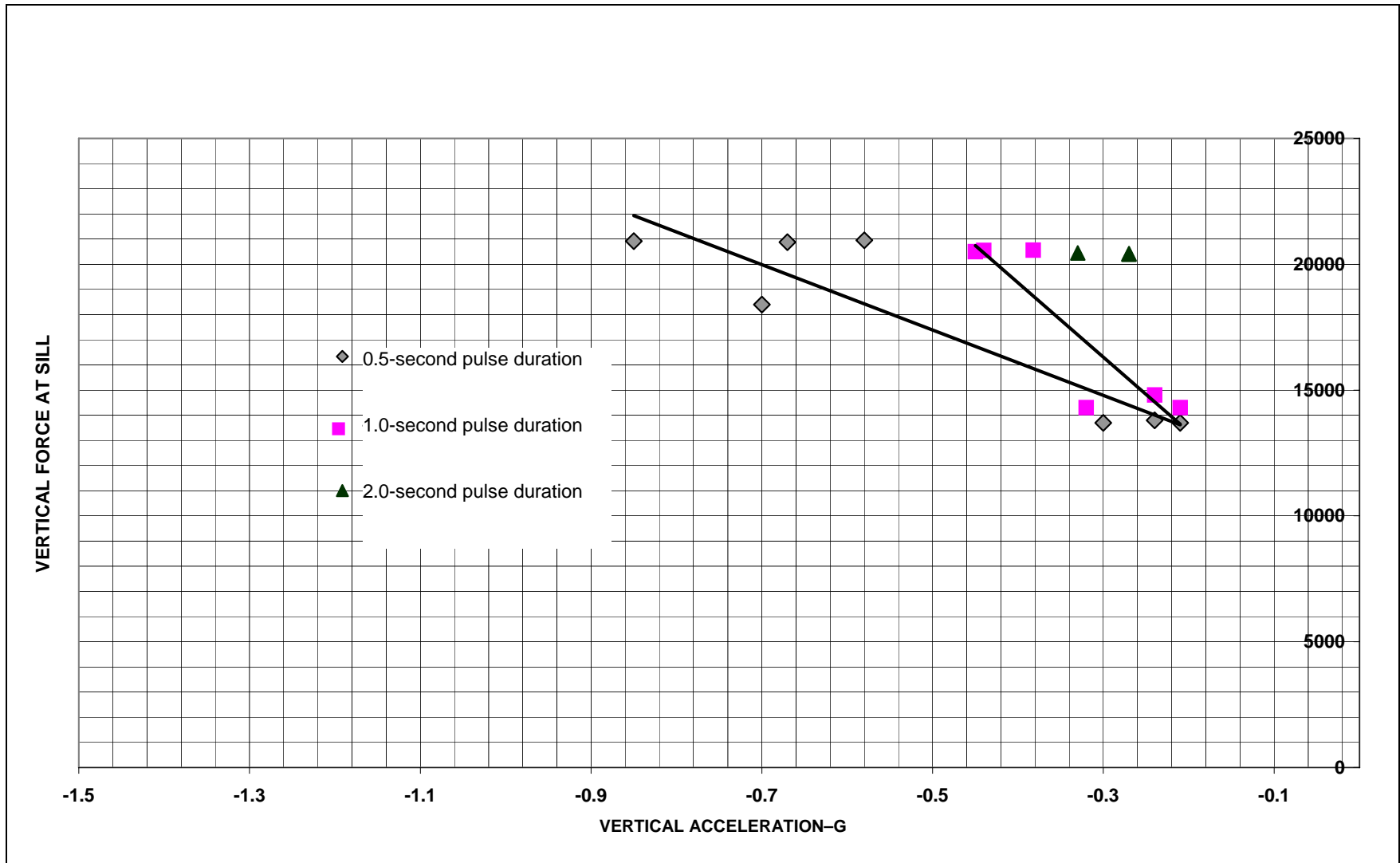
**Plots A-1 through A-22**



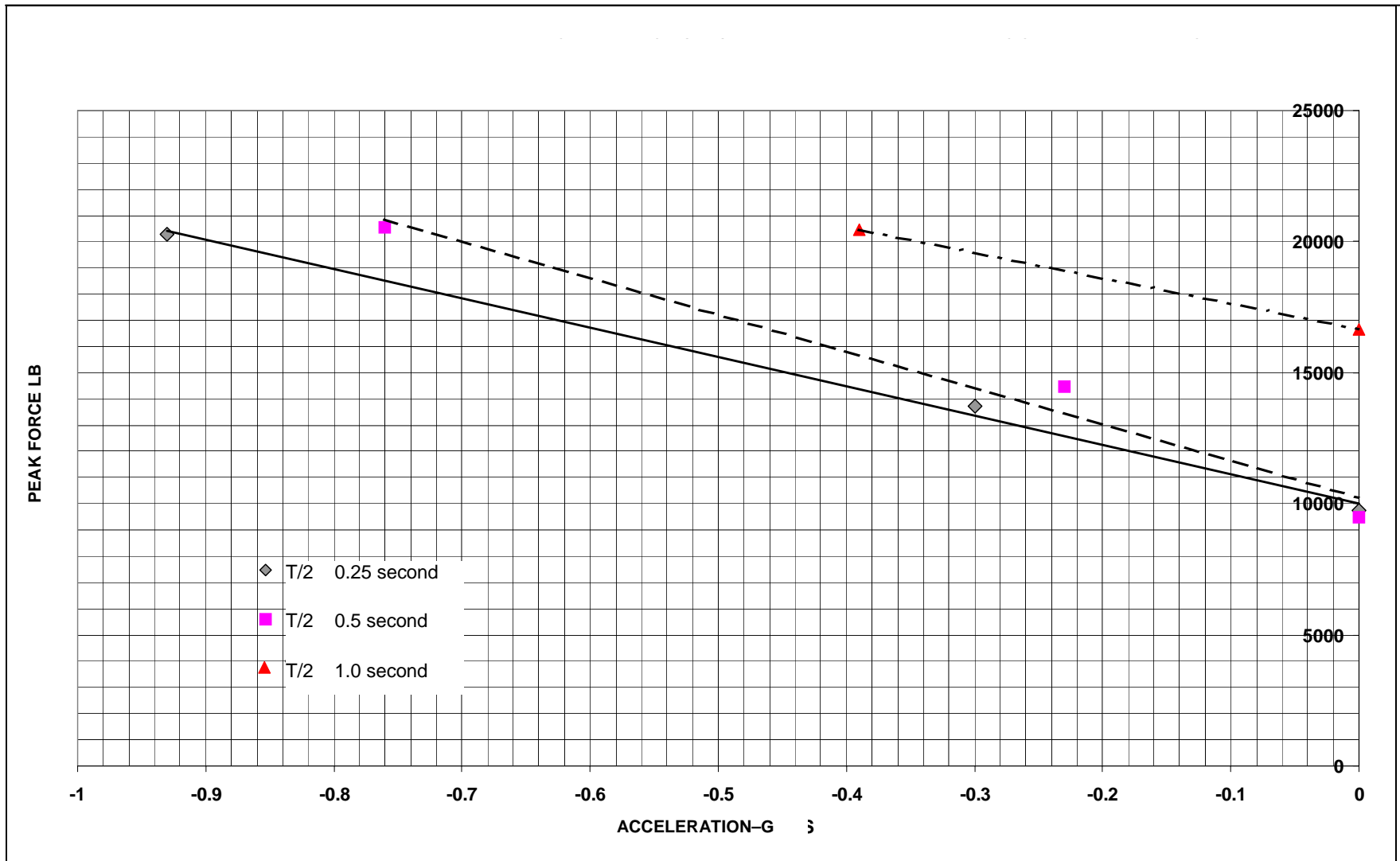
**Plot A-1. Strain versus Peak Vertical Sill Force—Gages 21-22**



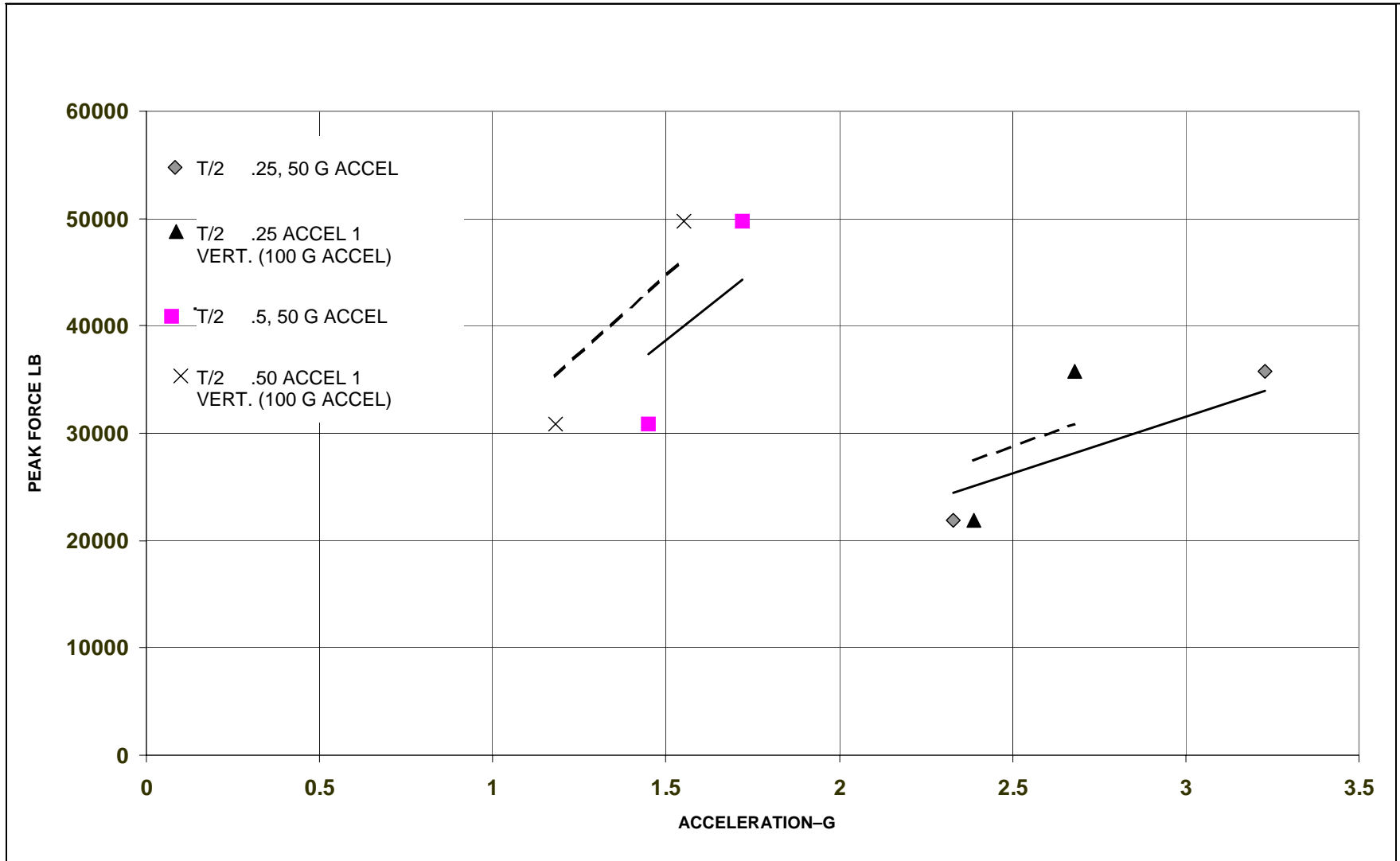
**Plot A-2. Peak Vertical Acceleration versus Maximum Vertical Sill Force—Acceleration 1 Vertical**



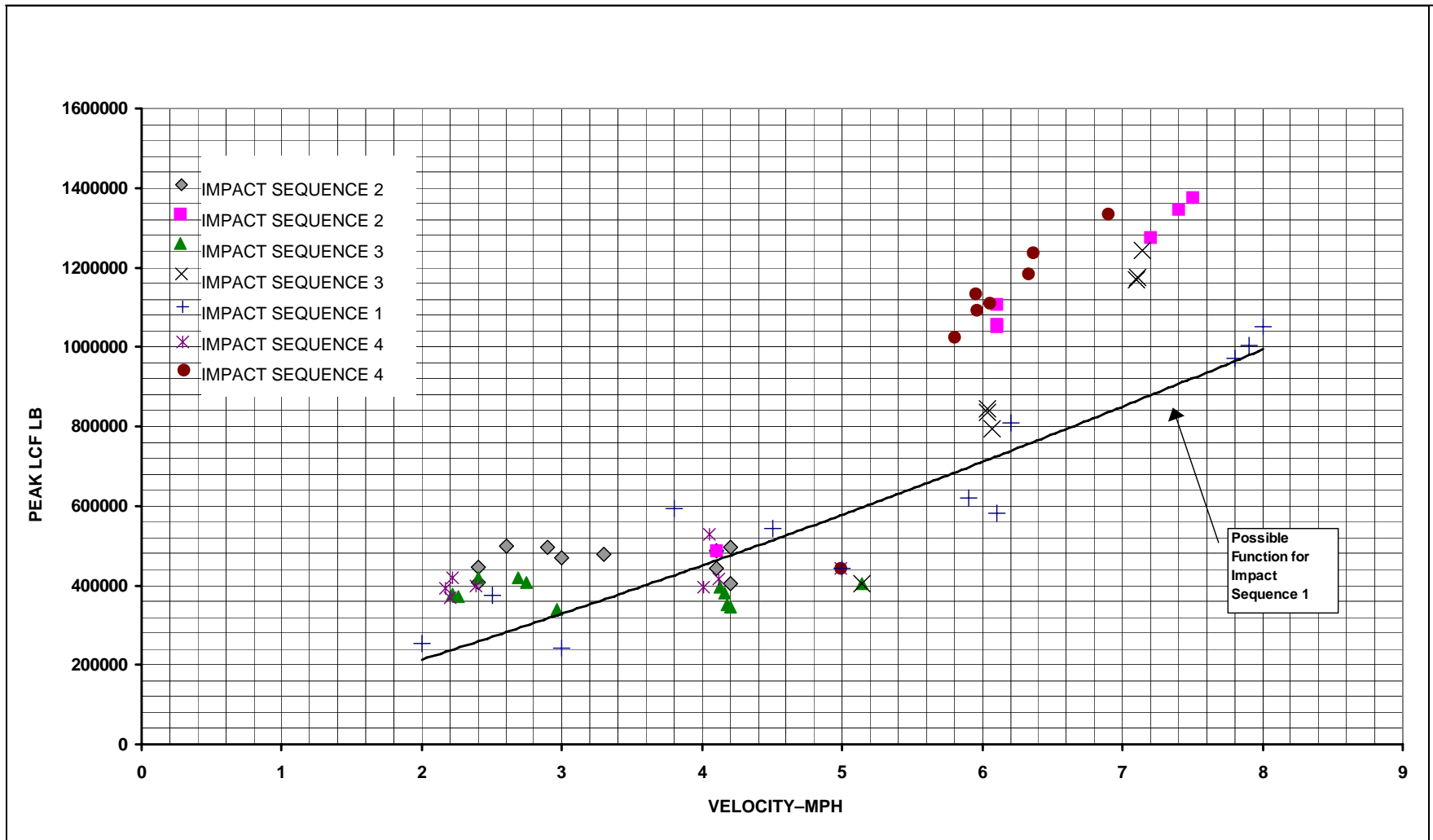
**Plot A-3. Peak Longitudinal Acceleration versus Vertical Sill Force—Acceleration 1A Vertical**



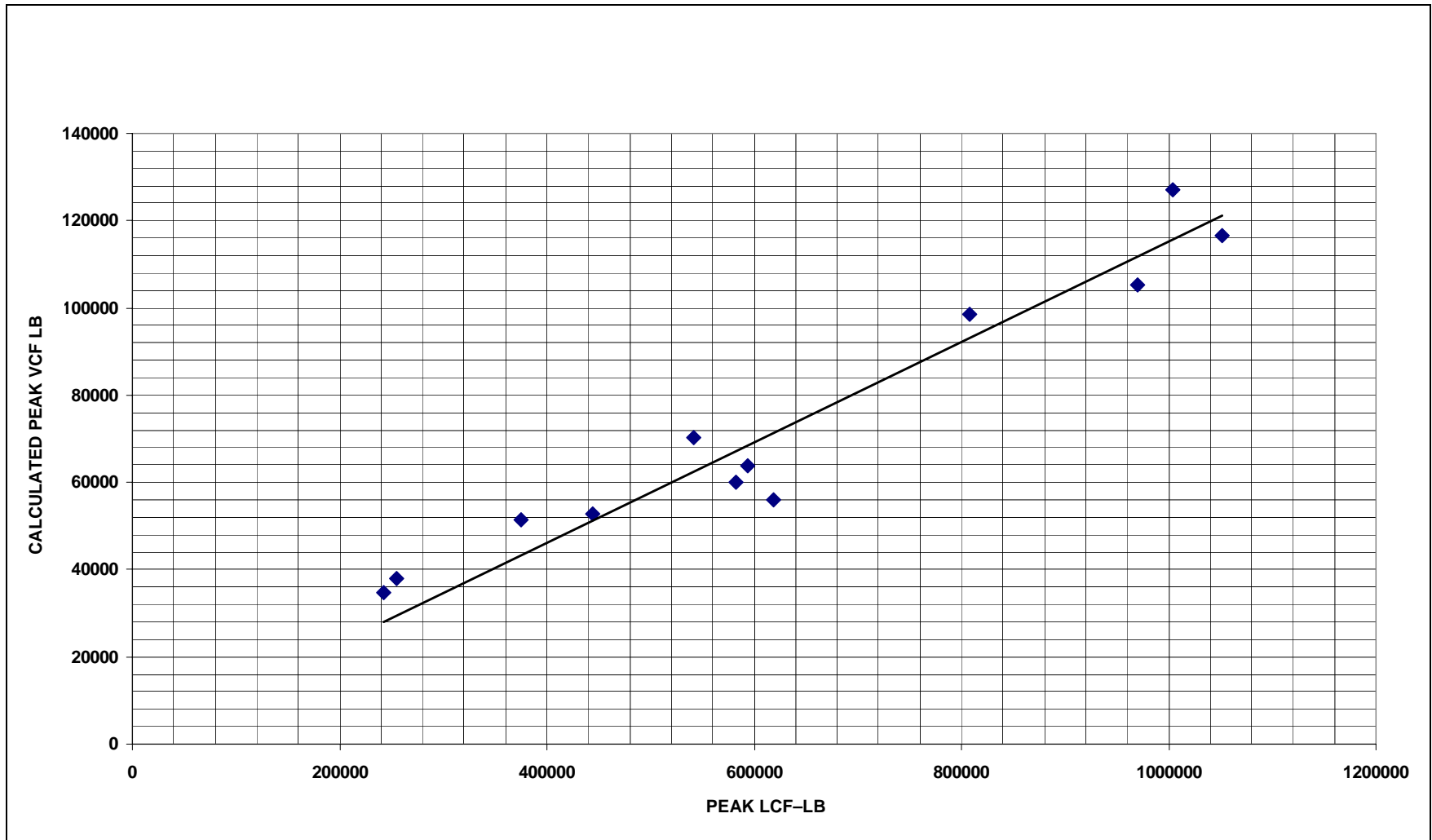
**Plot A-4. Average Peak Vertical Forces versus Average Peak Vertical—Acceleration #1 Empty Car**



**Plot A-5. Average of Peak Vertical Forces versus Average Peak Vertical Acceleration—Loaded**

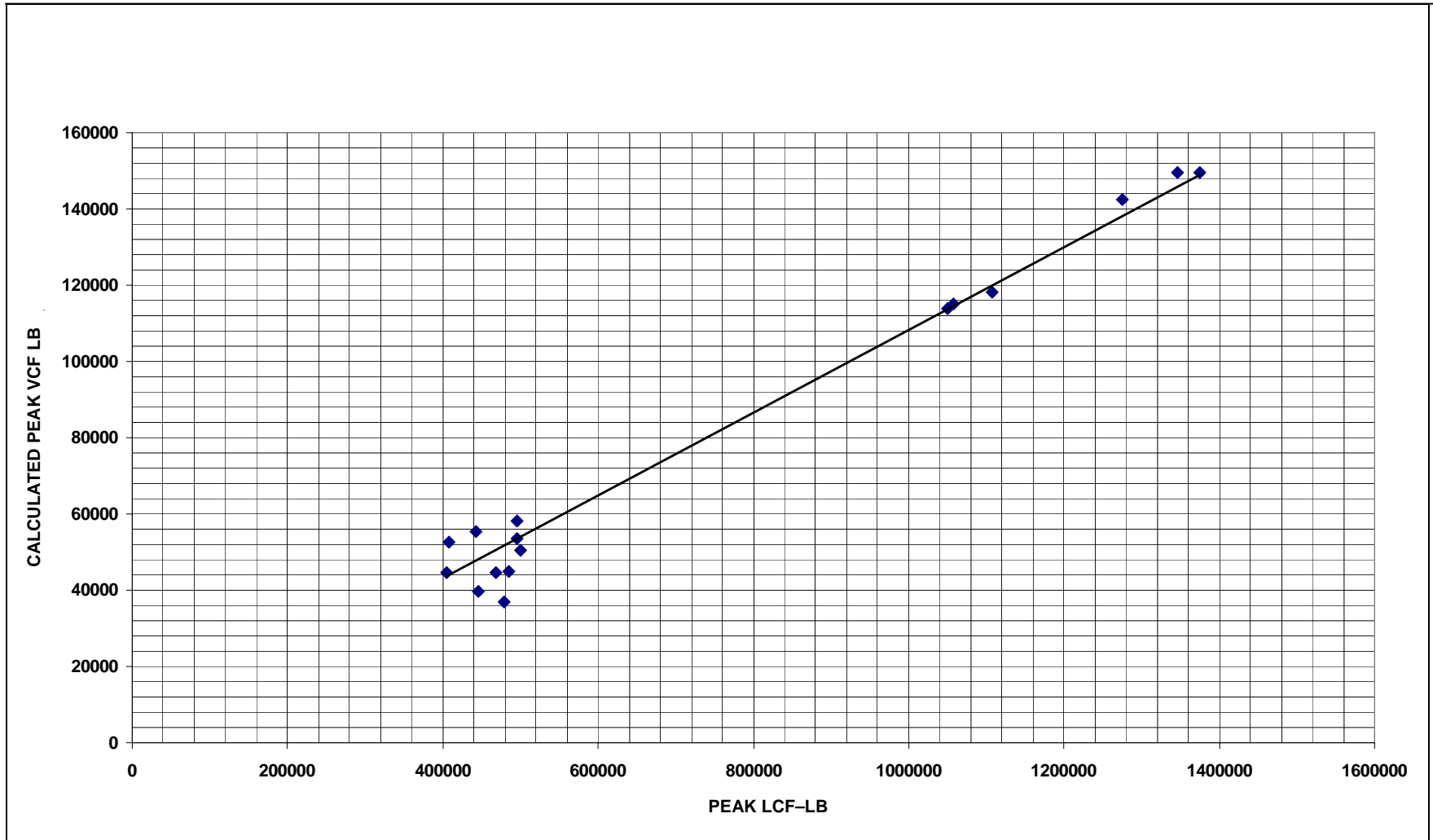


Plot A-6. Peak LCF versus Impact Velocity—All Impacts

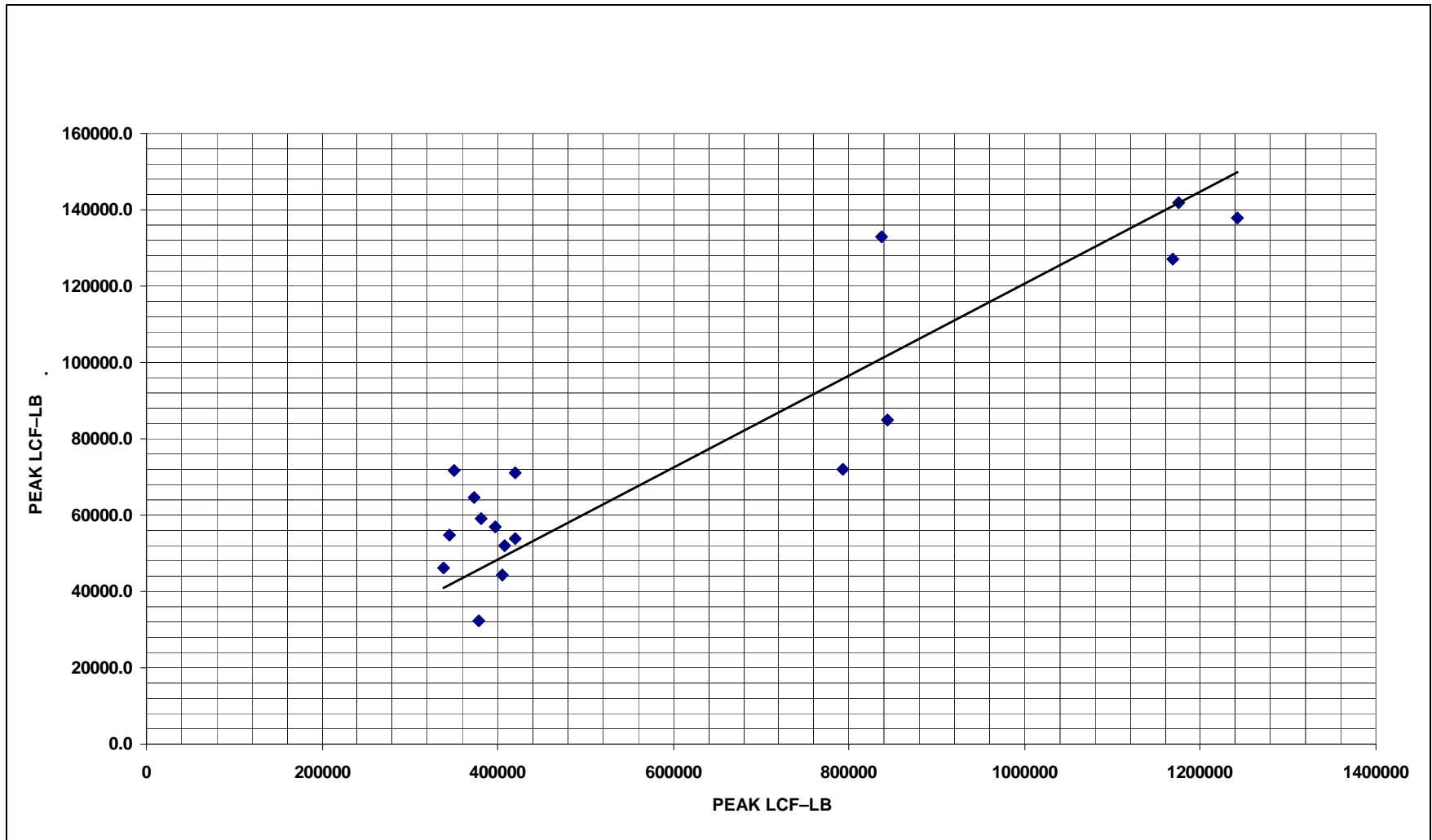


**Plot A-7. Calculated Peak VCF versus Peak LCF Impact Sequence 1**

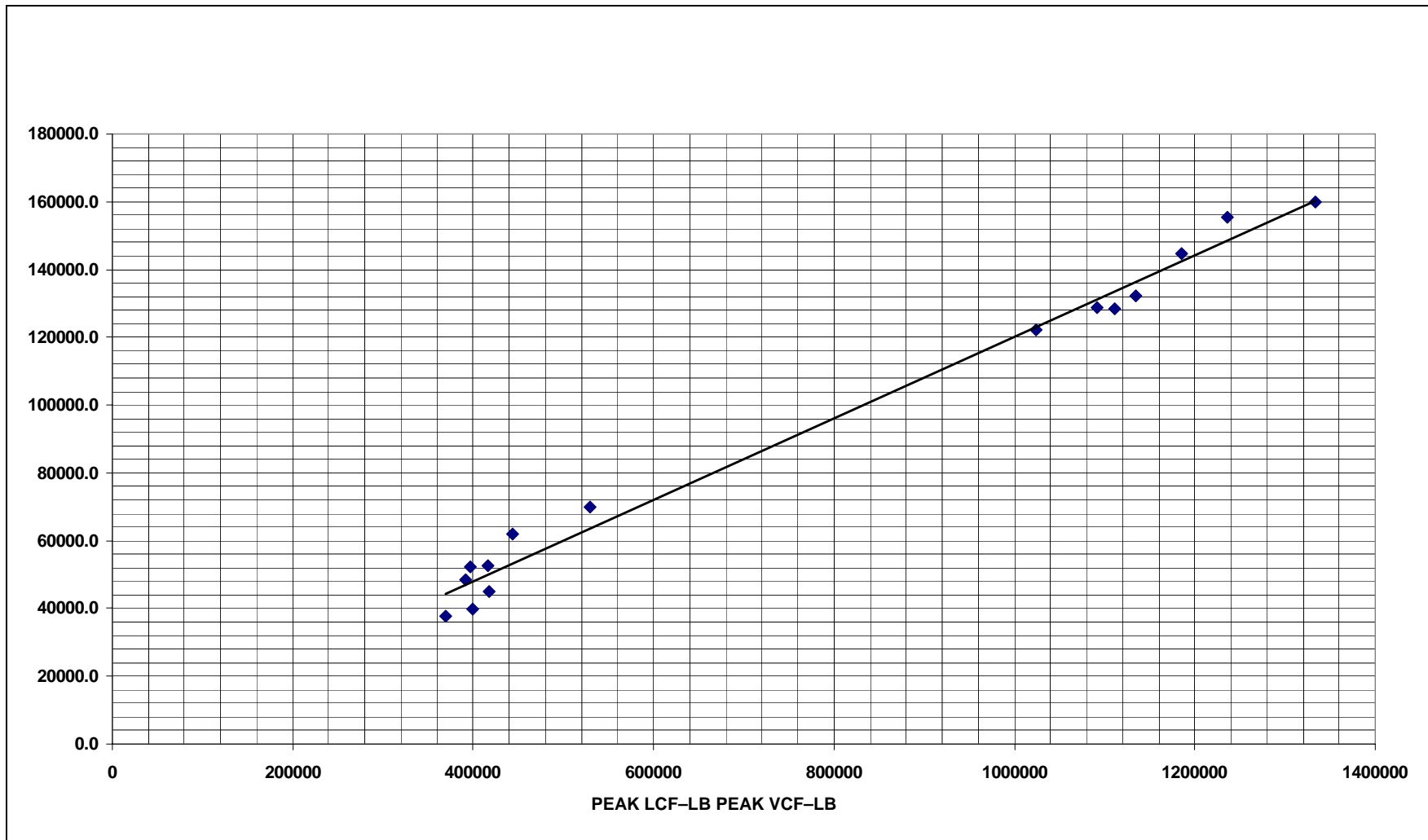




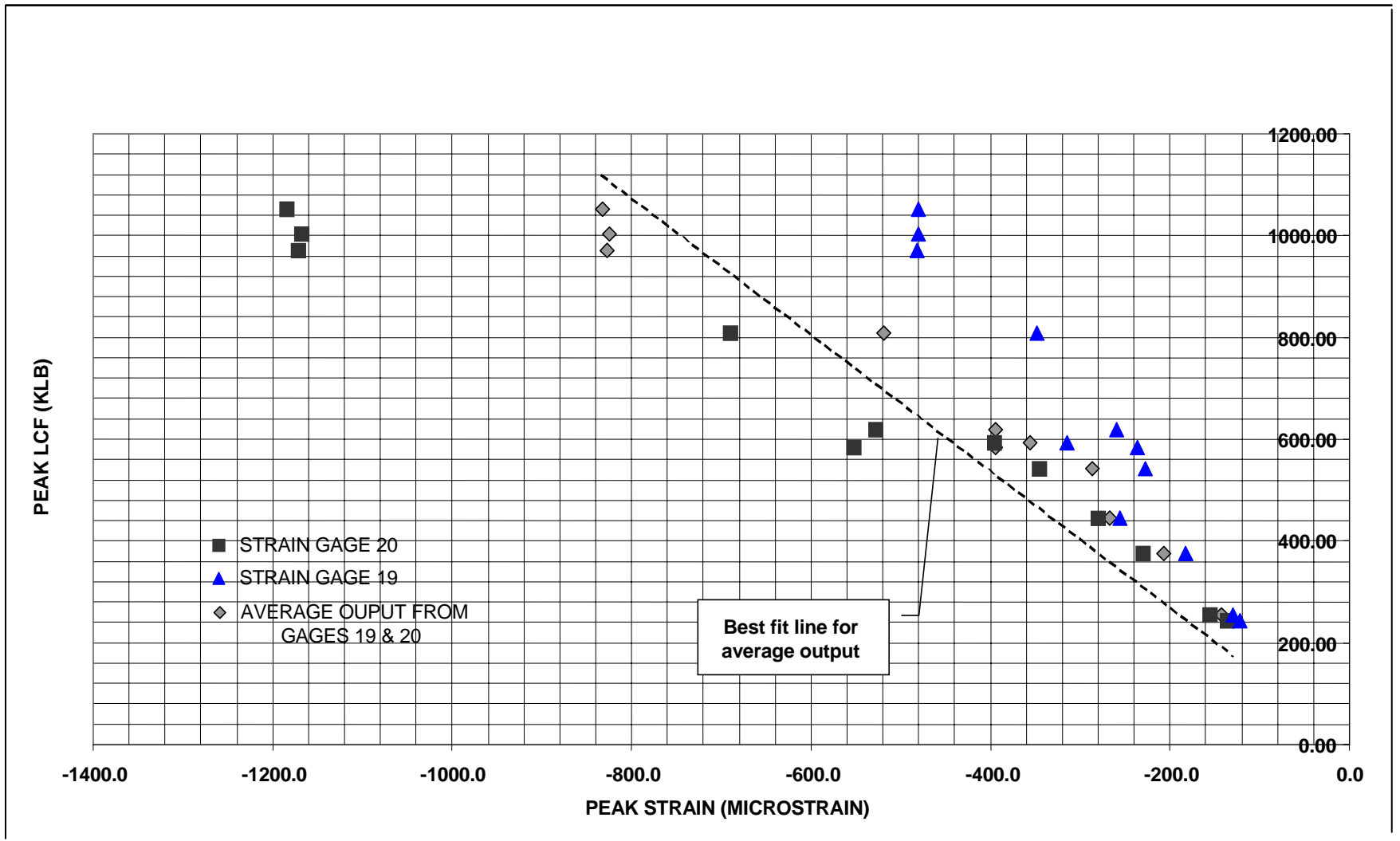
**Plot A-8. Calculated Peak VCF versus Peak LCF Impact Sequence 2**



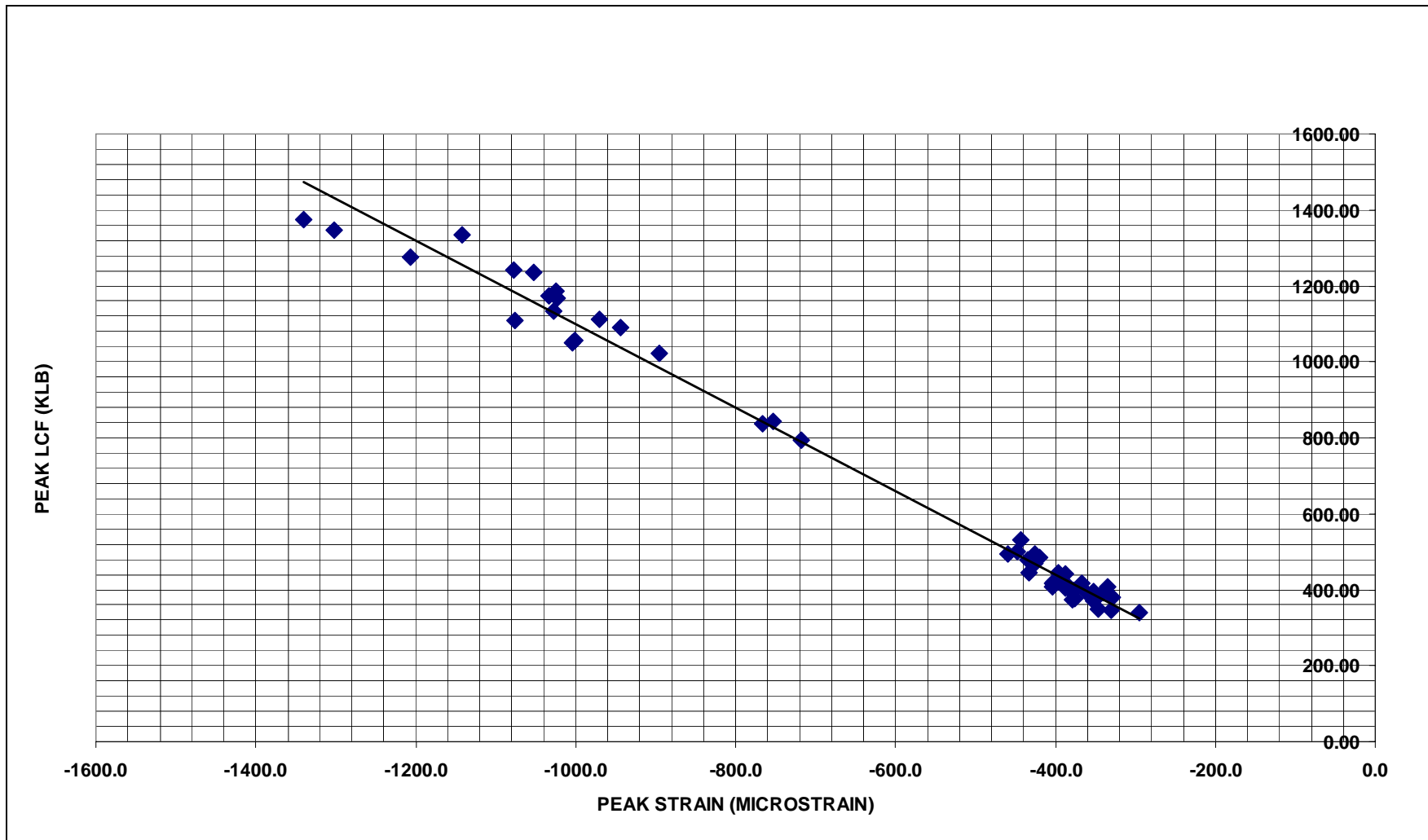
**Plot A-9. Calculated Peak VCF versus Peak LCF Impact Sequence 3**



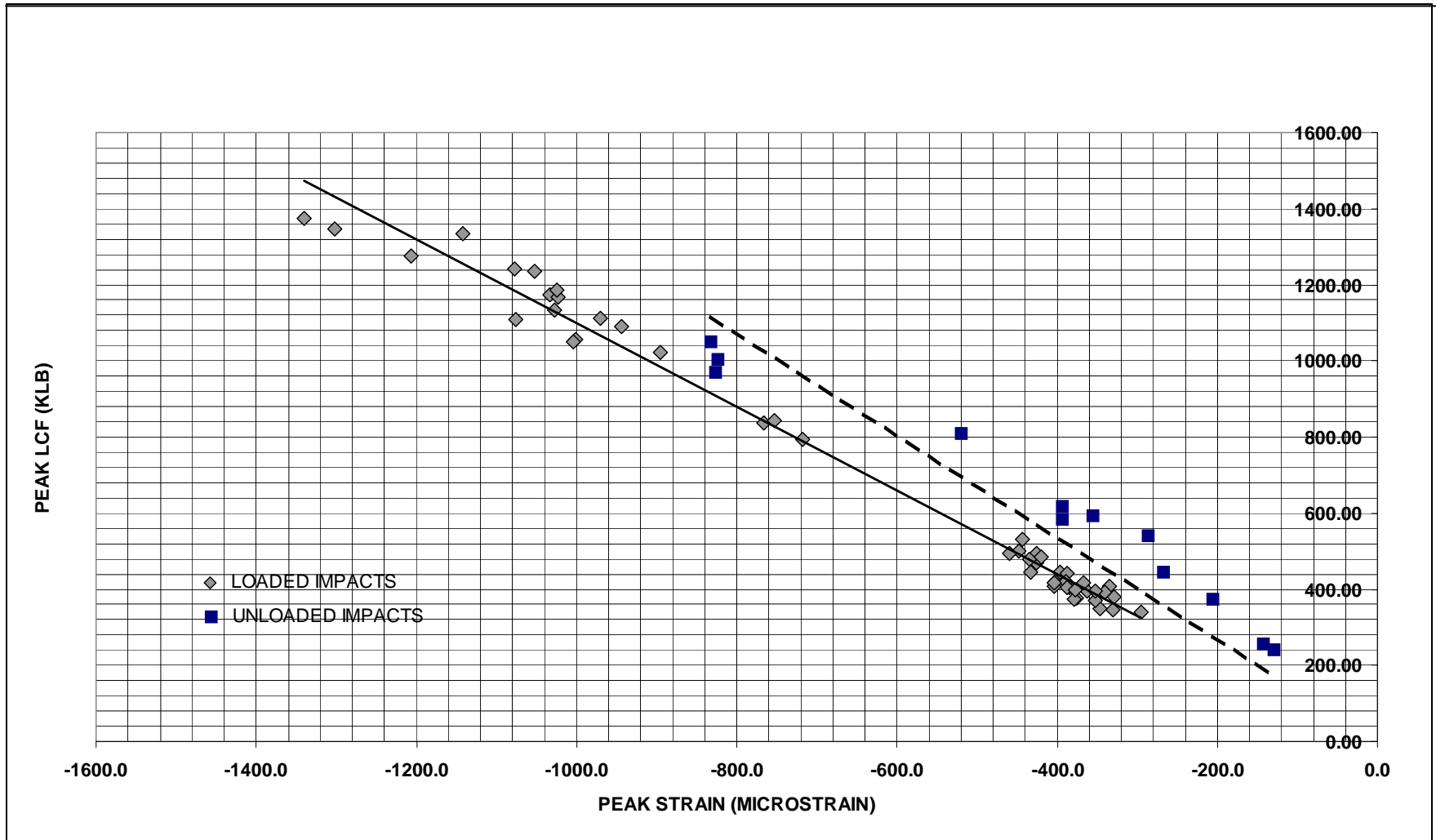
**Plot A-10. Calculated Peak VCF versus Peak LCF Impact Sequence 4**



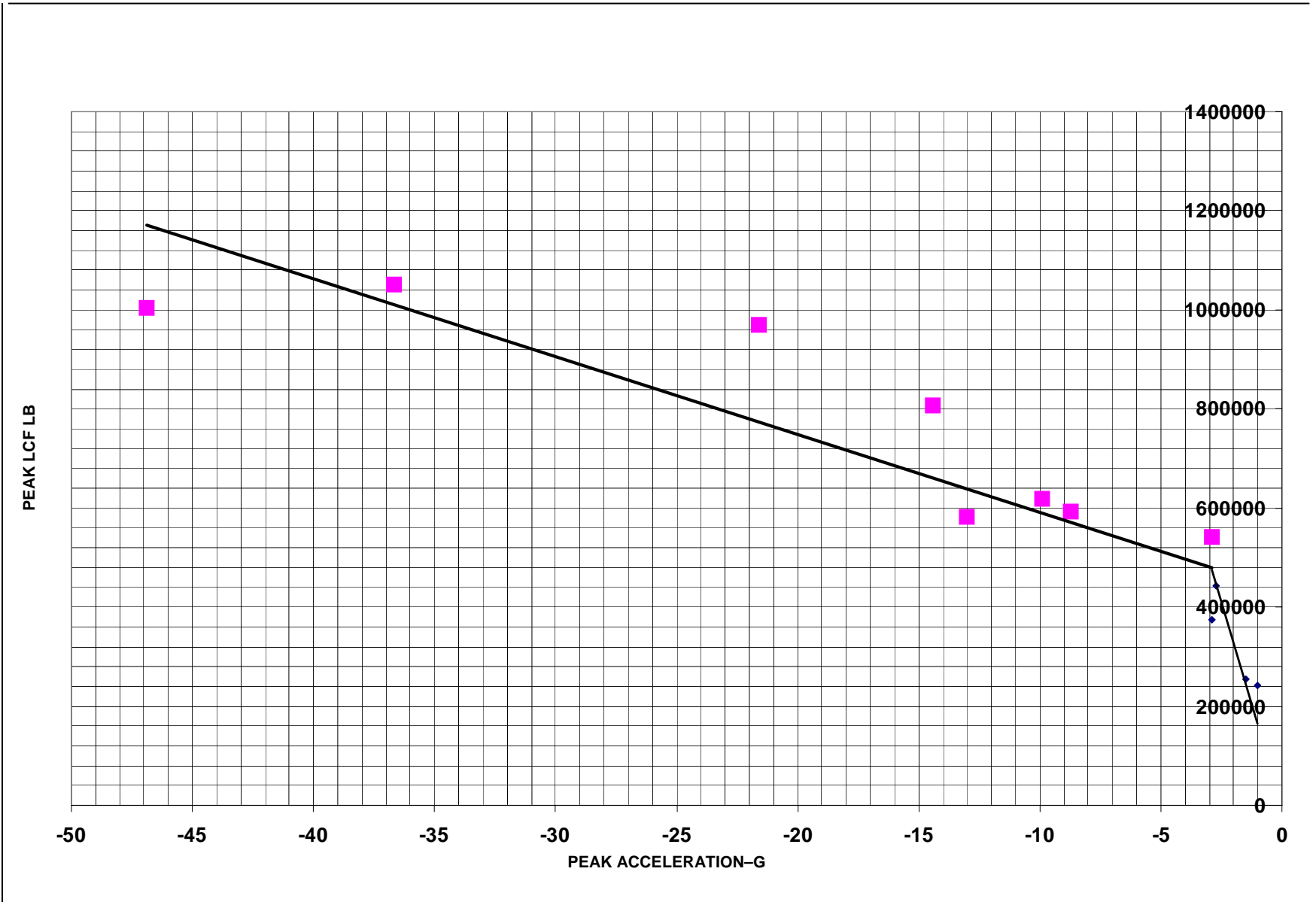
Plot A-11. Strain from Gages 19 and 20 versus Peak OCF Impact Sequence 1



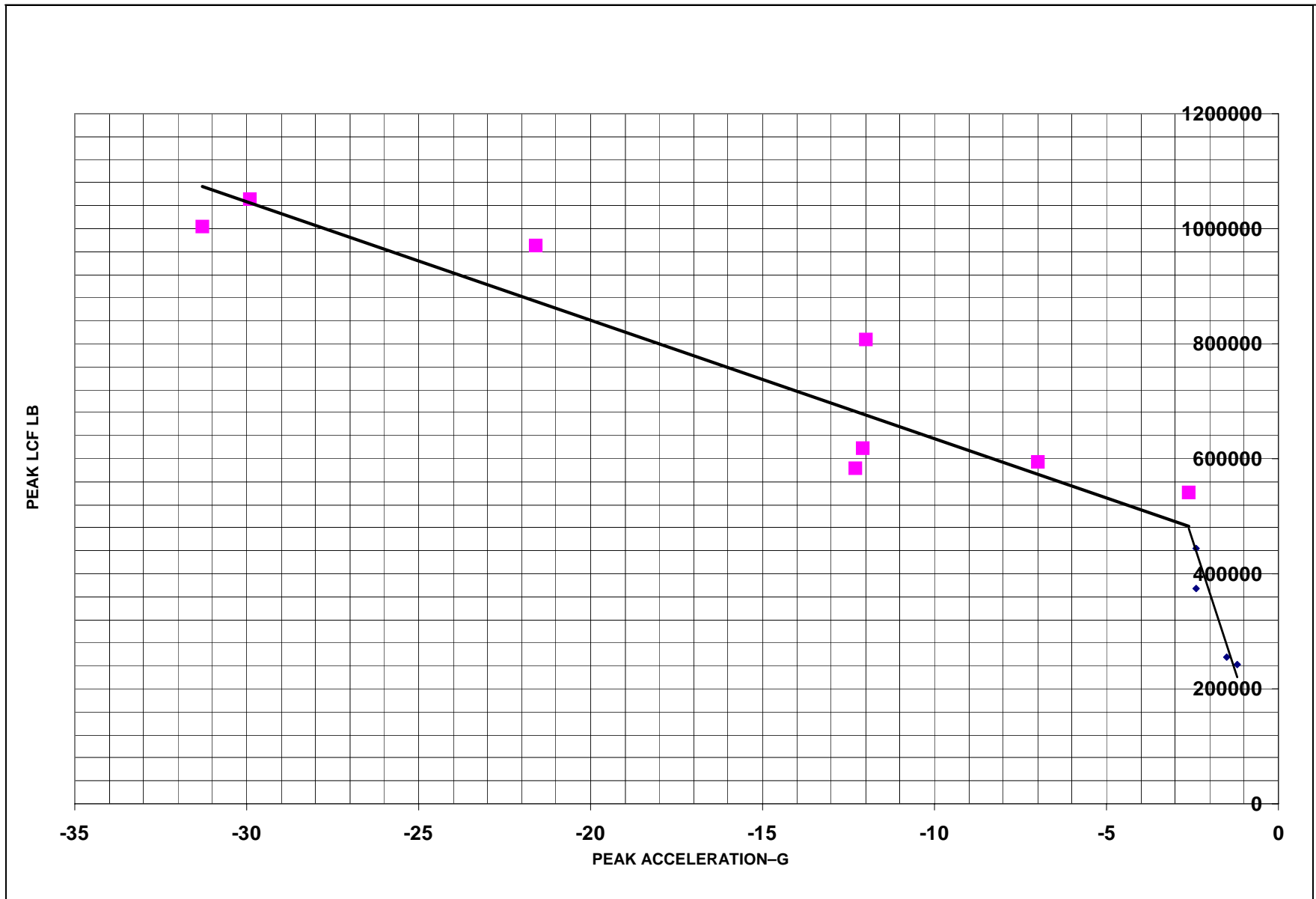
**Plot A-12. Average Strain from Gages 19 and 20 versus Peak LCF—All Loaded Impacts**



**Plot A-13. Average Strain from Gages 19 and 20 versus Peak LCF—All Impacts**

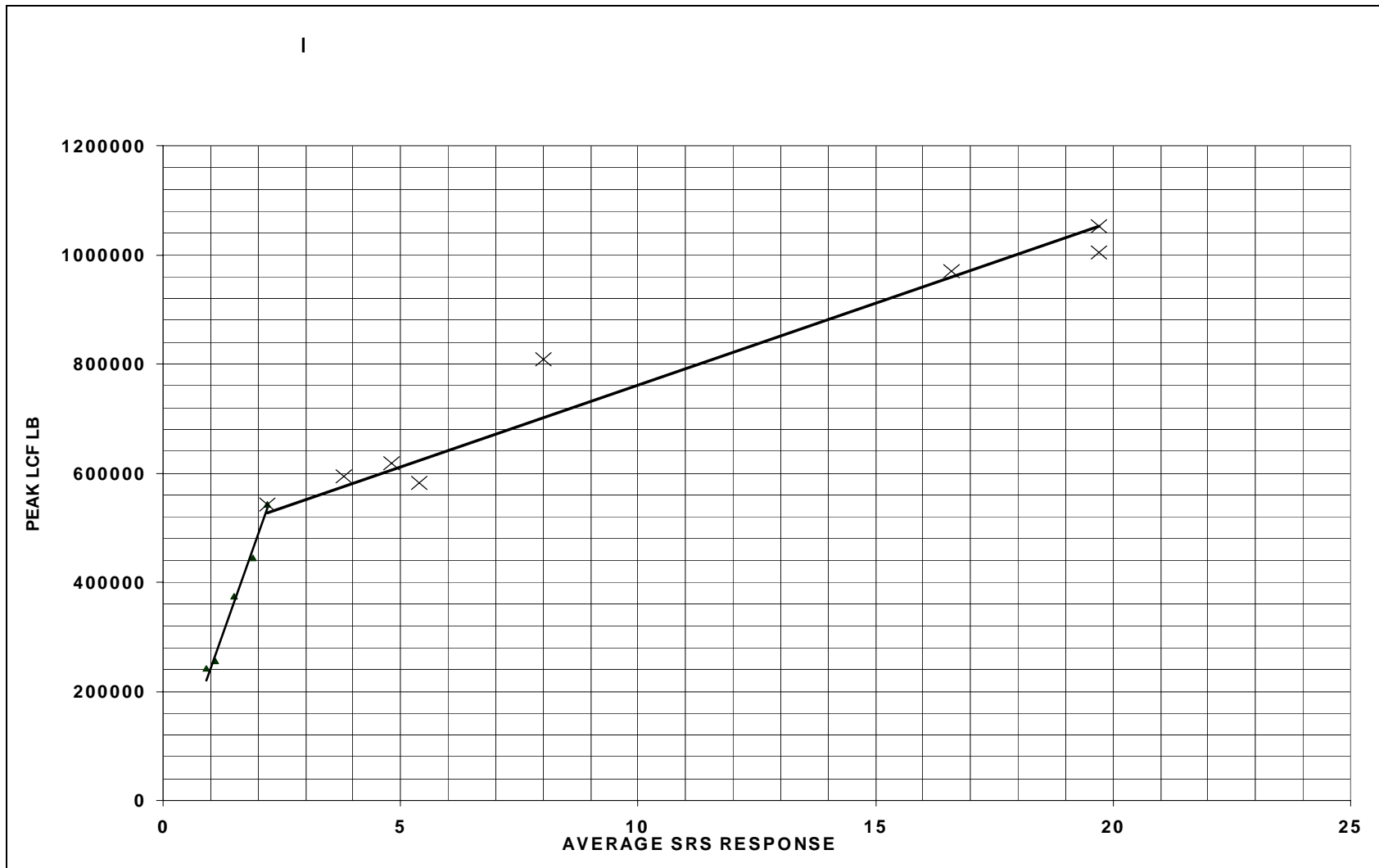


**Plot A-14. Peak Acceleration versus Peak LCF—Acceleration 6 Longitudinal**

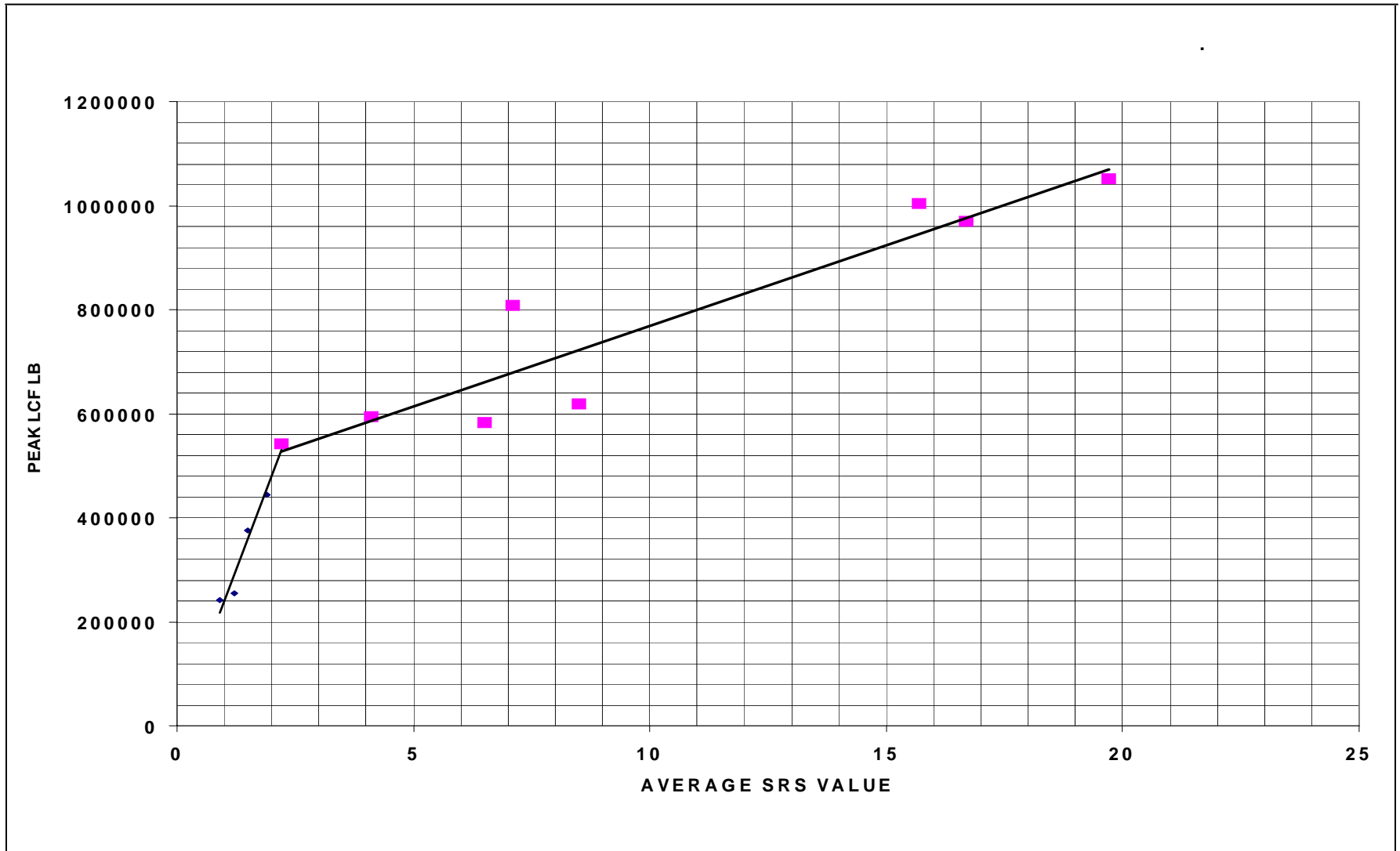


**Plot A-15. Peak Acceleration versus Peak LCF—Acceleration 18 Longitudinal**

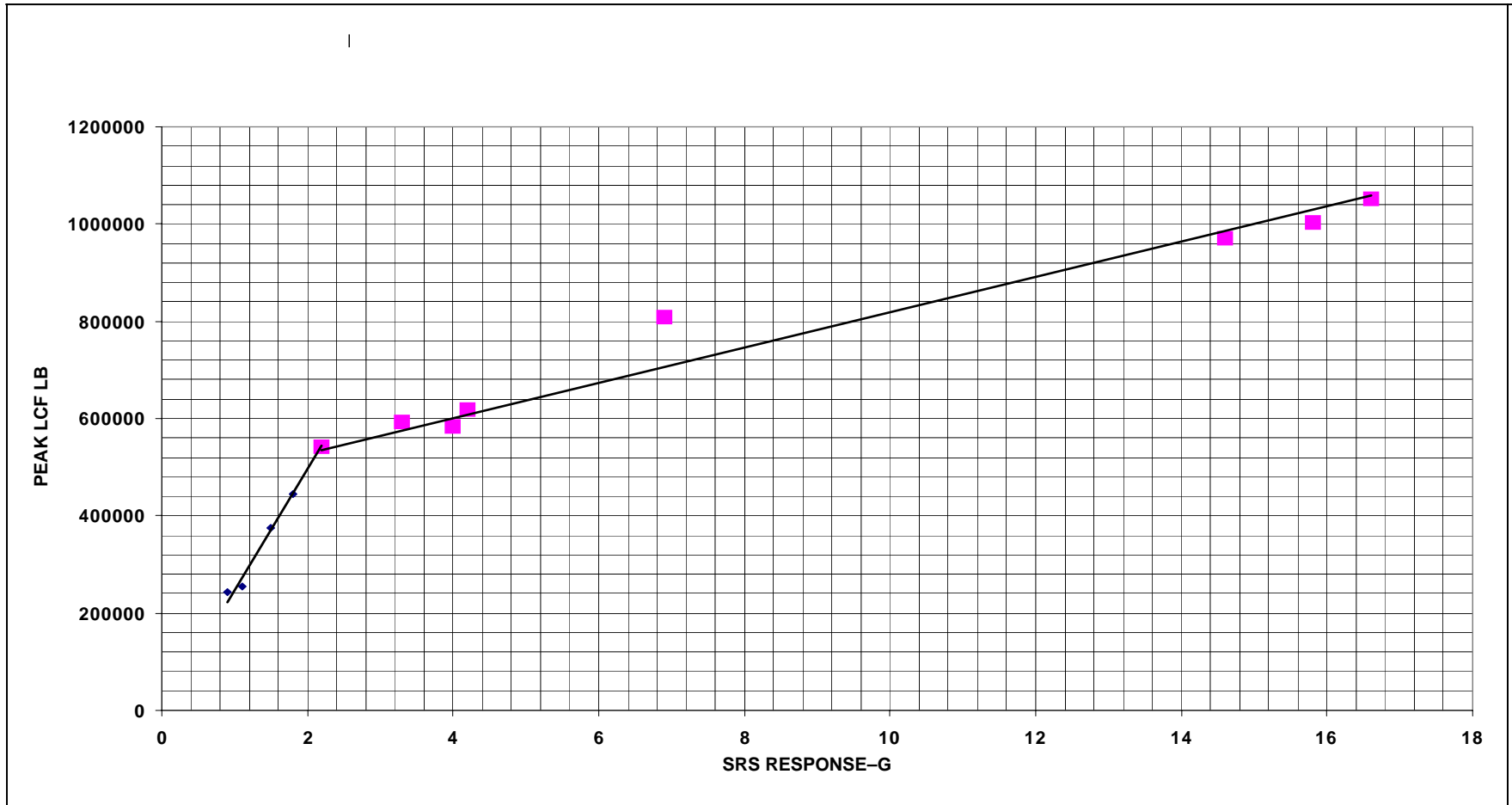




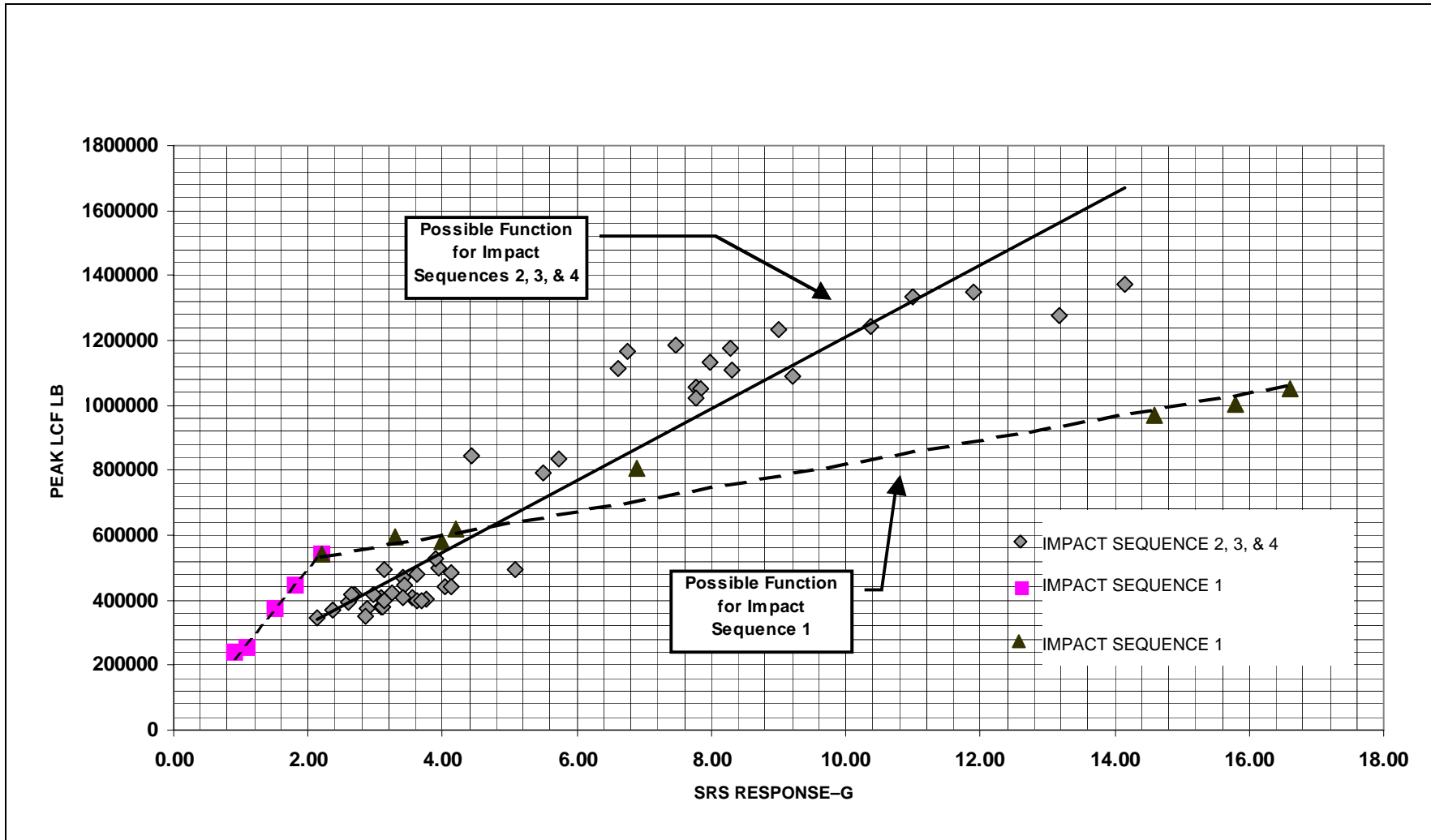
**Plot A-16. Average SRS Response, 10-100.8 HZ versus Peak LCF—Acceleration 6 Longitudinal**



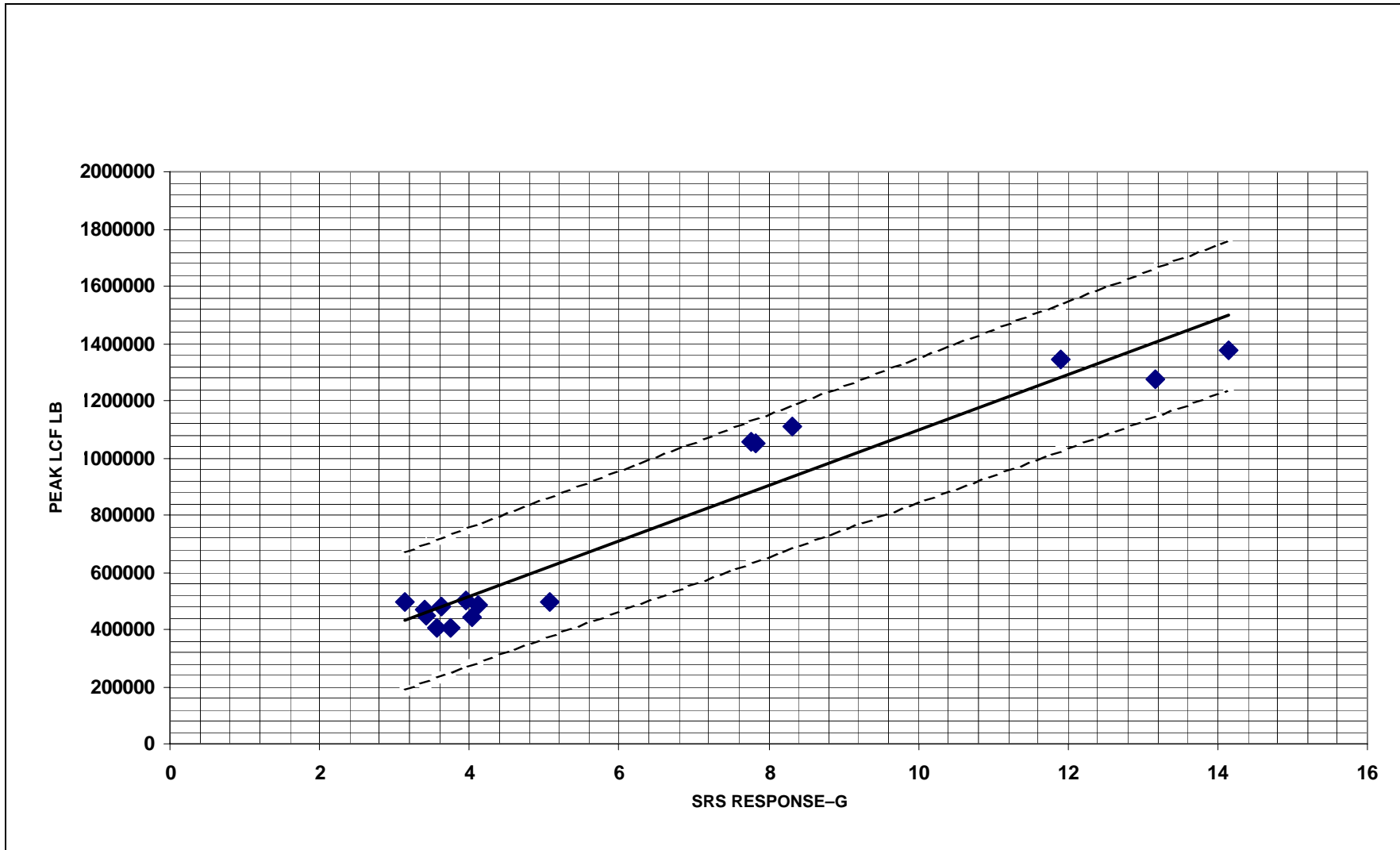
**Plot A-17. Average SRS Response, 10-100.8 Hz versus Peak LCF—Acceleration 18 Longitudinal**



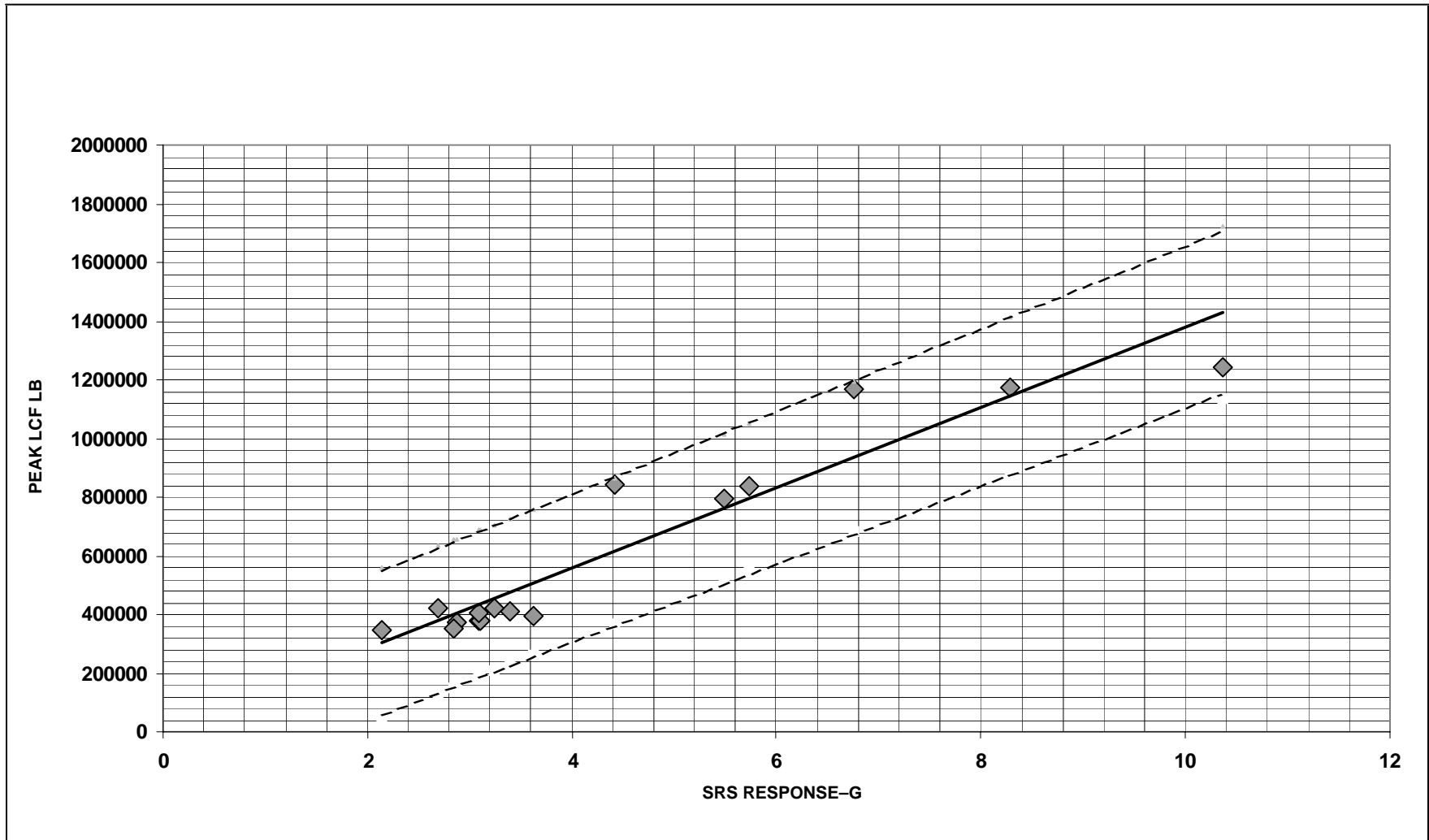
**Plot A-18. Average Longitudinal SRS Response (5-50 Hz) versus Peak LCF—Acceleration 6, Impact Sequence 1**



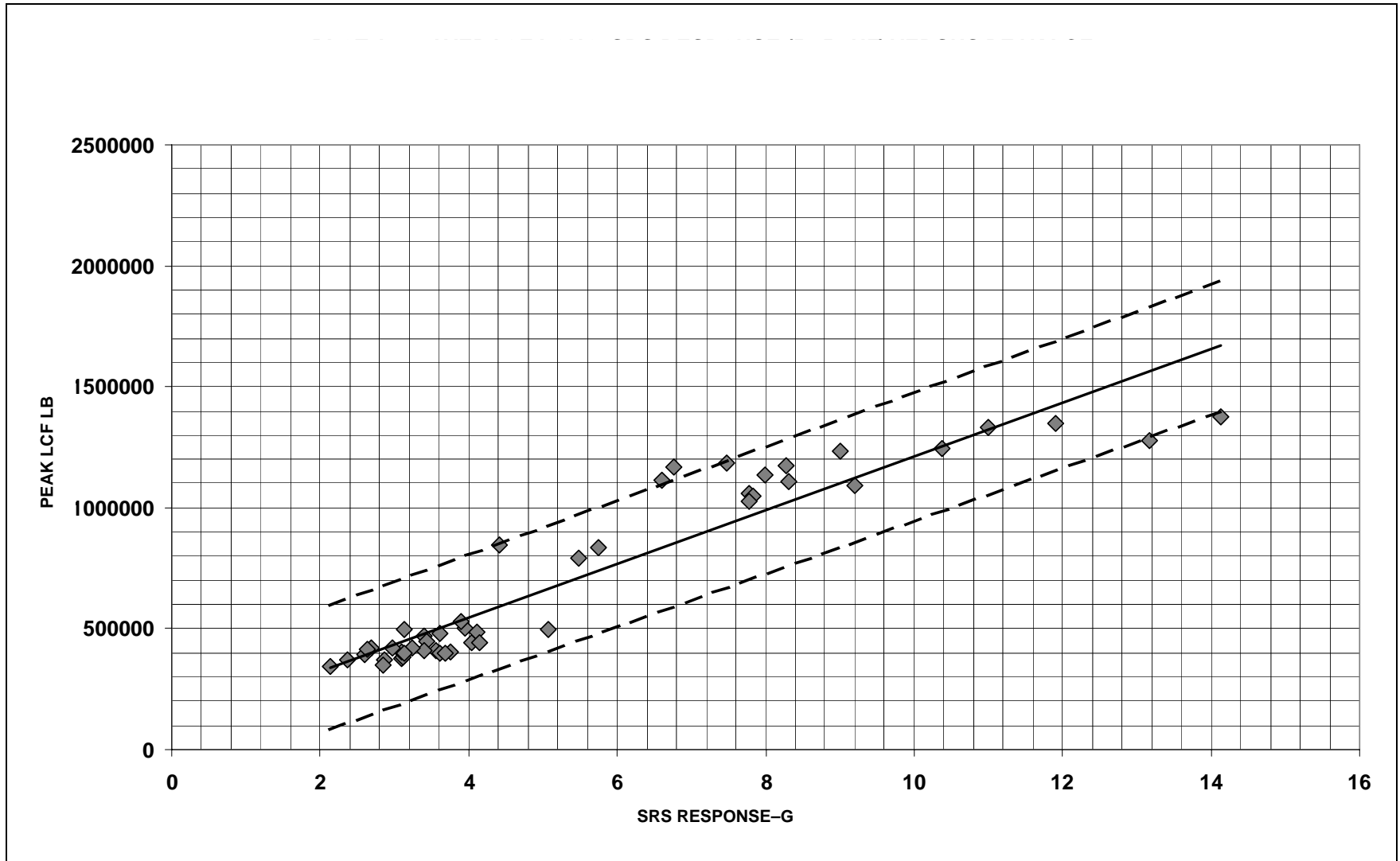
Plot A-19. Average Longitudinal SRS Response (5-50 Hz) versus Peak LCF—Acceleration 6, All Impacts—Sequence 1, 2, 3, and 4



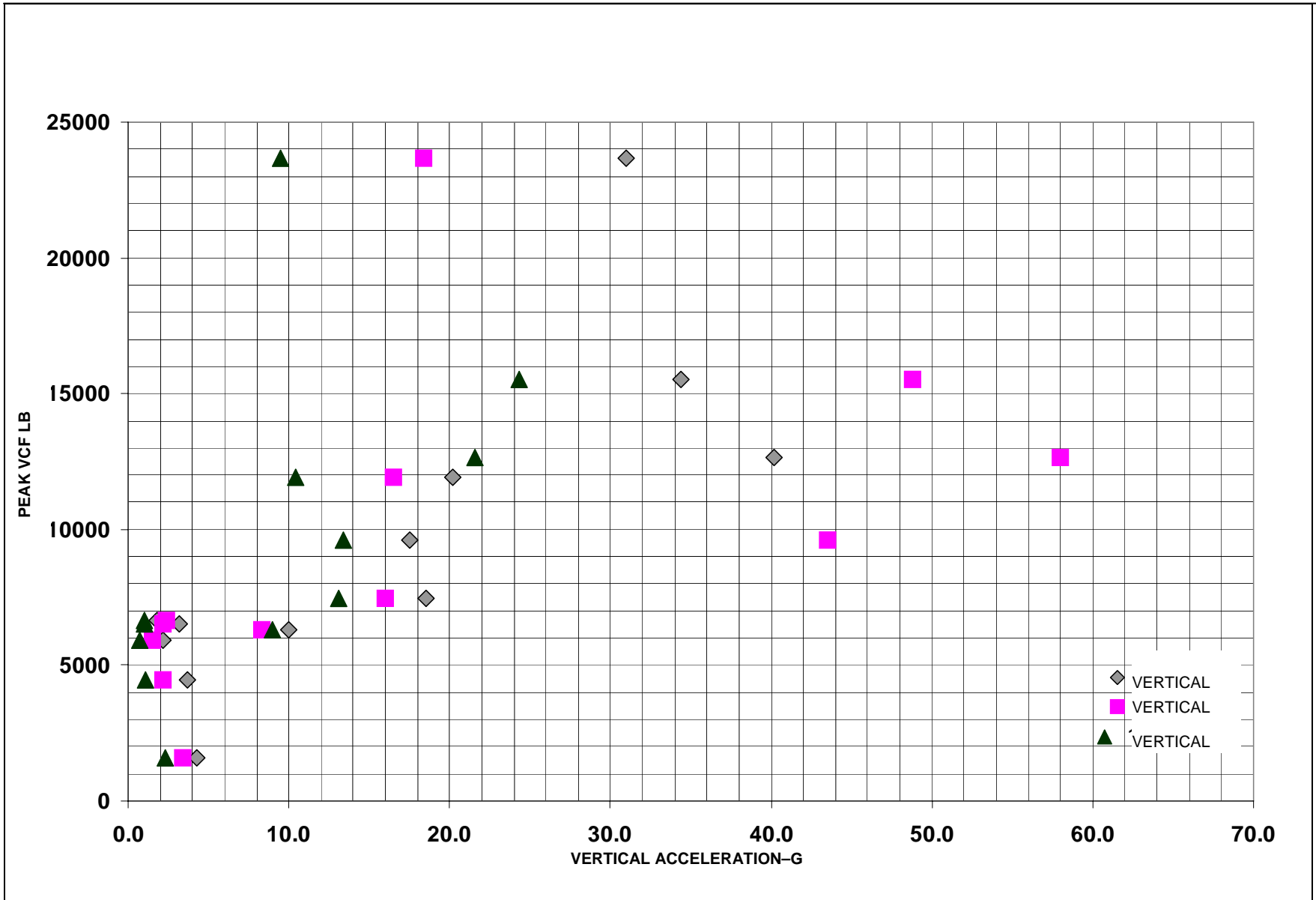
**Plot A-20. Average Longitudinal SFS Response (5-50 Hz) versus Peak LCF—Acceleration 6, Impact Sequence 2—Regression Analysis**



**Plot A-21. Average Longitudinal SRS Response (5-50 Hz) versus Peak LCF—Acceleration 6, Impact Sequence 3—Regression Analysis**

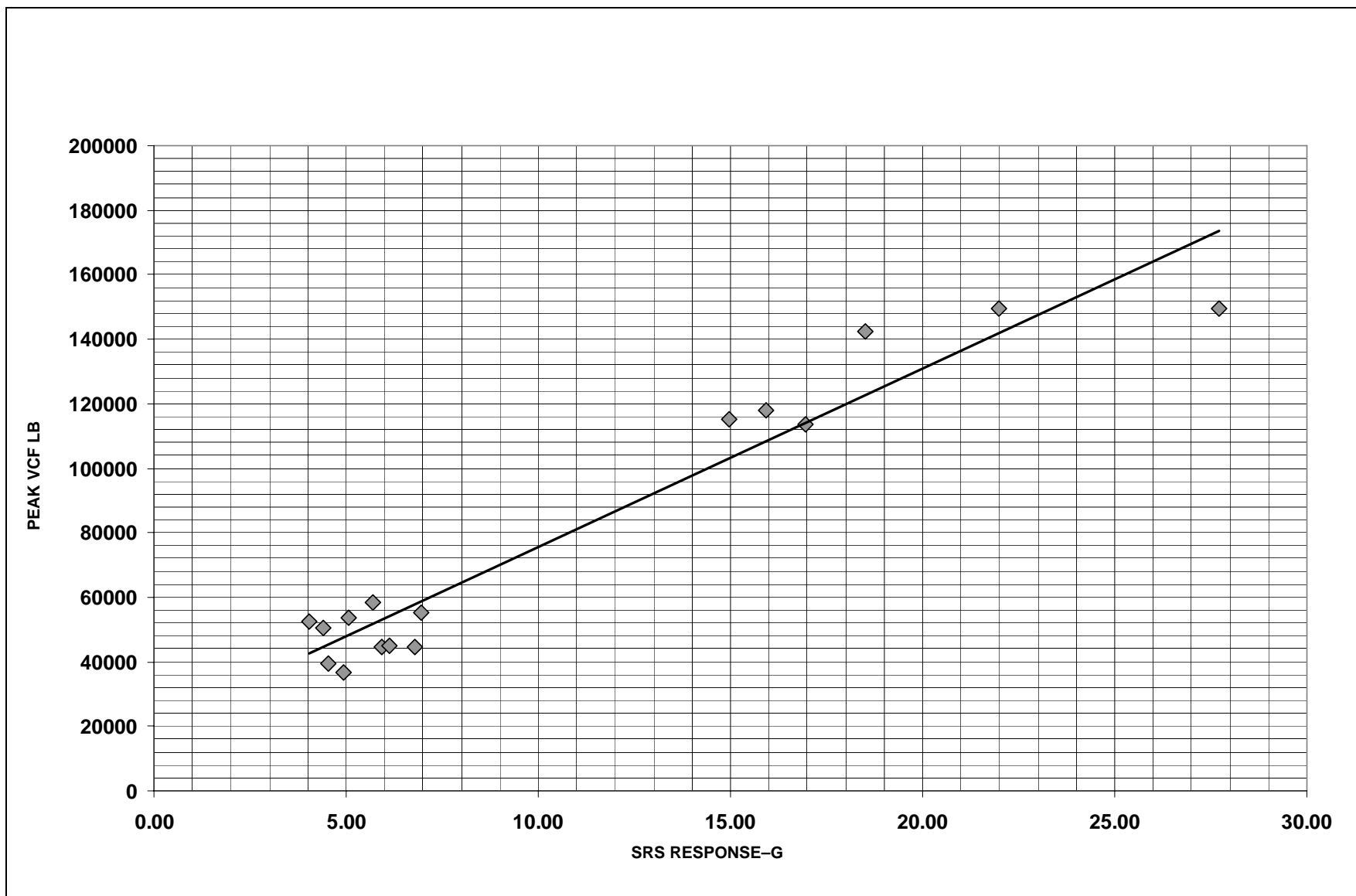


**Plot A-22. Average Longitudinal SRS Response (5-50 Hz) versus Peak LCF—Acceleration 6, Sequence 2, 3, and 4—Regression Analysis**

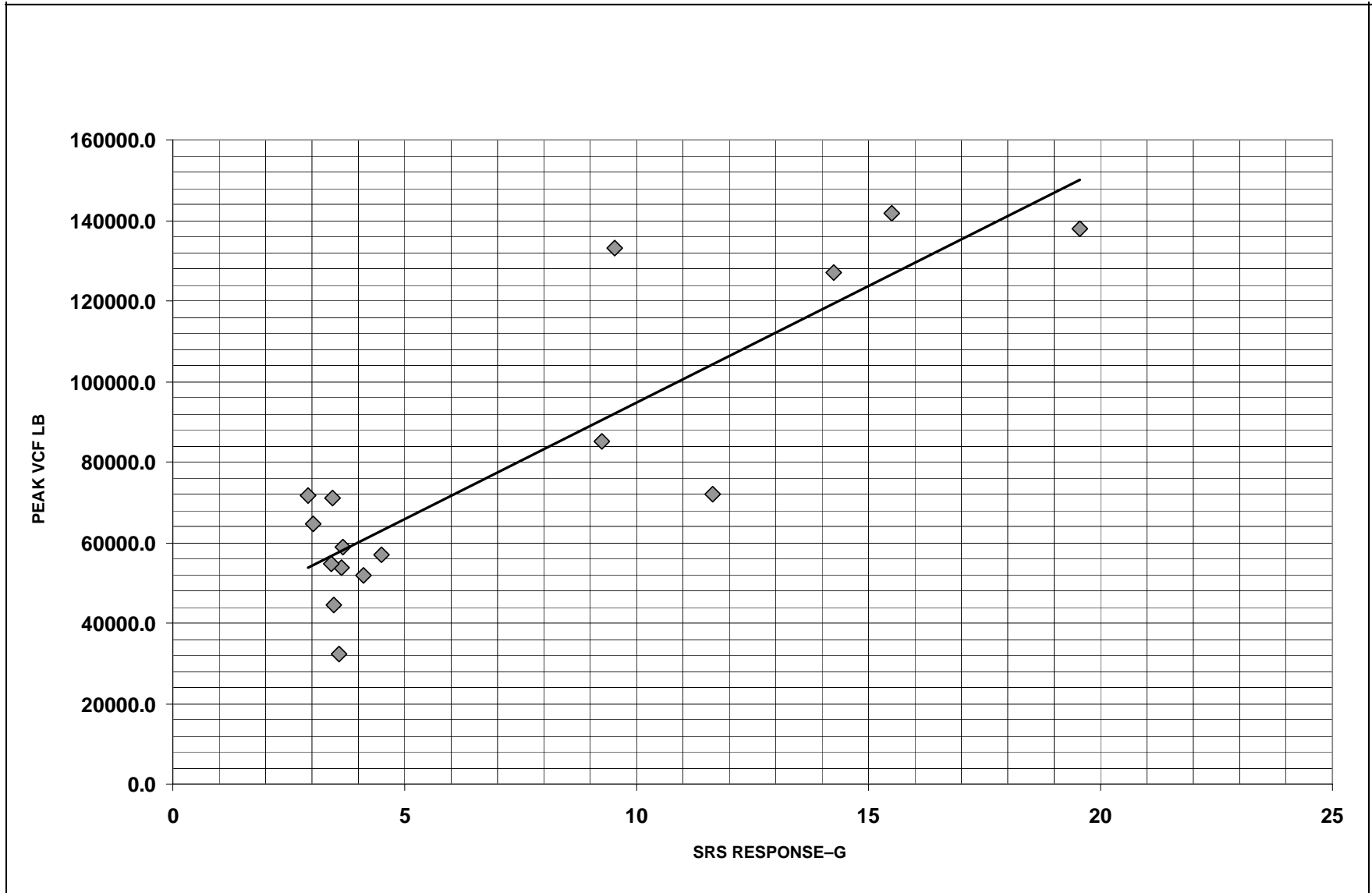


Plot A-23. Maximum Vertical Acceleration versus Peak LCF—Accelerations 5, 6, and 18 Vertical

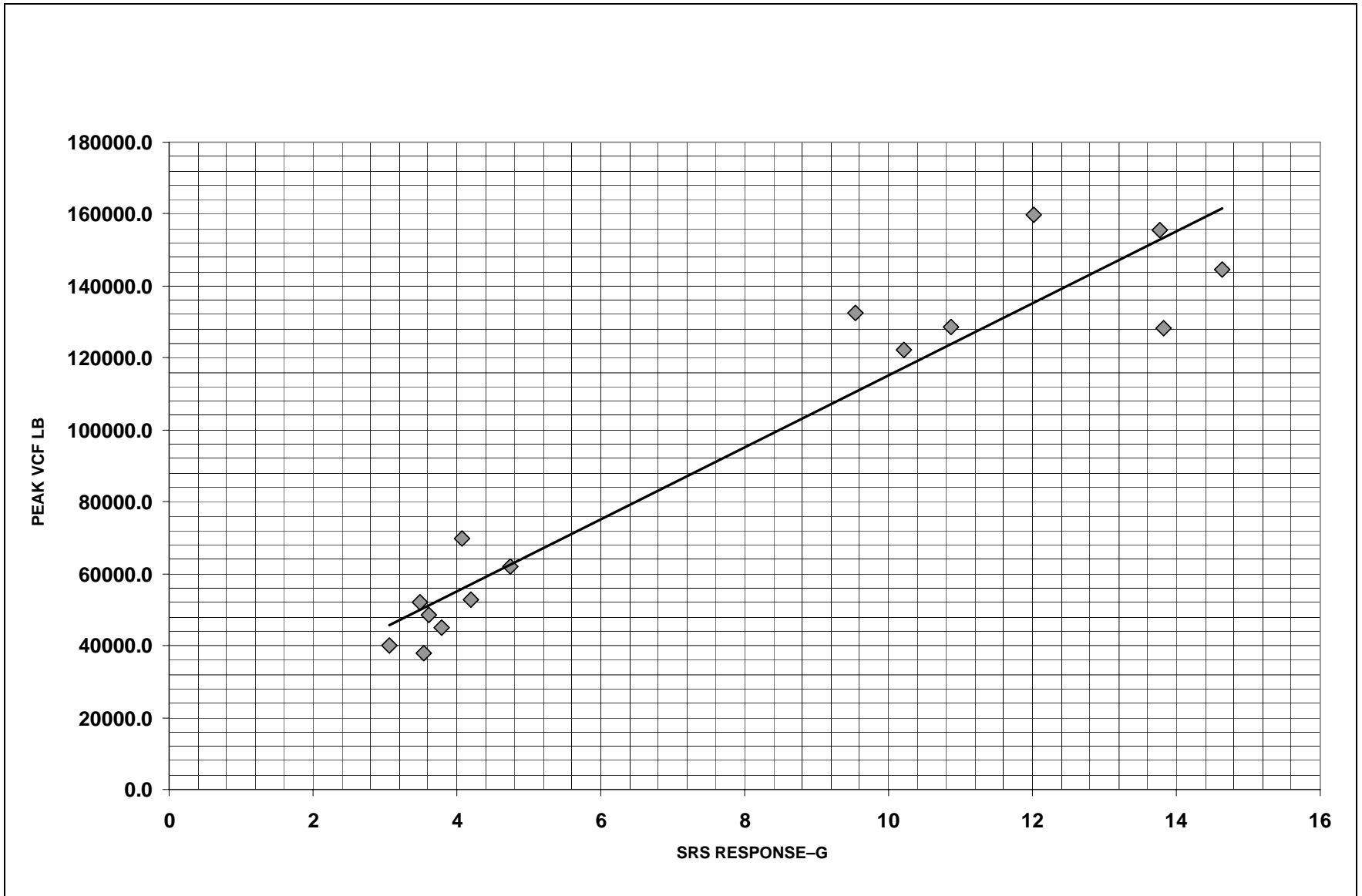




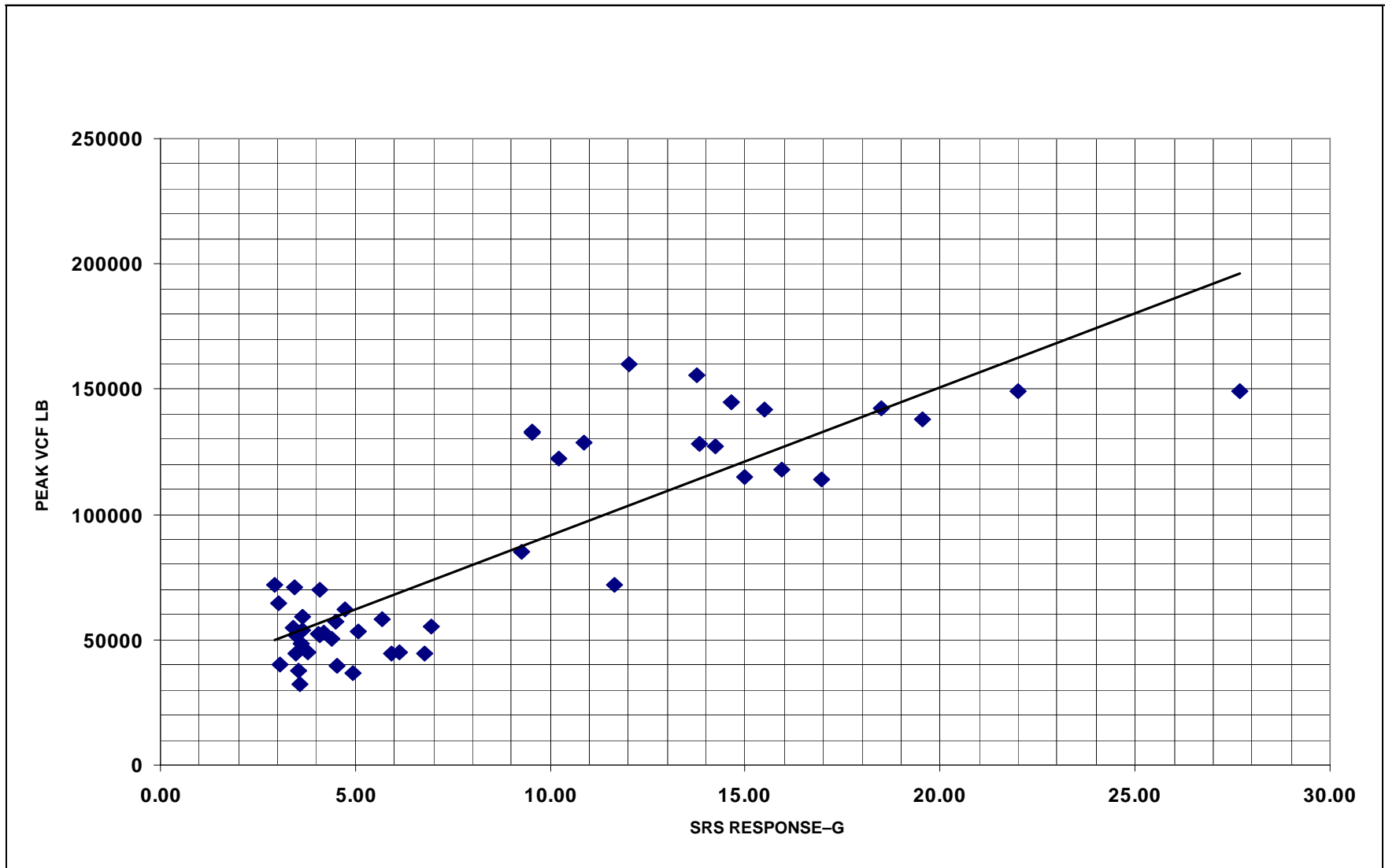
**Plot A-24. Average Vertical SRS Response (5-50Hz) versus Peak VCF Impact—Acceleration 6, Sequence 2**



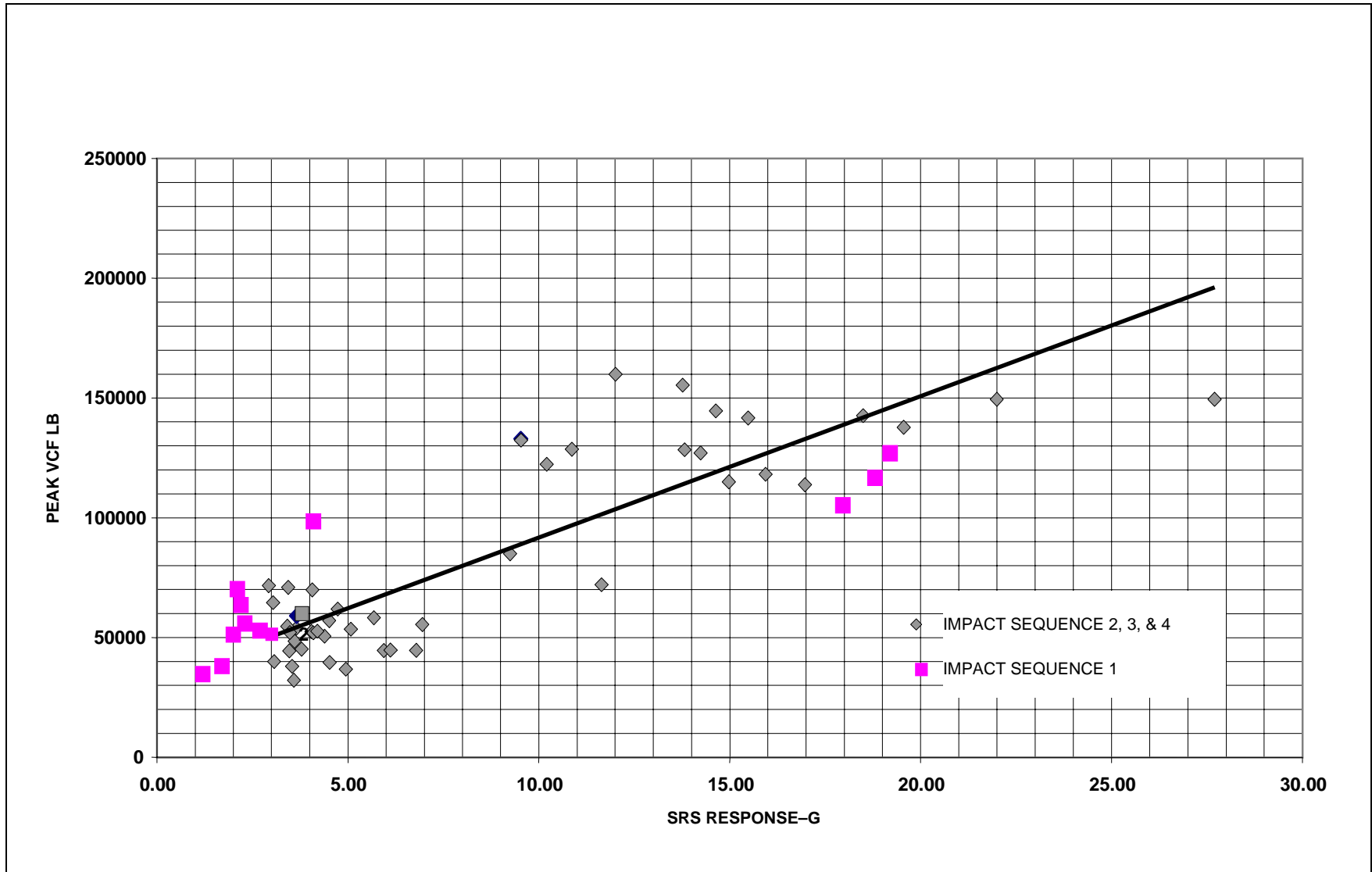
Plot A-25. Average Vertical SRS Response (5-50 Hz) versus Peak VCF Impact—Acceleration 6, Sequence 3



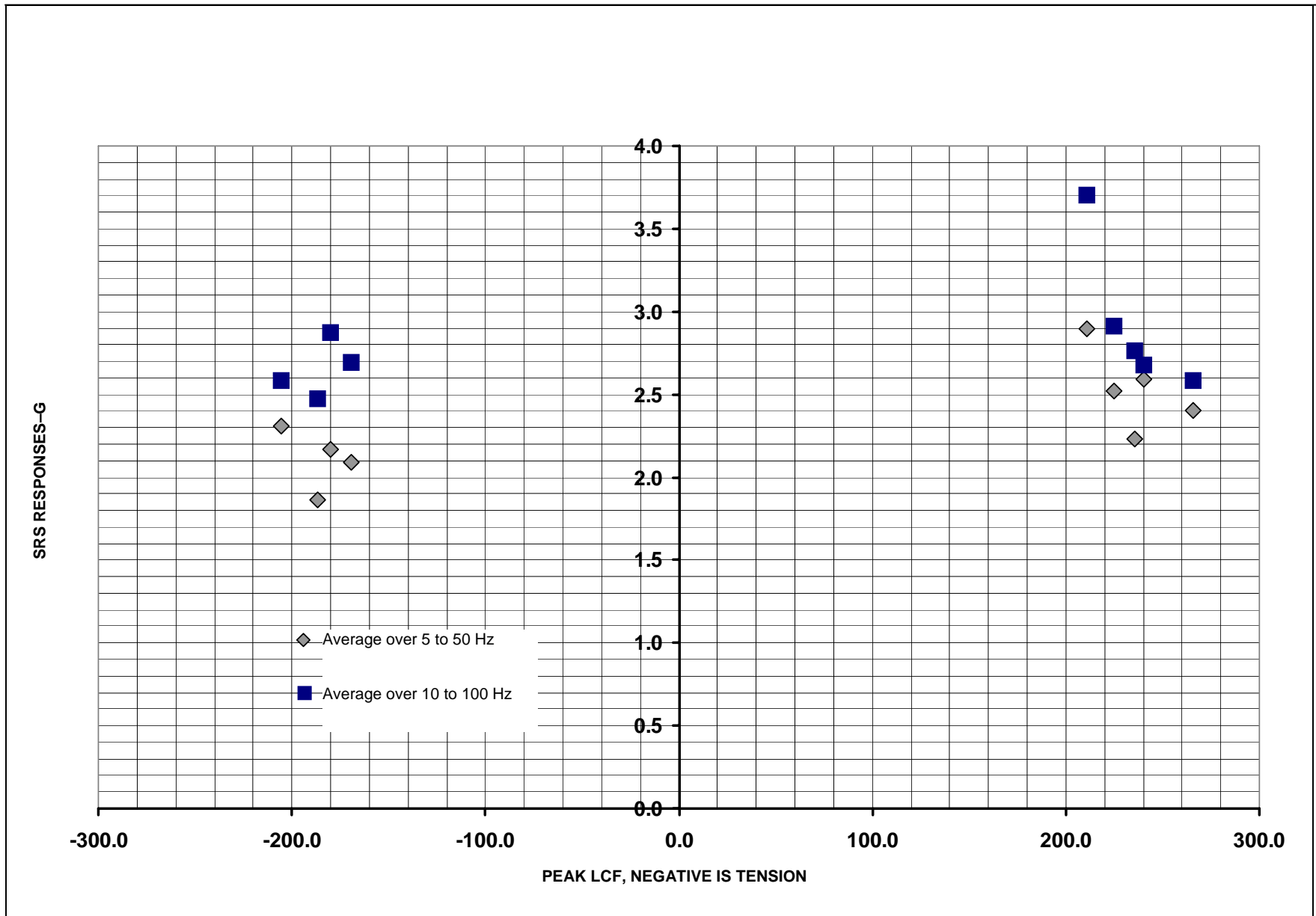
**Plot A-26. Average Vertical SRS Response (5-50 Hz) versus Peak VCF Impact—Acceleration 6, Sequence 4**



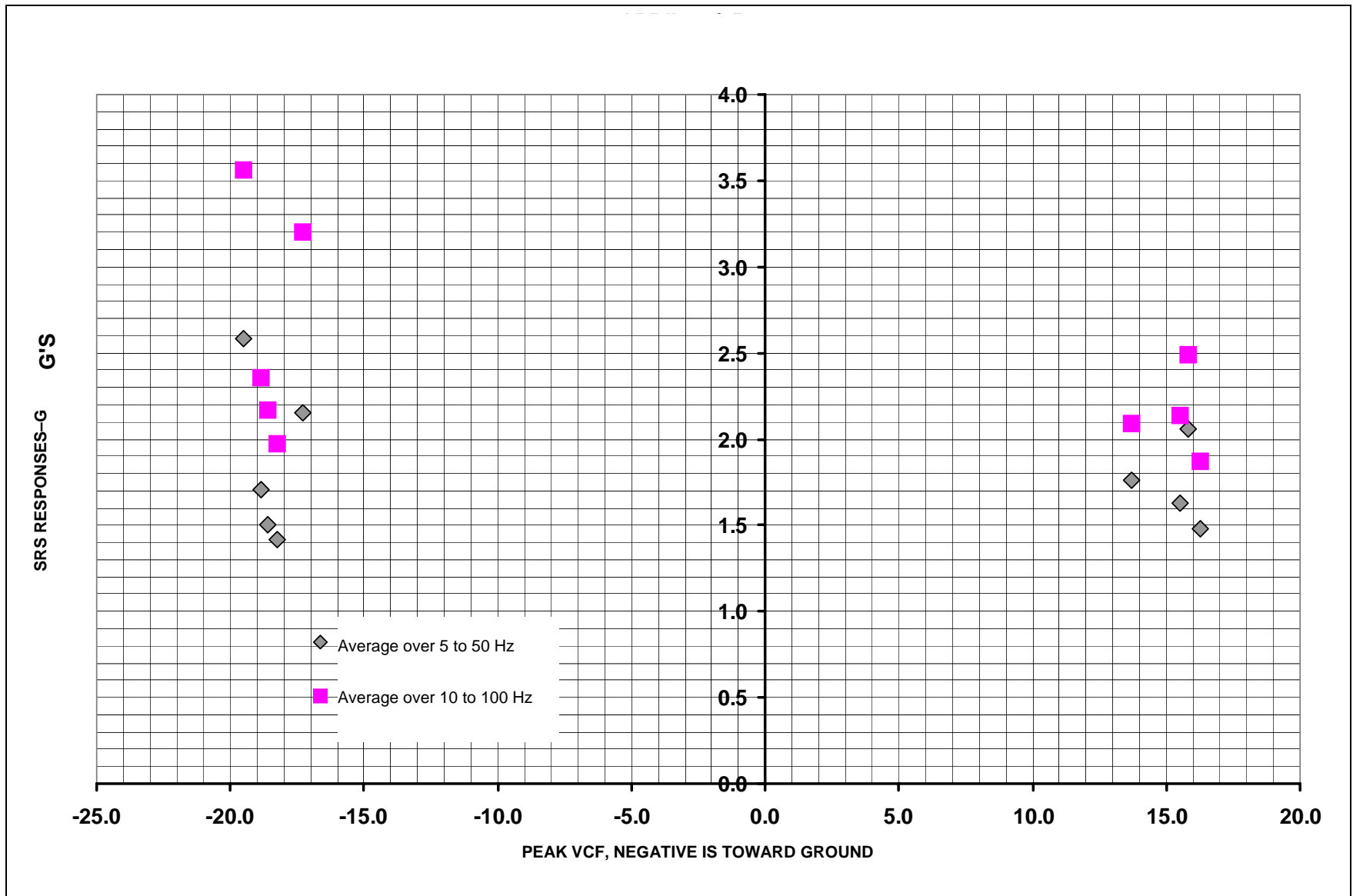
**Plot A-27. Average Vertical SRS Response (5-50 Hz) versus Peak VCF—Acceleration 6, Sequence 2, 3, and 4**



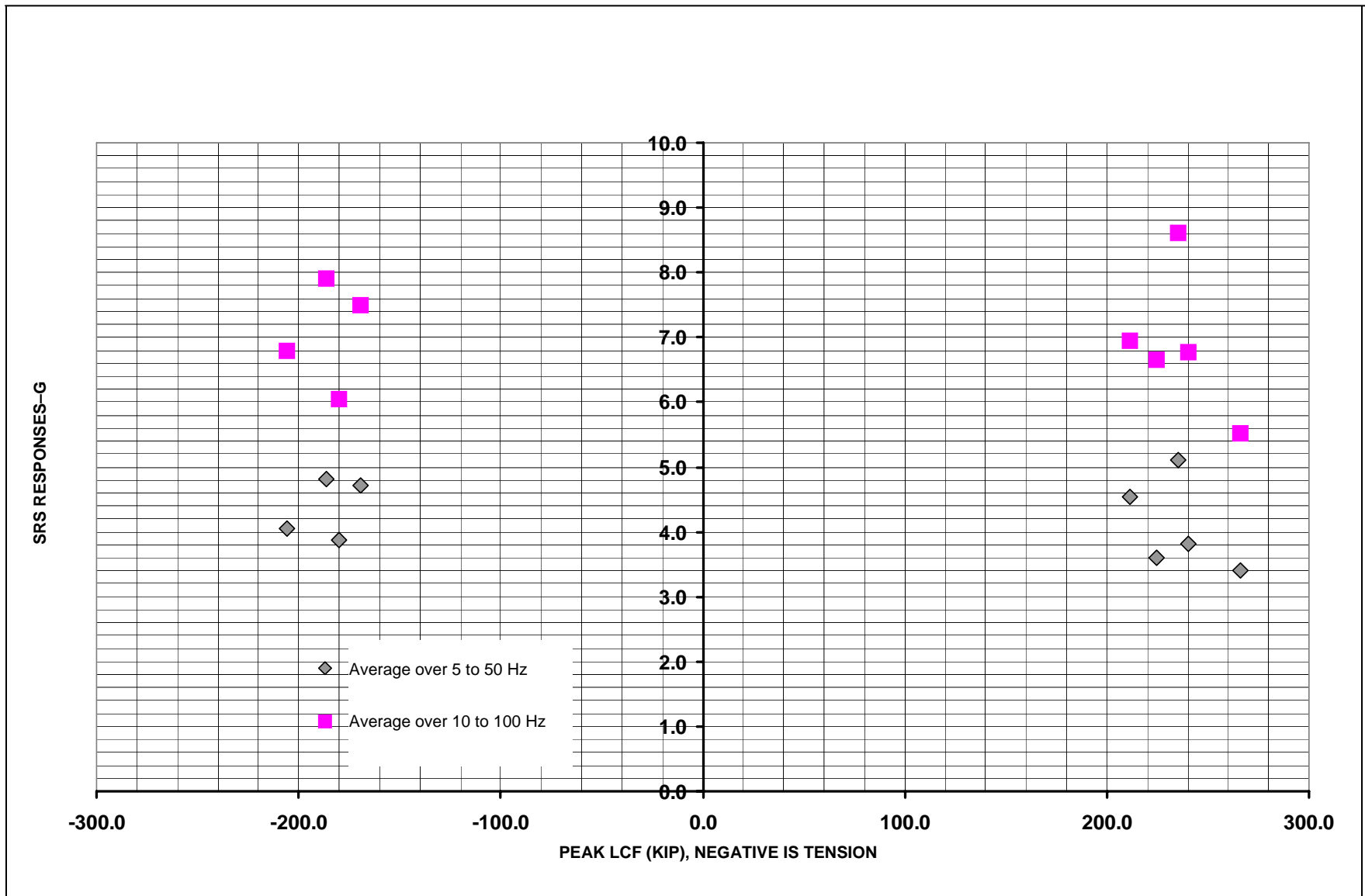
**Plot A-28. Average Vertical SRS Response (5-50 Hz) versus Peak VCF—Acceleration 6, Sequence 1, 2, 3, and 4**



Plot A-29. SRS Response versus Peak LCF—Acceleration 18 Longitudinal, April 14-15, 2003

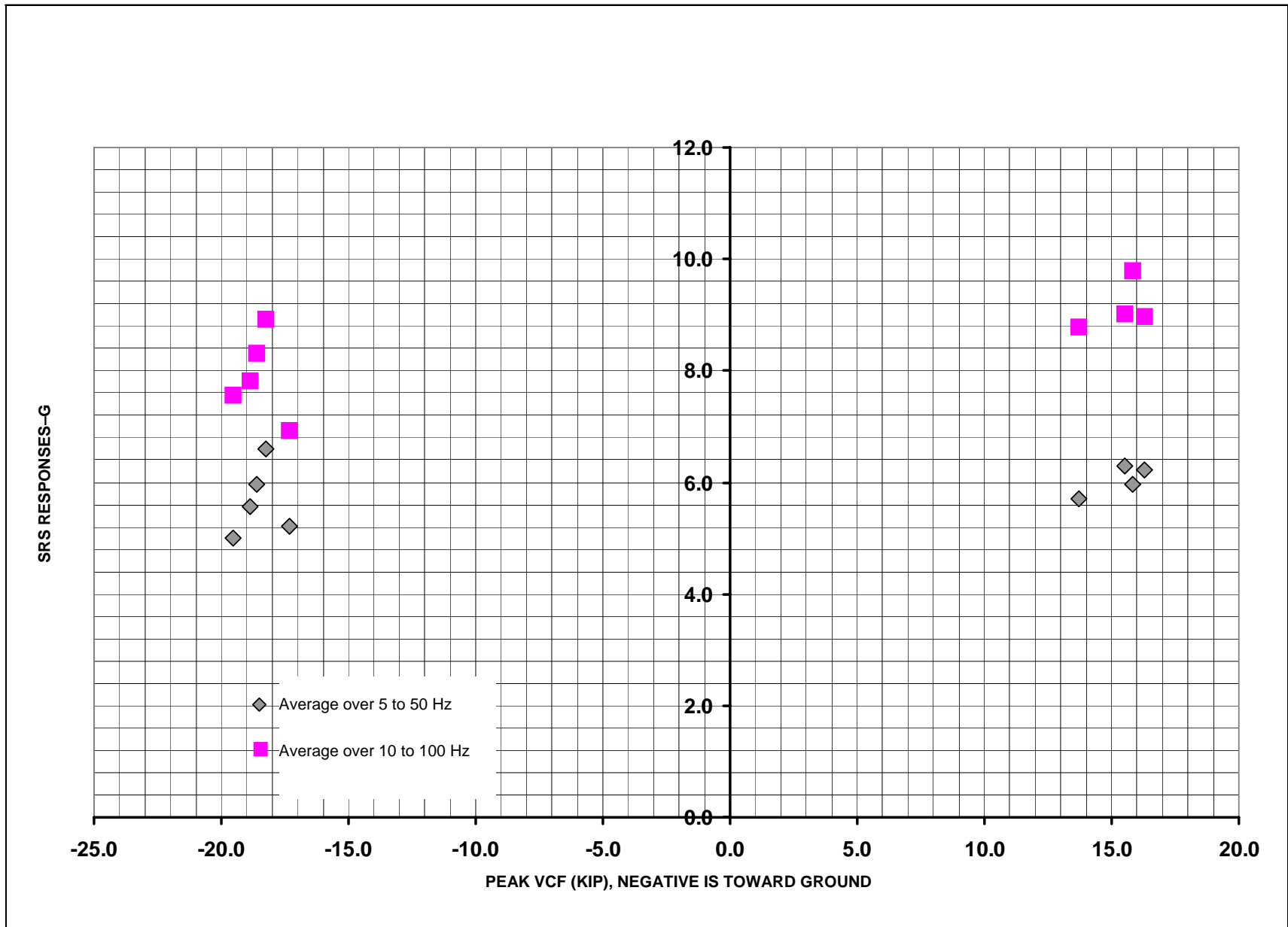


Plot A-30. SRS Response versus Peak VCF—Acceleration 18 Vertical, April 14-15, 2003



Plot A-31. SRS Response versus Peak LCF—Acceleration 6 Longitudinal, April 14-15, 2003





Plot A-32. SRS Response versus Peak VCF—Acceleration 6 Vertical, April 14-15, 2003

**Table A-1. Summary of TCOE FAST Test Data**

| DATE            | CAR LOCATION               | TRAIN DIRECTION | TOTAL NUMBER OF CARS | SAMPLE RATE | DATA USABLE | MAXIMUM LCF | MINIMUM LCF | MAXIMUM VCF | MINIMUM VCF |
|-----------------|----------------------------|-----------------|----------------------|-------------|-------------|-------------|-------------|-------------|-------------|
| 3/23/03–3/24/03 | 6 <sup>TH</sup> from front | CCW-Bypass      | 76                   | 4096        | No          |             |             |             |             |
| 3/24/03–3/25/03 | 6 <sup>th</sup> from front | CCW-Bypass      | 75                   | 4096        | No          |             |             |             |             |
| 3/25/03–3/26/03 | 6 <sup>th</sup> from end   | CCW-Bypass      | 76                   | 4096        | Yes         | 222.6       | -152.4      | 22.5        | -10.5       |
| 3/26/03–3/27/03 | 6 <sup>th</sup> from end   | CCW-Bypass      | 76                   | 4096        | Yes         | 203.2       | 186.9       | 41.6        | -11.4       |
| 3/30/03–3/31/03 | 6 <sup>th</sup> from end   | CCW-Main Loop   | 76                   | 4096        | Poor        | 166.1       | -236.8      | 21.1        | -31.2       |
| 3/31/03–4/01/03 | 6 <sup>th</sup> from end   | CCW-Main Loop   | 76                   | 4096        | No          |             |             |             |             |
| 4/7/03–4/8/03   | 4 <sup>th</sup> from front | CCW-Bypass      | 78                   | 4096        | Yes         | 1           | -185.3      | 21          | -8.2        |
| 4/13/03–4/14/03 | 6 <sup>th</sup> from end   | CCW-Bypass      | 77                   | 4096        | No          |             |             |             |             |
| 4/14/03–4/15/03 | 6 <sup>th</sup> from end   | CCW-Main Loop   | 76                   | 2048        | Yes         | 263.5       | -219.2      | 20.5        | -23.8       |
| 4/15/03–4/16/03 | 8 <sup>th</sup> from front | CW-Main Loop    | 77                   | 2048        | Yes         | 177         | -253.6      | 41.2        | -13.6       |
| 4/16/03–4/17/03 | 8 <sup>th</sup> from front | CW-Main Loop    | 77                   | 2048        | Yes         | -19.9       | -173.3      | 19.4        | -6.2        |
| 4/20/03–4/21/03 | 6 <sup>th</sup> from end   | CCW-Main Loop   | 76                   | 2048        | Yes         | 164.5       | -214.7      | 27          | -17.4       |
| 4/21/03–4/22/03 | 6 <sup>th</sup> from end   | CCW-Main Loop   | 75                   | 4096        | Yes         | 193.8       | -269.9      | 31.8        | -19.5       |

**Table A-2. Peak and SRS Acceleration Response versus Peak Coupler Force, April 14-15, 2003, Accelerometers 18L and 18V**

| FILE NAME | PEAK LCF KLB | PEAK VCF KLB | PEAK POS. LAT. ACCEL. | PEAK NEG. LAT. ACCEL. | PEAK POS. VERT. ACCEL. | PEAK NEG. VERT. ACCEL. | LAT. SRS 5-50 Hz | LAT. SRS 10-100 HZ | VERT. SRS 10-100 HZ | VERT. SRS 10-100 HZ |
|-----------|--------------|--------------|-----------------------|-----------------------|------------------------|------------------------|------------------|--------------------|---------------------|---------------------|
|           |              |              | 18L                   | 18L                   | 18V                    | 18V                    | 18L              | 18L                | 18V                 | 18V                 |
| 414225311 | 211.1        | -17.3        | 4.0                   | -4.8                  | 6.0                    | -4.1                   | 2.9              | 3.7                | 2.2                 | 3.2                 |
| 414225405 | -169.3       | 13.7         | 4.0                   | -3.1                  | 5.2                    | -3.4                   | 2.1              | 2.7                | 1.8                 | 2.1                 |
| 414225805 | -186.5       | 15.8         | 2.6                   | -4.9                  | 3.9                    | -4.4                   | 1.9              | 2.5                | 2.1                 | 2.5                 |
| 414230528 | 235.5        | -18.3        | 4.2                   | -3.3                  | 4.3                    | -2.5                   | 2.2              | 2.8                | 1.4                 | 2.0                 |
| 414230614 | -180.1       | 15.5         | 3.1                   | -5.2                  | 3.9                    | -2.7                   | 2.2              | 2.9                | 1.6                 | 2.1                 |
| 414230921 | 224.7        | -19.5        | 4.5                   | -3.9                  | 2.6                    | -3.4                   | 2.5              | 2.9                | 2.6                 | 3.6                 |
| 414232248 | -205.7       | 16.3         | 3.0                   | -2.5                  | 3.0                    | -2.3                   | 2.3              | 2.6                | 1.5                 | 1.9                 |
| 414232513 | 240.4        | -18.6        | 6.5                   | -4.4                  | 4.5                    | -4.4                   | 2.6              | 2.7                | 1.5                 | 2.2                 |
| 414235259 | 265.8        | -18.9        | 4.6                   | -3.7                  | 3.9                    | -3.4                   | 2.4              | 2.6                | 1.7                 | 2.4                 |

**Table A-3. Peak and SRS Acceleration Response versus Peak Coupler Force, April 14-15, 2003, Accelerometers 6L and 6V**

| FILE NAME | PEAK LCF KLB | PEAK VCF KLB | PEAK POS. LAT. ACCEL. | PEAK NEG. LAT. ACCEL. | PEAK POS. VERT. ACCEL. | PEAK NEG. VERT. ACCEL. | LAT. SRS 5-50 Hz | LAT. SRS 10-100 HZ | VERT. SRS 10-100 HZ | VERT. SRS 10-100 HZ |
|-----------|--------------|--------------|-----------------------|-----------------------|------------------------|------------------------|------------------|--------------------|---------------------|---------------------|
|           |              |              | 6L                    | 6L                    | 6V                     | 6V                     | 6L               | 6L                 | 6V                  | 6V                  |
| 414225311 | 211.1        | -17.3        | 2.2                   | -6.8                  | 3.2                    | -7.0                   | 4.5              | 6.9                | 5.2                 | 6.9                 |
| 414225405 | -169.3       | 13.7         | 2.4                   | -7.5                  | 3.2                    | -8.5                   | 4.7              | 7.5                | 5.7                 | 8.8                 |
| 414225805 | -186.5       | 15.8         | 4.7                   | -9.4                  | 7.3                    | -8.9                   | 4.8              | 7.9                | 6.0                 | 9.8                 |
| 414230528 | 235.5        | -18.3        | 2.9                   | -9.9                  | 3.8                    | -7.8                   | 5.1              | 8.6                | 6.6                 | 8.9                 |
| 414230614 | -180.1       | 15.5         | 3.2                   | -6.5                  | 3.6                    | -7.2                   | 3.9              | 6.1                | 6.3                 | 9.0                 |
| 414230921 | 224.7        | -19.5        | 5.2                   | -6.8                  | 6.2                    | -7.7                   | 3.6              | 6.7                | 5.0                 | 7.6                 |
| 414232248 | -205.7       | 16.3         | 2.6                   | -6.9                  | 2.7                    | -7.3                   | 4.1              | 6.8                | 6.2                 | 9.0                 |
| 414232513 | 240.4        | -18.6        | 2.7                   | -7.3                  | 3.3                    | -7.6                   | 3.8              | 6.8                | 6.0                 | 8.3                 |
| 414235259 | 265.8        | -18.9        | 3.0                   | -5.8                  | 2.8                    | -5.6                   | 3.4              | 5.5                | 5.6                 | 7.8                 |



## Acronyms

|         |  |
|---------|--|
| AAR     | Association of American Railroads                    |
| FAST    | Facility for Accelerated Service Testing             |
| FFT     | Fast Fourier Transfer                                |
| FRA     | Federal Railroad Administration                      |
| HTL     | High Tonnage Loop                                    |
| LCF     | longitudinal coupler force                           |
| PSD     | power spectral density                               |
| SDOF    | single-degree of freedom                             |
| SRS     | SRS  |
| SSWG    | Stub Sill Working Group                              |
| TC      | Transport Canada                                     |
| TCOE-TF | Tank Car Operating Environment Task Force            |
| TTC     | Transportation Technology Center (the site)          |
| TTCI    | Transportation Technology Center, Inc. (the company) |
| VCF     | vertical coupler forces                              |

